

# Iowa Research Online

---

## Functional genomic analyses of the impact of global hypomethylation and of tumor microenvironment in a rat model of human chondrosarcoma

Hamm, Christopher Allan

<https://iro.uiowa.edu/esploro/outputs/doctoral/Functional-genomic-analyses-of-the-impact/9983777114102771/filesAndLinks?index=0>

---

Hamm, C. A. (2009). Functional genomic analyses of the impact of global hypomethylation and of tumor microenvironment in a rat model of human chondrosarcoma [University of Iowa].  
<https://doi.org/10.17077/etd.6bfw4lta>

---

<https://iro.uiowa.edu>  
Free to read and download  
Copyright © 2009 Christopher Allan Hamm  
Downloaded on 2024/05/04 13:22:14 -0500

FUNCTIONAL GENOMIC ANALYSES OF THE IMPACT OF GLOBAL  
HYPOMETHYLATION AND OF TUMOR MICROENVIRONMENT IN A RAT  
MODEL OF HUMAN CHONDROSARCOMA

by  
Christopher Allan Hamm

An Abstract

Of a thesis submitted in partial fulfillment  
of the requirements for the Doctor of  
Philosophy degree in Genetics  
in the Graduate College of  
The University of Iowa

December 2009

Thesis Supervisor: Professor Marcelo B. Soares

## ABSTRACT

Chondrosarcomas are malignant cartilage tumors that do not respond to traditional chemotherapy or radiation. The 5-year survival rate of histologic grade III chondrosarcoma is less than 30%. To achieve a greater understanding of chondrosarcoma tumorigenesis, a model for human chondrosarcoma has been established in a rat system. The model, known as the Swarm rat chondrosarcoma (SRC), resembles human chondrosarcoma and provides a system to study tumor growth and progression. Here we examined the influence of the tumor microenvironment and the impact of genome-wide hypomethylation on the behavior of SRC tumors, two factors known to contribute fundamentally to the development and progression of solid tumors.

Previous studies with SRC revealed that tumor microenvironment can significantly influence chondrosarcoma malignancy, but the underlying biologic mechanisms have not been defined. To address this issue we carried out epigenetic and gene expression studies on the SRC tumors that were initiated at different transplantation sites. The epigenetic analysis revealed that microenvironmental changes could promote global DNA hypomethylation in SRC cells. Subsequent gene expression analyses revealed that the transplantation site had a significant impact on the gene expression profiles of SRC tumors. These SRC tumors had unique gene expression profiles, and we were able to identify genes that were differentially expressed between SRC tumors originating from different transplantation sites. Functional analyses of two differentially expressed genes, thymosin- $\beta$ 4 and c-fos, provided insight into the role that these genes may play in the development and progression of chondrosarcoma.

We also used the SRC model to examine the impact that DNA hypomethylation has on chondrosarcoma tumorigenesis. We induced DNA demethylation in SRC cells using 5-aza-2-deoxycytidine, a DNA demethylating agent. Loss of DNA methylation was accompanied by an increase in invasiveness of the rat

chondrosarcoma cells, *in vitro*, as well as by an increase in tumor growth *in vivo*. Subsequent microarray analysis provided insight into the gene expression changes that result from 5-aza-2-deoxycytidine-induced DNA demethylation. In particular, two genes that may function in tumorigenesis, *sox-2* and *midkine*, became overexpressed upon treatment with 5-aza-2-deoxycytidine. Promoter region DNA analysis revealed that these genes were methylated in control cells but became demethylated following 5-aza-2-deoxycytidine treatment.

Following withdrawal of 5-aza-2-deoxycytidine, the rat chondrosarcoma cells reestablished global DNA methylation levels that were comparable to that of control cells. Concurrently, invasiveness of the rat chondrosarcoma cells decreased to a level indistinguishable from that of control cells. Taken together these experiments demonstrate that global DNA hypomethylation induced by 5-aza-2-deoxycytidine promotes tumorigenesis in rat chondrosarcoma cells.

Overall, the studies with the SRC model indicate that changes in the microenvironment can induce DNA hypomethylation and gene expression changes in the SRC cells. Subsequent functional analyses of these changes demonstrated that both DNA hypomethylation and upregulation of specific genes may promote tumorigenesis in chondrosarcoma.

Abstract Approved: \_\_\_\_\_  
Thesis Supervisor

\_\_\_\_\_  
Title and Department

\_\_\_\_\_  
Date

FUNCTIONAL GENOMIC ANALYSES OF THE IMPACT OF GLOBAL  
HYPOMETHYLATION AND OF TUMOR MICROENVIRONMENT IN A RAT  
MODEL OF HUMAN CHONDROSARCOMA

by

Christopher Allan Hamm

A thesis submitted in partial fulfillment  
of the requirements for the Doctor of  
Philosophy degree in Genetics  
in the Graduate College of  
The University of Iowa

December 2009

Thesis Supervisor: Professor Marcelo B. Soares

Copyright by  
CHRISTOPHER ALLAN HAMM  
2009  
All Rights Reserved

Graduate College  
The University of Iowa  
Iowa City, Iowa

CERTIFICATE OF APPROVAL

---

PH.D. THESIS

---

This is to certify that the Ph.D. thesis of

Christopher Allan Hamm

has been approved by the Examining Committee  
for the thesis requirement for the Doctor of Philosophy  
degree in Genetics at the December 2009 graduation.

Thesis Committee: \_\_\_\_\_  
Marcelo B. Soares, Thesis Supervisor

\_\_\_\_\_  
Beverly L. Davidson

\_\_\_\_\_  
Raymond J. Hohl

\_\_\_\_\_  
Diane C. Slusarski

\_\_\_\_\_  
Edwin M. Stone

To my mother,  
Nancy Talarico Hamm,  
a constant source of inspiration for all of my research

## ACKNOWLEDGMENTS

I would like to thank my advisor, Dr. Bento Soares, for providing me with the opportunity to conduct my graduate research in his lab. Bento has been an excellent advisor, encouraging all aspects of my graduate studies. From the first exams of graduate school, to testing new hypotheses, to analyzing the expected and the sometimes unexpected results, Bento has always been a supportive mentor. He has fostered my development as a graduate student by sharing his research expertise, as well as sharing his skills in teaching, writing, and operating a productive lab.

I want to thank all members of the Soares lab for their support throughout graduate school. Most notably, I thank Maria de Fatima Bonaldo for her critical analysis and assistance with all aspects of my research projects. I also thank Hehuang Xie and Fabricio F. Costa for their help with the design and analysis of the methylation experiments; Elio F. Vanin for assistance with the design and construction of viral vectors; Tammy Kucaba and Christina Smith for DNA sequencing; and Jared Bischof for bioinformatic analyses.

Additionally, I would like to thank Jeff Stevens and Jose Morcuende for their assistance with the chondrosarcoma project; members of the Hendrix lab for help with invasion assays; and members of the Casavant lab for the bioinformatic analysis of the SAGE data.

I am thankful to all of my committee members for the time, effort, and guidance throughout graduate school and this thesis project. Furthermore, I want to acknowledge the Genetics program, Anita Kafer, and Linda Hurst for their continued support and assistance during graduate school.

Finally, I would like to express my gratitude to all of my family and friends, but especially Grandma, Brad, Melanie, and Juliette, for all of their support and encouragement throughout graduate school.

## ABSTRACT

Chondrosarcomas are malignant cartilage tumors that do not respond to traditional chemotherapy or radiation. The 5-year survival rate of histologic grade III chondrosarcoma is less than 30%. To achieve a greater understanding of chondrosarcoma tumorigenesis, a model for human chondrosarcoma has been established in a rat system. The model, known as the Swarm rat chondrosarcoma (SRC), resembles human chondrosarcoma and provides a system to study tumor growth and progression. Here we examined the influence of the tumor microenvironment and the impact of genome-wide hypomethylation on the behavior of SRC tumors, two factors known to contribute fundamentally to the development and progression of solid tumors.

Previous studies with SRC revealed that tumor microenvironment can significantly influence chondrosarcoma malignancy, but the underlying biologic mechanisms have not been defined. To address this issue we carried out epigenetic and gene expression studies on the SRC tumors that were initiated at different transplantation sites. The epigenetic analysis revealed that microenvironmental changes could promote global DNA hypomethylation in SRC cells. Subsequent gene expression analyses revealed that the transplantation site had a significant impact on the gene expression profiles of SRC tumors. These SRC tumors had unique gene expression profiles, and we were able to identify genes that were differentially expressed between SRC tumors originating from different transplantation sites. Functional analyses of two differentially expressed genes, thymosin- $\beta$ 4 and c-fos, provided insight into the role that these genes may play in the development and progression of chondrosarcoma.

We also used the SRC model to examine the impact that DNA hypomethylation has on chondrosarcoma tumorigenesis. We induced DNA demethylation in SRC cells using 5-aza-2-deoxycytidine, a DNA demethylating agent. Loss of DNA methylation was accompanied by an increase in invasiveness of the rat chondrosarcoma cells, *in vitro*, as well as by an increase in tumor growth *in vivo*. Subsequent microarray analysis provided insight into the gene expression changes that result from 5-aza-2-deoxycytidine-induced DNA demethylation. In particular, two genes that may function in tumorigenesis, *sox-2* and *midkine*, became overexpressed upon treatment with 5-aza-2-deoxycytidine. Promoter region DNA analysis revealed that these genes were methylated in control cells but became demethylated following 5-aza-2-deoxycytidine treatment.

Following withdrawal of 5-aza-2-deoxycytidine, the rat chondrosarcoma cells reestablished global DNA methylation levels that were comparable to that of control cells. Concurrently, invasiveness of the rat chondrosarcoma cells decreased to a level indistinguishable from that of control cells. Taken together these experiments demonstrate that global DNA hypomethylation induced by 5-aza-2-deoxycytidine promotes tumorigenesis in rat chondrosarcoma cells.

Overall, the studies with the SRC model indicate that changes in the microenvironment can induce DNA hypomethylation and gene expression changes in the SRC cells. Subsequent functional analyses of these changes demonstrated that both DNA hypomethylation and upregulation of specific genes may promote tumorigenesis in chondrosarcoma.

## TABLE OF CONTENTS

LIST OF TABLES .....	ix
LIST OF FIGURES .....	x
CHAPTER I. INTRODUCTION .....	1
Microenvironment in cancer .....	1
Components of the microenvironment.....	2
Microenvironment and gene expression .....	2
Microenvironment and epigenetics.....	3
Epigenetics in cancer.....	3
DNA hypermethylation.....	4
DNA hypomethylation.....	5
Chondrosarcoma .....	5
Chondrosarcoma subtypes and histologic grading.....	6
Genetic analysis of chondrosarcoma.....	7
Gene expression in chondrosarcoma.....	7
Epigenetic analysis of chondrosarcoma.....	9
Summary.....	9
Chondrosarcoma tumor model: Swarm rat chondrosarcoma.....	9
Transplantation site influences SRC phenotype .....	10
The SRC cell line .....	11
CHAPTER II. MICROENVIRONMENT ALTERS EPIGENETIC AND GENE EXPRESSION PROFILES IN SWARM RAT CHONDROSARCOMA TUMORS .....	12
Introduction.....	12
Gene expression profiles of the SRC tumors.....	13
SAGE.....	13
Functional analysis of differentially expressed genes.....	14
Materials and methods .....	14
Tumor induction and tissue harvesting.....	14
Total RNA Isolation.....	15
Sodium bisulfite-treatment of DNA.....	15
Pyrosequencing Primer design.....	16
SAGE library construction and data analysis .....	16
Real-Time Quantitative PCR .....	17
Thymosin- $\beta$ 4 and c-fos overexpression.....	18
Cell culture conditions and 5-Aza-2-deoxycytidine treatment.....	19
Invasion assay.....	19
Tumor Inductions in nude mice and tissue processing.....	20
Statistical Analysis.....	21
Results.....	21
Tumor transplantation site affects tumor phenotype.....	21
Epigenetic analysis of SRC tumors.....	22
SAGE library description.....	23
Gene expression differences between normal cartilage and the SRC tumors.....	23

Transplantation site influences gene expression .....	24
Endogenous thymosin- $\beta$ 4 expression in the SRC tumors .....	24
Endogenous c-fos expression in the SRC tumors .....	25
Growth factor expression in the SRC tumors .....	25
Functional analysis of differentially expressed genes.....	26
Overexpression of thymosin- $\beta$ 4 and c-fos.....	26
CTGF and the SRC cells.....	26
Discussion .....	27
CHAPTER III. GLOBAL DEMETHYLATION OF RAT CHONDROSARCOMA CELLS AFTER TREATMENT WITH 5-AZA-2'-DEOXYCYTIDINE RESULTS IN INCREASED TUMORIGENICITY .....	49
Introduction .....	49
5-Aza-2-deoxycytidine.....	49
Induction of DNA hypomethylation in a rat model for human chondrosarcoma .....	50
5-Aza-2-deoxycytidine treatment of SRC cells.....	50
Midkine and sox-2 .....	50
Effect of DNA hypomethylation in tumorigenesis .....	51
Materials and methods .....	51
Establishment of a bioluminescent rat chondrosarcoma cell line.....	51
Cell culture conditions and 5-Aza-2-deoxycytidine treatment.....	52
Tumor inductions .....	53
In vivo imaging.....	53
Primer design and pyrosequencing .....	54
Microarray.....	55
Real-Time quantitative PCR.....	56
CpG island identification .....	56
Analysis of DNA methylation by sequencing of sodium bisulfite- treated DNA .....	57
Invasion assay .....	57
Statistical analysis.....	58
Ethics statement .....	58
Results .....	58
5-Aza-2-deoxycytidine induces hypomethylation of LINE1 and Satellites 1 and 2 .....	58
Invasion Assay .....	59
Microarray analysis.....	60
Midkine and sox-2 .....	61
In vivo tumor formation.....	62
Methylation of SRC cells in vivo.....	63
Discussion .....	64
CHAPTER IV. CONCLUSION.....	91
APPENDIX A. COMPLETE SAGE DATA.....	97
APPENDIX B. DIFFERENTIALLY EXPRESSED SAGE TAGS.....	98
APPENDIX C. GENE LIST OF UNIQUE SAGE PROFILES .....	99
APPENDIX D. COMPLETE MICROARRAY DATA .....	100

APPENDIX E. DIFFERENTIALLY EXPRESSED GENES IDENTIFIED BY MICROARRAY ANALYSES .....	101
REFERENCES .....	102

## LIST OF TABLES

Table 1.	Effect of transplantation site on tumor weight. ....	33
Table 2.	Summary of SAGE tags generated from each normal cartilage and the SRC tumors. ....	34
Table 3.	Pathway analysis of differentially expressed genes between RNC and SRC tumors. ....	35
Table 4.	Summary of subcutaneous tumor weight following transplantation of SRC cells that overexpress thymosin- $\beta$ 4 or c-fos. ....	36
Table 5.	Pyrosequencing primer design and PCR conditions. ....	70
Table 6.	Bisulfite treated DNA primer design.....	71
Table 7.	Top pathways altered following 5-Aza-2-deoxycytidine treatment.....	72
Table 8.	In vivo: Subcutaneous transplantation of SRC tumor cells.....	73
Table 9.	Upregulation of dppa5, cryaB, cdh3, and sox-2 following 5-aza-2-deoxycytidine treatment. ....	74

## LIST OF FIGURES

- Figure 1. Schematic diagram of a SAGE experiment. SAGE (Serial Analysis of Gene expression) generates an expression profile that is based on the quantification of “tags”, which are a short nucleotide sequence that correspond to a mRNA transcript. (A) Polyadenylated RNA is used to construct a biotin-oligo d(T)-primed cDNA library. (B) The cDNA is cleaved with an anchoring enzyme, and the resulting 3’ end of the cDNA is isolated with streptavidin beads. (C) The cDNA is then split in half; one half is ligated to linker “A” and the other half is ligated to linker “B”. The linkers contain a tagging enzyme (TE) recognition site. Digestion with TE thus releases the “linker-SAGE tag” cDNA fragments of ~20bp (D) The two pools of tags are blunt ended, and then the pools are ligated to each other to form “Di-tags”. (E) The ligated “Di-Tags” are then PCR amplified with primer specific to linkers “A” and “B”. (F) The PCR amplified “Di-tags” are digested with the anchoring enzyme to remove the linker sequence (freeing the “Di-tag”). (G) Lastly the “Di-tags” are ligated and sequenced. The sequence is then computationally analyzed and the tags are quantified. Figure modified from (Velculescu *et al.*, 1995). ..... 37
- Figure 2. Transient transfection of 293T cells to produce viral particles. The viral vector has been modified so that it cannot, by itself, make proteins required for additional rounds of replication. The viral proteins that are needed for the initial infection can be provided in *trans*. 5’ and 3’ LTRs contain transcription factor recognition sites. The GAG sequence encodes for proteins that form the shell of the complete retroviral particle. The POL sequence encodes for reverse transcriptase, integrase and ribonuclease H (important for viral integration into host DNA). The ENV sequence encodes for an envelope glycoprotein that extends from the membrane of the viral particle (the ENV protein is the ligand for the receptor on the host cell). The “PR” sequence in the vector DNA contains the promoter sequence that drives the expression of the GAG-POL and ENV. “Ψ<sup>+</sup>” denotes the packaging signal (note that the packaging sequence is only present in the vector containing the gene of interest). The complete description of the viral vectors is located in the Materials and methods..... 38
- Figure 3. Phenotype of the Swarm Rat chondrosarcoma varies based on tumor transplantation site. (A) Transplantation of the SRC tumor into the tibia of Sprague-Dawley rats. Histologic micrographs at day 0, day 7, and day 34. Successive histologic micrographs revealed increased tumor volume and invasion of the tumor into the bony cortex. Cells stained with safranin O and fast green. (B) SRC tumor detected in the lung of a rat that had the SRC tumor transplanted into the tibia. Note the presence of multiple SRC tumors. Lung tumors were detected in 50% of the animals that had the SRC tumor transplanted into the tibia. The number of metastases in a single animal numbered from 1 to 54 (average=10). The average size of the tumors was 2mm. No lung tumors were detected in the animals with subcutaneous tumor transplants..... 39

Figure 4.	Transplantation microenvironment influences DNA methylation in SRC tumors. Pyrosequencing revealed that Satellite 1 DNA was hypomethylated compared to DNA from rat normal cartilage (control tissue). The satellite 1 DNA in the subcutaneous SRC tumor and the tibia SRC tumor was hypomethylated compared to the DNA in the lung SRC tumor. The graph illustrates the average DNA methylation that was calculated from a pool of tissues from each transplantation site. For each transplantation site, tissue was pooled from at least 10 separate animals. The error bars represent technical replicates of the pooled tissue samples. The p-values represent the significance of the comparison of a specific sample with normal rat cartilage (p-value<0.05 represents a statistically significant difference). .....	40
Figure 5.	Heat map displaying the differentially expressed genes between RNC and SRC tumor tissues. Rat normal (articular) cartilage has a unique expression profile when compared to the expression profiles of the SRC tumors. The changes in gene expression may represent critical differences between normal cartilage cells and chondrosarcoma, and they may also represent changes important for the development and progression of chondrosarcoma. Heat map displays the differentially expressed genes that were expressed at a level of at least 25 tags in one library. Color bar illustrates relative gene expression levels. Columns represent SAGE libraries and rows represent the expression of individual SAGE tags. For complete gene list and annotation see Appendix B.....	41
Figure 6.	SAGE reveals gene expression differences between the SRC tumors and normal cartilage as well as gene expression differences between SRC tumors. (A) Expression of extracellular matrix genes. (B) Expression of extracellular matrix modifying proteases. Heat map displays relative expression values. Actual expression values are listed to the right of the heat map. ....	42
Figure 7.	SAGE reveals gene expression differences between the SRC tumors and normal cartilage as well as gene expression differences between SRC tumors. (A) Expression of genes related to cell motility. (B) Expression of components of the AP-1 transcription factor complex. (C) Expression of growth factors. Heat map displays relative expression values. Actual expression values are listed to the right of the heat map.....	43

Figure 8. Tumor transplantation site significantly alters the gene expression profiles of the SRC tumors. Since the SRC tumors at different transplant sites originated from the same source tumor, the unique SRC gene expression profiles at each transplant site are likely a result of interactions in the microenvironment between tumor cells and host cells. (A) Differential gene expression between the Subcutaneous SRC tumor (highlighted in yellow) and SRC tumors at the other transplantation sites (200 genes upregulated and 107 genes downregulated in the Subcutaneous SRC tumor). (B) Differential gene expression between the Tibia SRC tumor (highlighted in yellow) and the SRC tumors at the other transplantation sites (106 genes upregulated and 108 genes downregulated in the tibia SRC tumor). (C) Differential gene expression between the Lung SRC tumor (highlighted in yellow) and the SRC tumors at the other transplantation sites (157 genes upregulated and 73 genes downregulated in the lung SRC tumor). Only genes with significantly different gene expression were included in each analysis ( $z > 1.96$ ; see Materials and methods). SAGE tags also needed to have an expression level of at least 25 in one tissue to be included in the analysis. Condition trees illustrate the relationship between the SAGE libraries with respect to the set of differentially expressed genes. Color bar illustrates relative gene expression levels. See Appendix C for complete data set and annotation of the genes presenting within this figure. .... 44

Figure 9. SAGE and quantitative RT-PCR confirm the expression of thymosin- $\beta$ 4 and c-fos in the SRC tumors. (A) Thymosin- $\beta$ 4 expression in the SRC tumors (SAGE analysis top panel; quantitative RT-PCR bottom panel). (B) C-fos expression in the SRC tumors (SAGE analysis top panel; quantitative RT-PCR bottom panel). Similar expression patterns were observed in both the SAGE and RT-PCR analysis. Note the increased expression of thymosin- $\beta$ 4 and c-fos in the tibia and lung SRC tumors. The bars in the RT-PCR graph represent the average expression ratio calculated on RNA that was collected from pooled tumor tissue. For RT-PCR at each transplantation site, tissue was pooled from at least 10 separate tumors. SAGE data was normalized to 100,000 tags/library for analysis. For the SAGE data, “\*” indicates expression levels that are significantly different than the “Subcutaneous SRC tumor” sample ( $z > 1.96$ ). .... 45

- Figure 10. Thymosin- $\beta$ 4 and c-fos overexpression in the SRC cells and histology following subcutaneous transplantation. (A) Confirmation of Thymosin- $\beta$ 4 and c-fos overexpression in the SRC cell line using real time quantitative-PCR. Expression of the transgene construct was detected in all cell lines that were transduced with the viral vector (SRC cell line-no insert vector, SRC c-fos cell line, and SRC Thymosin- $\beta$ 4 cell line). No expression of the transgene construct was detected in the untransduced SRC cell line (SRC cell line). The expression of the exogenous genes were detected with PCR primers specific for a sequence that is present in all of the expression constructs (see Material and methods). (B) Photomicroscopy of histological sections obtained from SRC tumors (20x magnification). Tumors induced from control cells (SRC cells expressing the empty viral vector), and from SRC cells overexpressing either Thymosin- $\beta$ 4 (Thymosin- $\beta$ 4 tumor) or c-fos (C-fos tumor). Approximately 30 days following tumor induction animals were sacrificed and tumors were removed for histology. Sections representative of each tumor are shown. All tumors were classified as histologic grade II chondrosarcomas. The SRC cells are stained with Safranin O (red)..... 46
- Figure 11. Tumor weight following induction of subcutaneous tumors with SRC cells overexpressing either thymosin- $\beta$ 4 or c-fos. Control tumors were initiated with SRC cells that express the MSCV viral vector with no insert (pMSCV-I-Hyrge vector). C-fos tumors were initiated with SRC cells that overexpress c-fos (MSCV-cfos-I-Puro). Thymosin- $\beta$ 4 tumors were initiated with SRC cells that overexpress thymosin- $\beta$ 4 (MSCV-Thy $\beta$ 4-I-Puro). Overexpression of c-fos resulted in the formation of tumors that were significantly smaller than control tumors. The bar represents the average invasion indices of biologic replicates, and the error bars represent the standard deviation of the biologic replicates. n=10 for control tumors and c-fos tumors. n=9 for thymosin- $\beta$ 4 tumors (one animal died prematurely and was found to have multiple chondrosarcoma lung metastases). See Table 4 for individual tumor weights. ‘\*’ Indicates that the tumor weight is significantly different than the tumor weight of the control tumors (p-value <0.05 considered significant)..... 47
- Figure 12. CTGF treatment decreases the invasiveness of SRC cells. Invasiveness was measured in control SRC cells (SRC Control) and in SRC cells treated with CTGF (50, 100, and 250ng/mL) at the start of the invasion assay. Twenty-four hours later, the invasiveness was calculated for all samples and the results are displayed as experimental sample compared to the untreated control SRC cells (100% invasion). The bar represents the average invasion indices of biologic replicates, and the error bars represent the standard deviation of 3 biologic replicates. ‘\*’ Indicates values that are significantly different than the ‘SRC Control’ sample (p<.05). ..... 48

- Figure 13. Expression of luciferase in a SRC cell line. SRC cells were transduced with a retrovirus containing the MSCV-Luc-I-Hyrgo plasmid (see Materials and methods). The number of transductions ranged from a single transduction to four transductions. Multiple transductions were done on consecutive days. Following antibiotic selection, the cell lines were tested for luciferase activity. The cell line with the highest luciferase activity was selected for use in subsequent experiments (SRC-LTC-MSCV3). The average luminescence signal is listed above each bar on the graph (the average was calculated from at least 5 biologic replicates). ..... 75
- Figure 14. Percent viability of SRC cells following 72-hour incubation with 5-Aza-2-deoxycytidine. Percent viability of SRC cells 72-hours following treatment with 0, 0.1, 0.3, 1.0, 3.0, 10, 30, 100, and 300uM 5-Aza-2-deoxycytidine. Each point on the graph represents the average viability of three biologic replicates, and the error bars represent the standard deviation of the biologic replicates. “\*\*\*” indicates a significant difference between a given sample and the control sample (0.0uM: no treatment). ..... 76
- Figure 15. Pyrosequencing of LINE and Satellite 1 and 2 *in vitro*. For each experiment the methylation pattern was analyzed in SRC untreated control cells (SRC-Control), SRC cells treated with 5-Aza-2-deoxycytidine for 5 passages (SRC 5AZA), and in SRC cells that were treated with 5-Aza-2-deoxycytidine for 5 passages and then allowed to grow for 5 additional passages without treatment (SRC 5AZA-STOP). Pyrosequencing assay: LINE1-S1; [2481 CpG’s], LINE1-S2; [3308 CpG’s]; Satellite I [15CpG’s], and Satellite II [411 CpG’s]. Treatment of MSCV3-LTC chondrosarcoma cells with 5-Aza-2-deoxycytidine leads to demethylation that can be detected throughout the genome. Altered DNA methylation patterns can be detected several weeks following removal of 5-Aza-2-deoxycytidine treatment. Bars represent the average DNA methylation % of biologic replicates, and error bars represent the standard deviation of these replicates. “\*” Indicates values that are significantly different than the “SRC Control” sample (p<.05). ..... 77
- Figure 16. 5-Aza-2-deoxycytidine treatment increases the invasiveness of rat chondrosarcoma cells. Invasiveness was measured in control SRC cells (SRC Control), SRC cells that were treated for 5 passages with 5-Aza-2-deoxycytidine (SRC 5AZA), and SRC cells 5-with 5 passages Aza-2-deoxycytidine and then grown for 5 additional passages without treatment (5AZA-STOP). The invasiveness was calculated for all samples and the results are displayed as experimental sample compared to the untreated control SRC cells (100% invasion). The bar represents the average invasion indices of biologic replicates, and the error bars represent the standard deviation of the biologic replicates. “\*” Indicates values that are significantly different than the “SRC Control” sample (p<.05). ..... 78

- Figure 17. Heat map of differentially expressed genes between SRC cells treated 5-Aza-2-deoxycytidine and untreated control SRC cells. Genes with at least a 5-fold difference were selected for analysis using the pathway program Ingenuity. Ingenuity revealed that, of the 977 differentially expressed genes (603 genes upregulated and 374 downregulated), 135 were identified as cancer related. A subset of these cancer related genes (see Materials and methods; see Appendix E for complete gene list and expression values) was then used for hierarchical clustering, and the results of that clustering are presented in this figure. Each vertical column represents microarray hybridizations from separate individual experiments. Microarray hybridizations were carried out on SRC cells treated with 5-Aza-2-deoxycytidine for 5 passages (SRC-5-AZA-P6 [1] and [2]), and microarray hybridizations were also carried out on SRC cells grown for 5 passages without 5-Aza-2-deoxycytidine treatment (SRC-No-Treat-P6 [1], [2], and [3]). ‘\*’ Indicates midkine and ‘\*\*’ indicates sox-2 in the heat map. The color bar corresponds the to the expression level in relative fluorescent units. .... 79
- Figure 18. Expression analysis of midkine. Quantitative real time PCR analysis of midkine expression in control SRC cells (SRC Control), SRC cells that were treated for 5 passages with 5-Aza-2-deoxycytidine (SRC 5AZA), and SRC cells 5-with 5 passages Aza-2-deoxycytidine and then grown for 5 additional passages without treatment (5AZA-STOP). Treatment with 5-Aza-2-deoxycytidine induces midkine expression. Five passages following 5-Aza-2-deoxycytidine removal the expression of midkine has dropped but it is greater than that of untreated control cells. Bars represent the average expression of three biologic replicates, and error bars represent the standard deviation of these replicates. ‘\*’ Indicates values that are significantly different than the “SRC Control” sample ( $p < .05$ ). Note that for graphical representation two different vertical scale bars are shown; the vertical scale bar on the left corresponds to the SRC Control and SRC 5AZA-STOP samples, and the vertical Scale bar on the right corresponds with the SRC 5AZA-STOP sample. .... 80
- Figure 19. Epigenetic analysis of Midkine methylation in SRC cells. Schematic representation of analyzed CpG islands in relation to the midkine transcriptional start site (TSS). Green bars indicate regions that were targeted for bisulfite sequencing. Bisulfite sequencing of midkine CpG Island 1 and CpG Island 2. Each row indicates an individual cloned sequence. Circles represent CpG sites. Black circles indicate a methylated CpG site and white circles indicate a unmethylated CpG site. These results demonstrate that 5-Aza-2-deoxycytidine treatment leads to the hypomethylation of CpG islands that span regions of the rat midkine gene. .... 81

- Figure 20. Expression analysis of sox-2 in SRC cells. Quantitative real time PCR analysis of sox-2 expression in control SRC cells (SRC Control), SRC cells that were treated for 5 passages with 5-Aza-2-deoxycytidine (SRC 5AZA), and SRC cells 5-with 5 passages Aza-2-deoxycytidine and then grown for 5 additional passages without treatment (5AZA-STOP). Treatment with 5-Aza-2-deoxycytidine induces sox-2 expression. Five passages following 5-Aza-2-deoxycytidine removal the expression of sox-2 has dropped. Bars represent the average expression of three biologic replicates, and error bars represent the standard deviation of these replicates. ‘\*’ Indicates values that are significantly different than the “SRC Control” sample (p<.05)..... 82
- Figure 21. Epigenetic analysis of sox-2. Schematic representation of analyzed CpG islands in relation to the sox-2 transcriptional start site (TSS). Green bars indicate regions that were targeted for bisulfite sequencing. Bisulfite sequencing of sox-2 CpG Island 47 and CpG Island 154. Each row indicates an individual cloned sequence. Circles represent CpG sites. Black circles indicate a methylated CpG site and white circles indicate an unmethylated CpG site. (A) CpG 47 Island was methylated in untreated SRC cells but following 5-Aza-2-deoxycytidine treatment it became hypomethylated. (B) CpG Island 154 was not methylated in either control or treated cells. .... 83
- Figure 22. Pyrosequencing of the midkine and sox-2 promoter. CpG sites in the midkine (A) and sox-2 (B) promoter sequence are methylated in untreated SRC cells but following 5-Aza-2-deoxycytidine treatment they become hypomethylated. The promoter regions of midkine and sox-2 were analyzed for DNA methylation status. Pyrosequencing was used to analyze bisulfite treated DNA with primers specific for midkine or sox-2. The bar represents the average DNA methylation of technical replicates, and the error bars represent the standard deviation of the technical replicates. ‘\*’ Indicates that the values are significantly different than the “SRC Control” sample (p<.05). Five CpG sites were examined with the midkine promoter analysis. Eight CpG sites were examined in the sox-2 analysis..... 84
- Figure 23. 5-Aza-2-deoxycytidine treated SRC cells produced larger tumors than untreated SRC cells. (A) *In vivo* bioluminescent imaging of SRC cells in nude mice.  $5 \times 10^6$  Control cells [animal a; left] and  $5 \times 10^6$  5-Aza-2-deoxycytidine treated cells [animal B; right] were injected subcutaneously. This image was collected 6 weeks after tumor induction. This Image corresponds to animal 3a and 3b in Table 8..... 85

- Figure 24. Summary of *in vivo* SRC injections. Tumors induced with 5-Aza-2-deoxycytidine-treated SRC cells produced larger tumors than the tumors induced with SRC control cells. A linear regression method was applied to analyze tumor weight between two tumor groups (SRC Control and SRC 5AZA) after adjusting for the number of cells injected. For graphical representation the tumor weights and the number of cells injected was log transformed. p-value is for comparison of the two tumor groups (SRC Control and SRC 5AZA), and indicates that there is a significant difference in tumor weight between the two groups. Results are shown for 7 animals with tumors induced from untreated cells (SRC control) and for 7 animals with tumors induced from 5-Aza-2-deoxycytidine-treated cells (SRC 5AZA). Detailed *in vivo* tumor summary is presented in Table 8. .... 86
- Figure 25. Photomicroscopy of histological sections obtained from SRC tumors (20x magnification). (A) Subcutaneous tumor induced from untreated SRC control cells. (B) Subcutaneous tumor induced from 5-Aza-2-deoxycytidine SRC cells. Approximately 60 days following tumor induction animals were sacrificed and tumors were removed for histology. Tumors from the SRC control cells and the 5-Aza-2-deoxycytidine cells showed considerable heterogeneity. There was no clear histological difference between tumors initiated from control cells or treated cells. Low grade (Grade 1) – Small nuclei with low variation in size and abundant cartilage matrix. Intermediate grade (Grade 2) – Higher cellularity, larger nuclei with increased atypia and hyperchromasia. High grade (Grade 3) – Pleomorphic cells with greater degree atypia and nuclear size. The SRC cells are stained with Safranin O (red). .... 87
- Figure 26. Macrometastasis detected in the lungs of mice injected with 5-Aza-2-deoxycytidine treated SRC cells. Macrometastases were detected in 3 of 9 animals injected with 5-Aza-2-deoxycytidine treated cells, but no macrometastases were detected in the lungs of mice injected with untreated cells. Metastases of varying size were detected in the in the lungs of the same animal. The SRC tumor cells form nodules of different sizes and resemble hyaline cartilage. Lungs from 3 separate mice are displayed in the figure. .... 88
- Figure 27. Pyrosequencing of LINE and Satellite 1 and 2 *in vivo*. Pyrosequencing results are also displayed from tumor samples: tumors initiated from untreated SRC cells (SRC Control) and tumors initiated from SRC cells that were treated for 5 passages with 5-Aza-2-deoxycytidine (SRC 5AZA). Results are shown for 3 SRC Control tumors and 3 SRC 5AZA tumors. Pyrosequencing assay: LINE1-S1; [2481 CpG's], LINE1-S2; [3308 CpG's], Satellite I [15CpG's], Satellite II [411 CpG's]. In all regions examined by pyrosequencing the SRC 5AZA tumors have a significantly lower level of methylation than the SRC Control tumors. Bars represent the average DNA methylation % of biologic replicates, and error bars represent the standard deviation of these replicates. ‘\*’ Indicates values that are significantly different than the “SRC Control” sample (p<.05). .... 89

- Figure 28. Identification of Sox-2 regulated genes. Genes with a 5-fold difference between control and 5-Aza-2-deoxycytidine treated cells were imported into the pathway program GeneGO. GenGO identified a network whereby sox-2 putatively activates the expression of Dppa5, Alpha crystallin B, and P-cadherin. Microarray data demonstrates that Dppa5, CryaB, Cdh3, and Sox2 are upregulated following 5-aza-2-deoxycytidine treatment (Table 9). The relative expression ratios of Dppa5, Alpha crystallin B, and P-cadherin are similar to that of sox-2, suggesting that sox-2 may play a role in the regulation of these genes. .... 90
- Figure 29. Schematic representation of the thymosin- $\beta$ 4 promoter. The thymosin- $\beta$ 4 promoter sequence in human (A) and rat (B) was examined for CpG islands. CpG islands were found to cover the first two exons of the thymosin- $\beta$ 4 gene in both species. Diagram is drawn to scale. Blue boxes represent exons. The green boxes represent the location of the CpG islands. .... 96

## CHAPTER I INTRODUCTION

In this thesis we characterize a rat model of human chondrosarcoma, the Swarm rat chondrosarcoma (SRC). The goal of this work was to obtain a greater understanding of the molecular mechanisms that underlie chondrosarcoma tumorigenesis. We have examined how changes to the tumor microenvironment impact the SRC cells and we have also examined how epigenetic changes impact the SRC cells. In this introduction, I will present a summary of information pertaining to the role that both the tumor microenvironment and epigenetic changes play in tumorigenesis. This information is followed by a detailed introduction to human chondrosarcoma and to the rat model of chondrosarcoma.

### Microenvironment in cancer

The microenvironment can broadly be defined by the interaction between tumor cells and surrounding normal cells. The importance of the tumor microenvironment was realized over 100 years ago with Stephen Paget's "seed and soil" hypothesis (Paget 1989). Paget suggested that organs might play an active role in tumor metastasis. Paget hypothesized that tumor cells ("the seed") can survive and grow only if they come in contact with a suitable microenvironment ("soil") (Paget 1989). More definitive proof of Paget's hypothesis came in 1980, when melanoma was shown to selectively metastasize to specific organs (Hart and Fidler 1980).

Although microenvironment is important for tumor metastasis, it also plays a key role in tumorigenesis. The tumor microenvironment can impact on genomic stability (Reynolds et al. 1996) and tumor malignancy (Stackpole et al. 1990). It has been

suggested that the microenvironment provides a selective pressure for the generation of tumor cells with varying degrees of tumorigenic potential (Young and Hill 1998).

### Components of the microenvironment

The microenvironment consists of fibroblasts, immune cells, tumor cells, and extracellular matrix molecules (Albini and Sporn 2007) surrounded by a vascular network. Physiologically, the tumor microenvironment is also characterized by changes in oxygen (Moulder and Rockwell 1987), pH (Wike-Hooley et al. 1984), and nutrient supply (Vaupel et al. 1989). These components of the microenvironment interact with each other and contribute to further changes in tumor cells.

Normal cells can produce growth factors that contribute to angiogenesis (Rehman et al. 2003), and fibroblasts are capable of producing growth factors that stimulate cell proliferation (Bhowmick et al. 2004). Immune cells may also produce factors that can promote tumor progression. Neutrophils and macrophages produce growth factors that foster angiogenesis and tumor cell growth (Balkwill and Mantovani 2001; Lewis et al. 2000; Scapini et al. 2004). Macrophages can also promote tumor invasion through the production of extracellular matrix-degrading proteases (Noel et al. 2008). Taken together, the non-tumoral cells of the microenvironment may contribute to the activation of pathways that promote tumorigenesis. These changes in tumorigenesis may be mediated by structural alterations in the microenvironment and/or by alterations in the tumor cells.

### Microenvironment and gene expression

The identification of gene expression changes that are induced by the microenvironment may provide insight into genes and pathways that are important for tumor progression, and thereby provide targets for therapeutic intervention. The microenvironment has previously been shown to significantly impact the gene expression of tumor cells (Bando et al. 2003; Fromigue et al. 2003). While these studies have

provided insight into the function of the microenvironment, there are many tumors in which the impact of the microenvironment has yet to be examined. Given that the same type of tumor may behave differently depending on the microenvironment, a comparative analysis of gene expression of tumor cells exposed to different microenvironments should provide an insight to the contribution of the microenvironment to the pathways that underlie tumorigenesis.

### Microenvironment and epigenetics

Additional insight into the tumor microenvironment was recently provided by work demonstrating that the microenvironment can contribute to epigenetic alterations in tumor cells (Shahrzad et al. 2007). Epigenetic alterations may have a significant impact on both genomic stability and gene expression in tumor cells (Hoffmann and Schulz 2005; Schmid et al. 1984). The microenvironment may mediate adaptive changes in tumor cell phenotype through epigenetic mechanisms (Fan et al. 2006).

### Epigenetics in cancer

Epigenetics is defined as the study of heritable changes in phenotype that do not involve alteration in the DNA sequence (Feinberg and Tycko 2004; Pogribny and Beland 2009). Epigenetic modifications have been documented for over forty years and they involve both modification of DNA binding proteins and methylation of DNA (Allfrey et al. 1964; Gold et al. 1963).

In eukaryotes, DNA methylation involves the covalent addition of a methyl group to the carbon atom 5 of the cytosine pyrimidine ring in a CpG (cytosine-guanine) dinucleotide (Chiang et al. 1996; Pogribny and Beland 2009). One of the main functions of DNA methylation is gene silencing. DNA methylation can inhibit gene expression by directly interfering with the binding of a transcription factor to DNA (Comb and Goodman 1990). Methylated DNA can also recruit DNA methyl binding proteins that

can promote a more condensed chromatin structure, and will ultimately lead to gene silencing (Szyf 2009).

DNA methylation is thought to be essential for normal development (Singer-Sam and Riggs 1993; Yoder et al. 1997). Conversely, abnormalities in DNA methylation have been detected in several human diseases, including cancer (Feinberg 2008). Increased activity of DNA methylating enzymes were initially detected in cancerous tissue and it was hypothesized that the enzymes may play a role in carcinogenesis (Magee 1971). Subsequent experiments have revealed the presence of two specific types of methylation abnormalities in cancer, DNA hypomethylation and DNA hypermethylation. DNA hypomethylation refers to a relative decrease in DNA methylation compared to a “normal” methylation level, and DNA hypermethylation refers to a relative increase in methylation compared to a “normal” methylation level (Dunn 2003). Cancer cells are thought to exhibit both types of DNA methylation alterations. Specifically, the genome of a cancer cell is thought to contain localized regions of DNA hypermethylation, while exhibiting an overall lower level of methylation, i.e. genome-wide hypomethylation (Hoffmann and Schulz 2005).

#### DNA hypermethylation

DNA hypermethylation has been detected in the promoter regions of specific genes, and hypermethylation is associated with abnormal gene silencing in several tumors (Esteller et al. 2001; Ohtani-Fujita et al. 1993). Experiments have demonstrated that DNA hypermethylation plays a role in gene inactivation in cancer (Feinberg and Tycko 2004). The epigenetic inactivation of genes, such as tumor suppressors, may have a significant impact on tumorigenesis. To address this issue, demethylation therapies have been developed to reverse DNA hypermethylation-induced gene silencing (Mund et al. 2006; Stresemann and Lyko 2008).

## DNA hypomethylation

In addition to DNA hypermethylation, DNA hypomethylation has also been reported in many tumors. The first report of epigenetic abnormalities in cancer was based on the observation that colon cancer DNA was hypomethylated compared to the corresponding normal tissue DNA (Feinberg and Vogelstein 1983). Subsequently, global DNA hypomethylation has been detected in other cancers, and it is proposed that DNA hypomethylation may be one of the most common alterations in cancer (Pogribny and Beland 2009). Associations between levels of DNA hypomethylation and tumor grade suggest that DNA hypomethylation may also have prognostic value (Kim et al. 1994; Watts et al. 2008).

Functionally, DNA hypomethylation has been shown to promote tumor formation in tumor-prone mice (Gaudet et al. 2003). DNA hypomethylation may promote carcinogenesis through transcriptional derepression of genes that are not expressed under normal conditions (Pogribny and Beland 2009). DNA hypomethylation may also promote tumor formation through derepression of transposition of repetitive elements, which is thought to result in genomic instability (Howard et al. 2008). Although these reports provide insight into the function of DNA hypomethylation, more research is needed to uncover the molecular basis for the relationship between global DNA hypomethylation and tumorigenesis.

## Chondrosarcoma

Chondrosarcoma is a malignant cartilage tumor (Dorfman and Czerniak 1995). Chondrosarcoma is the second most common primary bone malignancy, accounting for 25% of primary bone sarcomas (Sandberg and Bridge 2003; Unni 1996). Chondrosarcomas can arise skeletally or extraskeletally and have a peak incidence between the ages of 50-75 (Sandberg and Bridge 2003). Common sites of tumor formation are the pelvis, humerus, femur, tibia, spine and scapula (Evans et al. 1977;

Lee et al. 1999; Pant et al. 2005). Diagnosis is usually based on histologic grade of the tumor, but lack of prognostic markers (Aigner et al. 2002) and questions about the reliability of tumor grading have made it difficult to define the malignancy of these tumors (Lee et al. 1999). Currently the most common treatment for chondrosarcoma is surgical resection, but tumor removal is not always curative because local recurrence (Gitelis et al. 1981) and metastasis are common. High grade lesions may be treated with chemotherapy/radiation but chondrosarcomas are usually not responsive to these treatments (Gitelis et al. 1981; Mitchell et al. 2000), and as a result the 5-year survival rate of histologic grade III chondrosarcoma is only 29% (Aigner 2002).

#### Chondrosarcoma subtypes and histologic grading

There are five histologic subtypes of chondrosarcoma: conventional (classical), dedifferentiated, clear cell, mesenchymal, and mixoid. The conventional subtype is the most common, representing approximately 86% of all chondrosarcomas (Unni 2001). Dedifferentiated chondrosarcoma represents approximately 10% chondrosarcomas (Unni 2001), and the other subtypes account for less than 1% of all chondrosarcoma cases.

The conventional subtype can be further divided into three histological grades, grade I- grade III. Grading is an important factor in accessing the malignancy of the tumor (Evans et al. 1977), and tumor grading is also essential to the decision of treatment strategies (Riedel et al. 2009). Grade I chondrosarcoma is considered a low-grade tumor, and it accounts for approximately 60% of all chondrosarcomas (Unni 2001; Welkerling et al. 2003). Grade II and grade III tumors are high-grade lesions, and they account for approximately 30% and 10% of chondrosarcomas, respectively (Riedel et al. 2009). The rate of local tumor recurrence and the rate of distant metastasis increase with increasing tumor grade (Evans et al. 1977; Lee et al. 1999). Conversely, the overall survival rate decreases with increasing tumor grade (Gitelis et al. 1981).

Although grading is important, it is also highly subjective. Six different grading systems have been proposed for these tumors (Welkerling et al. 2003). Adding to the complexity of the diagnosis is the fact that the subsequent behavior of the tumor does not always correlate with the histologic classification (Dahlin and Henderson 1956; Evans et al. 1977), and patients diagnosed with the same tumor grade may have different clinical outcomes (Soderstrom et al. 2002). To address the limitations of the current grading systems, several studies have been designed to biochemically and molecularly classify chondrosarcoma. These studies have provided useful diagnostic information, and they have provided insight into the molecular basis of tumor progression.

#### Genetic analysis of chondrosarcoma

Approximately 55% of all conventional chondrosarcomas display an abnormal karyotype, which may include numerical and/or complex structural alterations (Mandahl et al. 2002; Tallini et al. 2002). Chondrosarcomas display considerable karyotypic heterogeneity, and no consistent chromosomal abnormalities are associated with a majority of conventional tumors (Sandberg and Bridge 2003). More recent comparative genomic hybridization studies have detected several low-level chromosomal abnormalities, but these abnormalities were also not detected in the majority of tumors (Hallor et al. 2009). Despite the lack of common chromosomal abnormalities, determining the degree of aneuploidy may be useful for chondrosarcoma diagnosis (Adler et al. 1995). Flow cytometric DNA analysis of chondrosarcomas has demonstrated that aneuploidy was less common in low-grade tumors than in high-grade tumors (Lee et al. 1999). Additionally, the analysis of chondrosarcoma DNA content may be useful for predicting outcome after surgical resection (Mankin et al. 2002).

#### Gene expression in chondrosarcoma

Several studies have examined the expression of genes, including tumor suppressors and oncogenes, which may be relevant to chondrosarcoma tumorigenesis.

One study identified altered patterns of expression of p53 primarily in high-grade tumors (Terek et al. 1998). Several reports have described alterations in oncogenes in chondrosarcomas (Barrios et al. 1994; Naka et al. 1997; Rong et al. 1993; Sakamoto et al. 2001; Weisstein et al. 2001). Growth factor expression has also been reported in several chondrosarcomas (McGough et al. 2002; Shakunaga et al. 2000).

Additional analysis has focused on the expression of genes that modify or contribute to the extracellular matrix of chondrosarcoma. Modification of the extracellular matrix is important for tumorigenesis and may contribute to the bone destruction that is observed in chondrosarcoma (Masciocchi et al. 1998; Mignatti and Rifkin 1993). Expression of matrix metalloproteases and cysteine proteinases have been detected in chondrosarcoma, and the expression of these proteases is thought to lead to the degradation of the extracellular matrix of the tumor cells and of the surrounding bone (Soderstrom et al. 2001a; Soderstrom et al. 2001b).

Chondrosarcomas also express several other genes that contribute to extracellular matrix. The expression of several types of collagen has been documented, and the expression of specific collagens is associated with longer survival (Aigner et al. 2002). The expression of certain collagens suggest a more “mature” phenotype (similar to that of normal cartilage), whereas decreased expression of these collagens represents a more “de-differentiated” phenotype that is associated with tumor cell proliferation and a poorer prognosis (Aigner 2002; Aigner et al. 2002).

Although these studies have provided insight into certain gene expression changes in chondrosarcoma, little is known about the global gene expression changes that occur during chondrosarcoma tumorigenesis. Global gene expression studies will provide insight into the pathways that promote chondrosarcoma tumor development and progression and they may lead to the identification of potential therapeutic targets.

## Epigenetic analysis of chondrosarcoma

Relatively little is known about the epigenetic changes that occur during conventional chondrosarcoma tumorigenesis. Aberrant DNA hypermethylation was detected in genes involved with the biosynthesis of heparan sulfate, and the aberrant methylation of these genes was linked to silencing of gene expression in chondrosarcoma (Bui et al. 2009). Other studies have examined individual promoter regions, but they have failed to find evidence for hypermethylated-related gene silencing (Kalinski et al. 2009; Tsuchiya et al. 2005; van Beerendonk et al. 2004). To date, there has been no report on global levels of methylation in chondrosarcoma, but based on observations in other tumors, the chondrosarcoma genome is anticipated to be hypomethylated with respect to that of normal tissue (Hoffmann and Schulz 2005).

## Summary

Research has provided insight into the genetic, gene expression, and epigenetic alterations that occur in chondrosarcoma. Several genes and pathways have been implicated in tumor progression, but rates of local recurrence, metastasis, and death have not changed in over 20 years (Lee et al. 1999). Since most chondrosarcoma studies focus on changes in a small number of genes, global changes may have been overlooked. The fact that chondrosarcoma is a relatively rare tumor -1 in 50,000 people- (Eefting et al. 2009), has limited the sample size of experiments, and has subsequently made the results difficult to interpret. To address the limitations of previous chondrosarcoma studies, a rat model has been developed to study chondrosarcoma tumorigenesis (Grimaud et al. 2002; Kenan and Steiner 1991)

## Chondrosarcoma tumor model: Swarm rat chondrosarcoma

To attain a greater understanding of tumor growth and progression, a model for human chondrosarcoma has been developed in rat. The rat model, known as the Swarm Rat Chondrosarcoma (SRC) (Choi et al. 1971), provides the opportunity to study tumor

growth and progression, the impact of the microenvironment, and it also provides a system to test therapeutic strategies.

The SRC is derived from a tumor that arose spontaneously in a Sprague-Dawley rat (Maibenco et al. 1967). The tumor has been maintained over several years by serial subcutaneous transplantations (Morcuende et al. 2002). The tumor originally contained both bone and cartilage elements, but the bone elements disappeared after successive transplantations (Breitkreutz et al. 1979). The histology and cytogenetics of the SRC are documented, and preliminary gene expression studies have been performed on SRC tumors (Breitkreutz et al. 1979; Morcuende et al. 2002; Stevens et al. 2005). The SRC has been the subject of numerous biochemical studies examining the production and function of various extracellular matrix molecules (Kimura et al. 1979; Mason et al. 1989; Stevens and Hascall 1981). In addition, the SRC has also been used to study the function of specific genes in tumor progression (Di Cesare et al. 1998; Fang et al. 2000; Fang et al. 2001).

#### Transplantation site influences SRC phenotype

Previous experiments have involved subcutaneous transplantation of SRC tumors into a rat. Studies on the subcutaneously grown SRC have provided valuable insight into chondrosarcoma, but chondrosarcomas do not originate from subcutaneous tumors in humans. To address this issue, since chondrosarcomas arise in cartilage tissue, Kennan and Steiner (Kenan and Steiner 1991) transplanted the SRC into the medullary cavity of the bone. Transplantation of the SRC tumor into the tibia resulted in the formation of tumors with growth patterns similar to that of human chondrosarcoma (Kenan and Steiner 1991). Specifically, SRC tumors were able to invade the surrounding bone, which is a characteristic important for the diagnosis of chondrosarcoma (Sanerkin 1980). Transplantation of the SRC into the tibia also resulted in the formation of lung metastasis

(Kenan and Steiner 1991). Lung metastasis has not been reported following subcutaneous transplantation of the SRC tumor.

Additional studies of the SRC model have revealed that transplantation of the SRC tumor into the tibia leads to the formation of a higher-grade tumor than of that grown outside of the bone (Grimaud et al. 2002). The tibia SRC tumors induced extensive bone remodeling, and it was hypothesized that the interaction between the bone environment and the SRC cells was responsible for the higher grade of the tibia SRC tumor (Grimaud et al. 2002).

Overall, the studies with the transplantable SRC tumor indicate that the SRC is an appropriate model to study chondrosarcoma. These studies have also revealed that the bone environment can influence tumor malignancy (Grimaud et al. 2002). This is in agreement with findings in human chondrosarcoma, which suggest that tumor location may impact malignancy (Lee et al. 1999). Although the rat model has been characterized histologically, the molecular changes that underlie these histologic changes are not defined. Epigenetic and gene expression analyses of the SRC tumor model will provide insight into the role of the tumor microenvironment in the development and progression of chondrosarcoma.

#### The SRC cell line

The aforementioned studies have been carried out on SRC tumors *in vivo*, but a stable SRC cell line has also been established (King and Kimura 2003). The SRC cell line is useful for functional chondrosarcoma studies because it can be manipulated *in vitro*. Following *in vitro* manipulation, the cell line can be further studied *in vitro* or it can be used to initiate *in vivo* tumors (Stevens et al. 2005). Taken together, the SRC tumor model and the SRC cell line provide a useful system to identify genes and pathways that may be involved in tumorigenesis and metastasis of chondrosarcoma.

## CHAPTER II MICROENVIRONMENT ALTERS EPIGENETIC AND GENE EXPRESSION PROFILES IN SWARM RAT CHONDROSARCOMA TUMORS

### Introduction

Chondrosarcoma is the second most common primary bone malignancy (Ozaki et al. 1996) accounting for 25% of primary bone sarcomas (Sandberg and Bridge 2003). High grade lesions may be treated with chemotherapy/radiation but chondrosarcomas are usually not responsive to treatment (Gitelis et al. 1981; Mitchell et al. 2000) and as a result the 5-year survival rate of histologic grade III chondrosarcoma is only 29% (Aigner 2002).

To obtain a greater understanding of chondrosarcoma tumorigenesis, a rat model of human chondrosarcoma has been developed (Breitkreutz et al. 1979; Grimaud et al. 2002; Kenan and Steiner 1991). The model, known as the Swarm rat chondrosarcoma (SRC), histologically resembles the human tumor, indicating that the SRC is a suitable model to study chondrosarcoma (Grimaud et al. 2002; Kenan and Steiner 1991). Experiments with the SRC tumors have demonstrated that transplantation site can effect the malignancy of the tumor, and more specifically, transplantation of the SRC tumor into the tibia results in the formation of a higher grade tumor compared to those arising from extraosseous transplantation (Grimaud et al. 2002). Since tumors were initiated from the primary tumor in these transplantation studies, the increase in malignancy observed with the SRC tibia tumor is likely to result from the interaction between the tumor and its microenvironment.

Although the SRC tumors have undergone extensive histological characterization, no studies have examined the effect that the transplantation site has on epigenetic and gene expression profiles of the SRC tumors.

In our study, tumors were transplanted subcutaneously, or into the tibia of Sprague-Dawley rats. Subcutaneous tumor transplantation led to the formation of

significantly larger tumors than those tumors transplanted into the tibia. However, similar to previous SRC experiments (Grimaud et al. 2002), transplantation of the SRC tumor into the tibia resulted in the formation of more aggressive tumors that were capable of invading the surrounding bone. SRC tumors were also detected in the lungs of rats that had SRC tumor transplanted into the tibia, but no SRC tumors were detected in the lungs of rats in which tumor cells were injected subcutaneously.

Epigenetic analysis was performed on the tumors to determine how the transplantation environment effected DNA methylation. The analysis revealed that the tumor transplantation site could significantly affect DNA methylation levels in the SRC tumors.

#### Gene expression profiles of the SRC tumors

To complement the epigenetic analysis, SAGE (Serial Analysis of Gene Expression) (Velculescu et al. 1995) was used to identify the gene expression changes that accompanied the changes in phenotype of the SRC tumors at the different transplantation sites. This global gene expression analysis revealed that the SRC tumors have gene expression profiles that are unique to each transplantation site.

#### SAGE

SAGE is a technique that allows for the quantitative analysis of a large number of transcripts without prior knowledge of the genes that are expressed in any given sample (Velculescu et al. 1995) (Figure 1). SAGE has previously been used to analyze the gene expression of several cancers (Iacobuzio-Donahue et al. 2002; Lee et al. 2003; Zhang et al. 1997), and it has also aided in the identification of new cancer markers (Argani et al. 2001; Porter et al. 2003; Walter-Yohrling et al. 2003). In the SAGE technique, cDNA is reverse transcribed from mRNA from a given cell line or tissue. A short 14 bp sequence

tag is isolated from each cDNA by series of enzymatic reactions. The sequence tags are collected, ligated together, sequenced, counted, and finally the tags are matched to EST's or mRNAs. The collection and quantitation of individual tags, that represent a specific transcript, allows for the generation of a gene expression profile from any given sample. The final SAGE data output is a list of SAGE tags along with the total number of counts for each tag.

There has not been extensive studies examining the global gene expression of chondrosarcoma, and there is not sufficient knowledge of the types of genes expressed in this tumor. Since SAGE can provide quantitative analysis of gene expression without preexisting knowledge of the genes that are expressed in the SRC, it has an advantage over other expression analysis techniques.

#### Functional analysis of differentially expressed genes

Analysis of the differentially expressed genes provided insight into the pathways that are altered between the SRC tumors, and subsequent functional analysis provided insight into the role that specific genes, thymosin- $\beta$ 4, c-fos and connective tissue growth factor (CTGF), play in chondrosarcoma tumorigenesis. Overall, our study highlights the influence of the microenvironment on epigenetic and gene expression profiles of SRC tumors. Such profiles provide an insight into the biological pathways that may be affected by the microenvironment, while underscoring the complex nature of SRC tumorigenesis.

### Materials and methods

#### Tumor induction and tissue harvesting

The tumor line SRC-JWS tumor line (Jeff Stevens, The University of Iowa) was used for all transplantation studies. We demonstrated by microscopy and immunohistochemistry that tumors derived from transplantation of the SRC-JWS tumor

line are similar to human conventional chondrosarcoma. Subcutaneous tumors were induced as previously described (Morcuende et al. 2002; Stevens et al. 2005). Subcutaneous tumors were induced as previously described. Briefly, SRC-JWS tumor cells were isolated from a subcutaneous SRC tumor, and  $5 \times 10^6$  tumor cells were injected subcutaneously into the lower lumbar region of 4-week-old male Sprague-Dawley rats. For the tibia transplantations,  $5 \times 10^6$  SRC-JWS tumor cells were injected into the proximal tibia as previously described (Kenan and Steiner 1991). Injection of SRC-JWS tumor cells into the tibia also resulted in the formation of SRC tumors in the lungs. Since this was observed even in the animals that had their legs amputated within minutes of transplantation, the observed SRC lung tumors were considered to result from colonization of SRC tumor cells into the lungs, as opposed to representing true lung metastases. The animals were euthanized 35 days post tumor induction, and the tumor tissues were frozen in liquid nitrogen immediately after excision and stored at  $-80^\circ\text{C}$ .

Normal rat cartilage was obtained from femoral head cartilage of 37-40 day old male Sprague-Dawley rats as previously described (Morcuende et al. 2002).

#### Total RNA Isolation

Total RNA was obtained from frozen tissues using TRIZOL reagent (Life Technologies, Inc.) Total RNA was treated with DNase (Promega #M6101), and subsequently treated with Proteinase K (Promega # 9PIV302). Total RNA was further purified using RNeasy kit (Qiagen) and then used for subsequent reactions.

#### Sodium bisulfite-treatment of DNA

Genomic DNA was obtained by digestion with proteinase K (Quiagen) followed by phenol/chloroform extraction, and was subjected to sodium bisulfite treatment to modify unmethylated cytosine to uracil using the 'CpGenome<sup>TM</sup> DNA Modification Kit' (Chemicon International, CA).

### Pyrosequencing Primer design

The rat genome sequence (rn4/ version 3.4, Nov. 2004) and the annotation for repetitive elements were obtained from the UCSC Genome Database. Satellite 1 sequences were extracted and subjected to *in silico* bisulfite conversion based on their genomic coordinates in the UCSC database. Full-length Satellite 1 sequences were identified and used for alignment to generate a Satellite 1 nucleotide base matrix. A region within Satellite 1 sequence with dense CpG dinucleotides was selected for PCR primer design. An electronic PCR was performed with the primers designed for rat Satellite 1 sequences. A minimum of 137 distinct Satellite I elements were predicted to be targeted in PCR reactions with the primer set designed. Using a single sequencing primer, a total of 3 CpG dinucleotides were sequenced for each Satellite 1 element targeted. The global methylation data generated was derived from a minimum of 411 CpG dinucleotides in Satellite elements.

### SAGE library construction and data analysis

Poly (A)+ RNA was isolated from total RNA using mRNA DIRECT Kit (Dynal) according to manufacturers instructions. The poly(A)+ RNA and a biotinylated oligo d(T) primer were used for cDNA synthesis according to a previously described method(Adams et al. 1993). SAGE was carried out as previously described (Velculescu et al. 1995).

Approximately 100,000 tags were derived from each SAGE library. The initial sequencing files from each SAGE library were processed with SAGE2000 (Johns Hopkins University). For all analyses, each SAGE library was normalized to 100,000 tags. SAGE libraries were annotated using SAGEmap (<http://www.ncbi.nlm.nih.gov/projects/SAGE/>). Mitochondrial tags were identified using previously described annotation(Anisimov 2005). Genespring was used to perform

hierarchical gene tree clustering (Pearson correlation; centroid linkage), and to graphically represent the SAGE data. See Appendix A for complete SAGE data.

All SAGE data is (Gene Expression Omnibus) GEO compliant. The raw SAGE data has been submitted to the GEO database. The accession number for the Swarm rat chondrosarcoma SAGE data is GSE1517.

#### Real-Time Quantitative PCR

Total RNA was isolated using Trizol; RNA was treated with TURBO RNase-free DNase (Ambion Cat# AM1907). Total RNA (1 $\mu$ g) was used to make cDNA with the iScript cDNA Synthesis kit (BioRad). Real time PCR was performed with the iQ SYBR Green Supermix (BioRad), and rat specific primers. Real time PCR primers were designed with Beacon Designer 6.0 (Premier Biosoft International; Palo Alto CA). Thymosin- $\beta$ 4 primers (Forward: CACATCAAAGAATCAGAACTAC; Reverse: TCTCAATTCCACCATCTCC). C-fos primers (Forward: ACCACGACCATGATGTTC). For SYBR green PCR's, 18S-RNA was used as a reference gene (Zhu and Altmann 2005) (Forward: GGGAGGTAGTGACGAAAATAACAAT; Reverse: TTGCCCTCCAATGGATCCT).

To measure the expression of the transgene construct, primers were designed for the IRES (Internal Ribosome Entry Sequence). The IRES sequence is present in all expression vectors used within this report. The primer sequence; MSCV-IRES-F: TCTGTAGCGACCCTTTGC and MSCV-IRES-R: TTCCACAACACTATCCAACACTCAC. For the analysis of transgene expression 18S-RNA was used a reference gene as described above.

The Pfaffl method was used to calculate the normalized gene expression (Pfaffl 2001). For each real time PCR analysis the individual sample being examined was used as the test sample in the Pfaffl method. The calibrator sample, for the Pfaffl method, was an equal mixture of cDNA from rat normal cartilage, SRC tumor, and/or SRC cell line.

All real time qPCR results are displayed as a ratio of the target gene relative to the reference gene, in a specific test sample, compared to the expression of the target gene relative to the reference gene in the calibrator sample.

#### Thymosin- $\beta$ 4 and c-fos overexpression

Two vectors were made for the overexpression experiments: MSCV-Thy $\beta$ 4-I-Puro and MSCV-cfos-I-Puro. The expression of Thy $\beta$ 4 and c-fos was driven by the retroviral LTR, and the expression of the Puromycin resistance gene was controlled by the IRES sequence. For overview of viral production see Figure 2.

The rat thymosin- $\beta$ 4 coding sequence was PCR amplified from a rat normal cartilage cDNA library clone (UI-R-DY1-cns-1-12-0-UI) using the following primers; Forward: CTCTGAGCAGGAATTCTCTCCTTGTTTCGCCAGCTC and Reverse: CTCAGTCAGTCTCGAGTGCCCTGCCTTCTCTGACTG. The resulting thymosin- $\beta$ 4 PCR product was digested with EcoRI and XhoI. The digested PCR product was ligated to an EcoRI-XhoI digested MSCV-I-Puro vector.

The rat c-fos coding sequence was PCR amplified from a Swarm rat chondrosarcoma cDNA library clone (UI-R-DZ0-crj-j-07-0-UI) using the following primers; Forward: TCTACCCCTGGAATTCTCGCCGAGCTTTGCCAAAC and reverse: CTCAGTCAGTCTCGAGTGCCCTGCCTTCTCTGACTG. The resulting c-fos PCR product was digested with EcoRI and XhoI. The digested PCR product was ligated to an EcoRI-XhoI digested MSCV-I-Puro vector.

A murine stem cell virus was prepared by transfecting 293T cells with three plasmids; pMSCV-I-Hyrgo vector (for control cells: pMSCV-I-Hyrgo; for thymosin- $\beta$ 4: MSCV-Thy $\beta$ 4-I-Puro; for c-fos expression MSCV-cFos-I-Puro), pEQ-Pam3(-E) (which encodes retroviral gag and pol) and pSR $\alpha$ -G (which encodes glycoprotein G from Vesicular Stomatitis Virus) (Rose and Gallione 1981). Forty eight hours post-transfection media containing retroviral vector was collected, aliquoted, frozen, and stored at -80°C.

This vector was then used to transduce the Swarm rat chondrosarcoma cell line (SRC-LTC (Long Term Culture) (King and Kimura 2003), [obtained from Jeff W. Stevens, University of Iowa]), in the presence of 5µg/ml polybrene on three successive days allowing the cells to recover in the media generally used overnight. Transduced cells were selected by incubation with puromycin at a concentration of 3µg/ml for 14 days. The overexpression of thymosin-β4 and c-fos was confirmed following puromycin selection.

#### Cell culture conditions

SRC-LTC cells were cultured in DMEM high glucose (4.5g glucose/ml) supplemented with 10% FBS and Penicillin/Streptomycin. Cells were plated at  $2.5 \times 10^4$  cells with 6ml of media in a 25 cm<sup>2</sup> T flask. Cells were grown until they became 80-90% confluent (6days), and at this time the cells were trypsinized and split.

#### Invasion assay

A Membrane Invasion Culture System (MICS) was used to measure the *in vitro* invasiveness of all SRC cell lines as previously described (Hendrix et al. 1987). Briefly, a polycarbonate membrane with 10-um pores was uniformly coated with a defined matrix. Both upper and lower wells of the chamber were filled with RPMI. For CTGF treatment, the RPMI was supplement with 50ng, 100ng, or 250ng/mL of CTGF. Recombinant CTGF obtained from PeproTech Inc.(Rocky Hill, NJ) (C-terminal peptide; product# 120-19). SRC cells were seeded into upper wells at a concentration of  $5 \times 10^5$  cells per well. After a 24-hour incubation in a humidified incubator at 37°C with 5% CO<sub>2</sub>, cells that had invaded through the basement membrane were collected, stained, and counted by light microscopy (Sood et al. 2004).

### Tumor Inductions in nude mice and tissue processing

The SRC cells were grown until they were 80% confluent, the cells were then washed with PBS, and then cells were removed from the plate using TrypLE Express (GIBCO cat#: 12605-010) according to manufactures instructions. Following removal of SRC cells from plates, the cells were washed with PBS, centrifuged, and resuspended in PBS.  $5 \times 10^6$  cells were injected subcutaneously into the lower lumbar region of 4 week old nude mice (Males; Charles River, Strain code: 088). For the control group, the SRC-LTC-MSCV-I-Hyrgo (cells expressing the empty viral vector) were injected into 10 separate mice. For one experimental group, the SRC-LTC-MSCV-Thy $\beta$ 4-I-Puro cells were injected into 10 separate mice. For the other experimental group, the SRC-LTC-MSCV-cFos-I-Puro cells were injected into 10 separate mice.

Following the injection, the animals were monitored twice weekly for 60 days. After 60 days the animals were euthanized by CO<sub>2</sub> gas inhalation followed by cervical dislocation. Immediately following euthanization, tumors and other tissues were frozen in liquid nitrogen or placed in paraformaldehyde for histology.

Nude mice were selected for this study because previous experiments in our lab have demonstrated that the SRC-LTC cell line grows in nude mice without host rejection. Since the SRC-LTC was modified with a retrovirus, we wanted to reduce the chance that the tumor cells would be rejected by the host immune response. Previous experiments in our laboratory have also indicated that the subcutaneous injection of SRC-LTC cells (modified with retrovirus) in to nude mice would lead to the formation of palpable tumors in 4 weeks. Subcutaneous injection of SRC-LTC cell line into rats resulted in slower tumor growth than in nude mice. Palpable tumors were detected at 4 months in rats compared to less than 1 month in nude mice. Additionally, some rats did not have a palpable tumor at 4 moths. To limit experimental time, and to prevent the rejection tumor cells by the host, nude mice were selected for the transplantation experiments with SRC-LTC cells.

## Statistical Analysis

Significant differences in tag count between SAGE tag libraries were determined using a Z-test ( $\alpha=0.05$ ) (Ruijter et al. 2002). When the significance level is set at 0.05, a z-value greater than 1.96 is considered as a statistically significant difference.

DNA methylation level data were analyzed with the analysis of variance (ANOVA) method and mean DNA methylation levels from three groups were compared with the normal rat cartilage group and resulted p-values were adjusted using the Dunnett method. We used statistical software SAS 9.1 and R to conduct analysis and generate figures. The statistically significant level is 0.05 for all comparisons.

## Results

### Tumor transplantation site affects tumor phenotype

Tumors were initiated by transplanting SRC tumor cells subcutaneously or into the tibia of Sprague-Dawley rats. The tumors exhibited different growth characteristics depending on the tumor transplantation site. Approximately 3 weeks following subcutaneous transplantation tumors were isolated and determined to have an average weight of 35.05g (Table 1). However, 3 weeks following tumor transplantation into the tibia the tumors weighed an average of 75.22mg (Table 1). As reported previously (Grimaud et al. 2002), transplantation of the SRC tumor into the tibia resulted in tumor invasion into the surrounding bone (Figure 3A). Tumor transplantation into the tibia also led to the formation of SRC tumors in the lungs of rats (50% of animals; Figure 3B). No SRC lung tumors were detected in the lungs of rats that had the SRC tumor transplanted subcutaneously.

Although 50% of the animals with the tibia SRC tumor also developed lung SRC tumors, the latter most likely result from colonization of tumor cells in the lungs rather than metastasis. As pointed out before, animals that had their leg amputated immediately following tumor transplantation did exhibit tumors in the lungs. Hence, we do not refer

to the SRC lung tumor as a metastatic tumor. Since chondrosarcoma does metastasize to the lungs in humans, we feel that including the SRC lung tumors in subsequent analyses might provide relevant information relating to chondrosarcoma tumorigenesis.

#### Epigenetic analysis of SRC tumors

Epigenetic analyses were carried out to determine if there was a difference in the DNA methylation profiles of the tumors that were initiated at different transplantation sites. Methylation levels of cytosines in repetitive elements has been used as a surrogate marker for genome-wide methylation (Yang et al. 2004), and therefore the Satellite 1 repetitive element was selected as a surrogate methylation marker. Rat specific pyrosequencing assays were designed to examine the methylation of Satellite 1 sequences throughout the genome. Pyrosequencing was performed on DNA isolated from control tissue, rat normal (articular) cartilage (RNC), and on SRC tumor tissue from the different transplantation sites.

Pyrosequencing of rat satellite 1 revealed methylation differences between the SRC tumors and rat normal cartilage, as well as among the SRC tumors at different transplantation sites. Specifically, the SRC tumors have a lower level of methylation than rat normal cartilage (Figure 4). For the SRC tumors, the subcutaneous tumor and tibia tumor have lower Satellite 1 methylation levels than the lung tumor (Figure 4).

These results demonstrate that the Satellite 1 DNA is hypomethylated in SRC tumors compared to control tissue, and the results also indicate that transplantation site can influence DNA methylation levels in SRC tumors. Since the changes in methylation levels were detected in satellite 1 DNA sequences throughout the genome, the changes in methylation may be indicative of other changes in methylation that are a result of tumor growth at different transplantation sites.

### SAGE library description

Based on the aforementioned differences between the SRC tumors, we hypothesized that tumors would also exhibit significant differences in gene expression. To test this hypothesis, SAGE was used to generate gene expression profiles for the SRC tumors. SAGE profiles were generated for rat normal cartilage, the subcutaneous SRC tumor, the tibia SRC tumor, and the SRC lung tumor. Over 400,000 SAGE tags were sequenced for this analysis, and the total number of SAGE tags sequenced for each library and the number of unique tags in each library are shown in Table 2.

### Gene expression differences between normal cartilage and the SRC tumors

The SRC tumors have significantly different gene expression profiles compared rat normal cartilage (control tissue), and these gene expression changes distinguish tumors from RNC (Figure 5). Analysis of the differentially expressed genes revealed changes in several pathways that may be important to chondrosarcoma tumorigenesis. (Table 3). The most significantly altered pathway, “Skeletal and muscular system development and function”, highlighted differences in gene expression that could directly impact the extracellular matrix of both tumor cells and surrounding host cells. Specifically, gene expression alterations were detected for structural extracellular matrix genes (Figure 6A) and for extracellular matrix modifying proteases (Figure 6B).

Most structural extracellular matrix genes were expressed at lower levels in the SRC tumors than in normal cartilage, but closer analysis revealed changes in gene expression that were unique to the SRC tumor at each transplantation site (Figure 6A). The expression of specific proteases varied among tumors and the expression changes of the proteases may represent changes that are unique to the SRC tumors at specific transplantation sites (Figure 6B).

Changes to the extracellular matrix have prognostic value in chondrosarcoma. Decreased expression of specific extracellular matrix molecules has been associated with

high grade human chondrosarcomas (Aigner et al. 2002). Increased expression of specific proteases has also been reported in human chondrosarcoma (Soderstrom et al. 2001a; Soderstrom et al. 2001b).

These results indicate that gene expression alterations in the SRC tumors are similar to changes observed in human chondrosarcoma, and they provide additional support to previous work demonstrating that the SRC tumor model resembles human chondrosarcoma (Kenan and Steiner 1991).

#### Transplantation site influences gene expression

The SRC tumors have gene expression profiles that are unique to their transplantation site (Figure 8). Although each SRC tumor originated from the same source tumor, significant gene expression differences were detected among the SRC tumors. Further characterization of these differences revealed changes in the expression of genes involved in regulating “Cellular Assembly and Organization” (Table 3). Several genes related to cell motility were upregulated in both the tibia and lung SRC tumors (Figure 7A). The altered expression of cell motility related genes suggest that both the tibia and the lung microenvironments may promote changes in the actin cytoskeleton, which in turn may have a direct impact on the invasiveness of SRC cells

#### Endogenous thymosin- $\beta$ 4 expression in the SRC tumors

It is noteworthy that one of the genes identified in cell motility pathway, thymosin- $\beta$ 4, is significantly upregulated in the tibia and lung SRC tumors (Figure 9A). Thymosin- $\beta$ 4 is thought to play a role in the cytoskeletal organization of chondrocytes (Blain et al. 2002), and overexpression of thymosin- $\beta$ 4 may influence tumorigenicity and metastasis (Kobayashi et al. 2002).

### Endogenous c-fos expression in the SRC tumors

The second most significantly altered pathway was “Cellular Growth and Proliferation”(Table 3). More detailed examination of this pathway identified several differentially expressed genes that are components of the AP-1 transcription factor complex (Figure 7B). AP-1 is a potent transcription factor that has multiple functions in tumor cells (Eferl and Wagner 2003). One particular component of AP-1, c-fos, was differentially expressed in both the tibia and lung SRC tumors (Figure 9B). Expression of c-fos has been investigated in human chondrosarcoma (Weisstein et al. 2001). Overexpression of c-fos leads to the development of chondrogenic tumors (Wang et al. 1991), and c-fos activity has been associated with increased invasiveness of chondrosarcoma cells (Tuckermann et al. 2001).

### Growth factor expression in the SRC tumors

These results demonstrate that gene expression varies with transplantation site. Gene expression changes in the SRC could promote additional expression changes in the SRC cells and they could also promote expression changes in the surrounding host cells. For example, changes in growth factor expression were detected in the SRC tumors (Figure 7C). These growth factors could be secreted into extracellular matrix where they have the potential to interact with tumor and/or host cells. Taken together, these results indicate that the tumor transplantation site has a significant impact on the gene expression profile of the SRC cells. These analyses provide insight into the interaction between the SRC cells and the transplantation site, as well as to the specific pathways that may contribute to SRC tumorigenesis.

## Functional analysis of differentially expressed genes

### Overexpression of thymosin- $\beta$ 4 and c-fos

Based both on their differential expression (Figure 7) and their potential role in tumorigenesis, thymosin- $\beta$ 4 and c-fos were selected for additional analyses. Thymosin- $\beta$ 4 and c-fos were independently overexpressed in a SRC cell line and the cell lines were used to induce subcutaneous SRC tumors (Figure 10A). Control tumors were induced with SRC cells expressing the empty viral vector, while the tumors in the experimental groups were induced by injection of SRC cells overexpressing either c-fos or Thymosin- $\beta$ 4. Histologically, the tumors were classified as grade II chondrosarcomas (Figure 10B), but other phenotypic differences were observed between the tumors.

Overexpression of thymosin- $\beta$ 4 resulted in the formation of the largest SRC tumors (Table 4). However, the size of the thymosin- $\beta$ 4 overexpressing tumors varied among animals and the average tumor weight was not statistically different from that of tumors derived from control cells (Figure 11). Although thymosin- $\beta$ 4 tumors did not exhibit a statistically significant difference in size relative to the control tumors, it should be noted that one of the mice (with the thymosin- $\beta$ 4 tumor) died before the end of the *in vivo* experiment (n=10; 1 mouse died; see Table 4). Histologic analysis of this animal revealed multiple lung chondrosarcoma micrometastases.

C-fos overexpression resulted in the formation of tumors that were significantly smaller than control tumors (Figure 11 and Table 4). Micrometastasis was not detected in any animals with c-fos overexpressing tumors.

### CTGF and the SRC cells

Growth factor expression varied with the tumor transplantation site (Figure 7C), but the functional consequences of these changes are unknown. One growth factor, CTGF (Connective Tissue Growth Factor), was selected for further analysis because of its differential expression and previously reported altered expression in several cancers

(including chondrosarcoma) (Chang et al. 2004; Kondo et al. 2006; Pan et al. 2002; Shakunaga et al. 2000). To test the influence of CTGF, the invasiveness of the SRC cells was examined following incubation with varying concentrations of CTGF. SRC cells were incubated with varying concentrations of CTGF. The lower doses of CTGF (50 and 100ng/mL) did not significantly alter the invasiveness compared to that of control cells, but a higher concentration of CTGF resulted in a significant decrease (30%) in SRC invasiveness (Figure 12).

### Discussion

Tumor microenvironment is an important factor that can influence the malignancy of SRC tumors (Grimaud et al. 2002). Previous studies have characterized the histological changes that accompany SRC tumor growth at different transplantation sites (Grimaud et al. 2002). However, little is known about the gene expression changes that underlie the histological changes. To address this issue, we examined the epigenetic and gene expression changes following SRC growth at different tumor transplantation sites. Epigenetic and gene expression changes were detected between the SRC and normal tissue, and additional analysis revealed gene expression changes among SRC tumors grown at different transplantation sites. Closer examination of differentially expressed genes and subsequent functional analysis provided insight into the involvement that specific genes may have in chondrosarcoma tumorigenesis.

Subcutaneous SRC tumor transplantation resulted in the formation of tumors that were significantly larger than SRC tumors induced into the tibia. Although the tibia tumor was smaller, the tibia tumor displayed increased tumor infiltration and bone destruction over time. These findings are in agreement with previous findings indicating that tibia transplantation of the SRC results in tumor infiltration (Kenan and Steiner 1991) and changes in the malignancy of the SRC cells (Grimaud et al. 2002).

Epigenetic analysis of the SRC tumors revealed that the SRC tumors are hypomethylated compared to normal rat cartilage. The epigenetic analysis also demonstrated that the tumor transplantation site can influence the DNA methylation levels of the SRC tumors, and this result supports previous findings that suggest that the microenvironment may modulate epigenetic events in solid tumors (Shahzad et al. 2007). Although the impact of hypomethylation on the SRC cells is not completely known, DNA hypomethylation has been observed in several types of cancer (Hoffmann and Schulz 2005), and previous studies have demonstrated that DNA hypomethylation may have a significant impact on tumorigenesis (Eden et al. 2003; Gaudet et al. 2003).

In addition to differences in DNA methylation, the SRC tumors possessed significantly different gene expression profiles depending on the transplantation site. Furthermore, the SRC tumors also have a significantly different gene expression profile as compared to normal rat cartilage. These include significant decrease in the expression of several extracellular matrix molecules (Figure 6A). Studies with human chondrosarcoma have indicated that the expression of Collagen type II and aggrecan is indicative of a mature neoplasm with low reoccurrence and low chance for metastasis (Aigner 2002). A decrease in the expression of extracellular matrix molecules, as observed in SRC tumors, may represent a change in the nature of the SRC tumors from a mature neoplasm to a more aggressive dedifferentiated neoplasm.

The SRC tumors also expressed several matrix metalloproteases and cathepsins (Figure 6B). The expression of these proteases varied depending on the SRC transplantation site, but since these proteases alter the extracellular matrix, their expression may have a significant impact on tumor progression. Altered expression matrix metalloproteases and cathepsins has previously been reported in human chondrosarcoma (Soderstrom et al. 2001a; Soderstrom et al. 2001b), and their expression may play an important role altering the extracellular matrix and promoting tumor invasion. For example, cathepsin K, is thought to play a role in human chondrosarcoma

progression (Soderstrom et al. 2001b), and cathepsin K is expressed at highest levels in SRC tumors grown in the tibia. Cathepsin K is a protease that has the ability to degrade collagen type I (Bromme et al. 1996), a major component of bone. The expression of cathepsin K may explain the degradation of bone that is observed with the tibia SRC tumors (Figure 3A). The expression of cathepsin K combined with the expression of other proteases may lead to extracellular matrix degradation and subsequent SRC tumor progression.

Further analysis of the SAGE data revealed additional gene expression changes that may also contribute to chondrosarcoma tumorigenesis. Both the tibia SRC tumor and the lung SRC tumor displayed elevated levels of genes regulating the actin cytoskeleton (Figure 7A), and the SRC tumors also displayed elevated levels of genes controlling cellular growth and proliferation (Figure 7B). Overexpression of a cell motility related gene, thymosin- $\beta$ 4, did not produce tumors that were significantly larger than control tumors (Figure 11). However, overexpression of thymosin- $\beta$ 4 resulted in chondrosarcoma lung metastasis and subsequent death in one animal. In human chondrosarcoma, tumor size does not always correlate with tumor malignancy (Lee et al. 1999), and although the thymosin- $\beta$ 4 tumors are not larger than control tumors, they may have a greater malignant potential.

Although the function of thymosin- $\beta$ 4 in the SRC is not completely known, high levels of thymosin- $\beta$ 4 have been detected in human chondrosarcoma (National Cancer Institute: SAGE Genie database). Overexpression of thymosin - $\beta$ 4 has previously been shown to regulate motility and invasiveness in fibrosarcoma (Kobayashi et al. 2002), and reports in melanoma suggest that thymosin- $\beta$ 4 can stimulate metastasis through the activation of cell migration and angiogenesis (Cha et al. 2003). The ability of thymosin- $\beta$ 4 expression to increase tumor cell motility may be related to its function in the regulation of the actin cytoskeleton (Ridley 2000), but thymosin- $\beta$ 4 may have other functions in the SRC cells. Thymosin- $\beta$ 4 can be secreted into the extracellular matrix

(Huang and Wang 2001), and extracellular stimulation with thymosin- $\beta$ 4 may lead to increased AP-1 activity.

C-fos is a component of the AP-1 transcription factor complex, and AP-1 is thought to play multiple roles in tumorigenesis (Eferl and Wagner 2003). C-fos overexpression has previously been shown to lead to the development of chondrogenic tumors (Wang et al. 1991). However, overexpression of c-fos in SRC cells resulted in the formation of tumors that are significantly smaller than those derived from control tumor cells (Figure 11). The inability of c-fos overexpression to promote tumor progression may be explained by the fact that c-fos has different transcriptional activation potential depending on which protein it heterodimerizes with to form the AP-1 transcription factor complex (Hess et al. 2004).

C-fos can interact with several proteins to form variations of the AP-1 transcription factor complex (Eferl and Wagner 2003). Indeed, analysis of the SAGE data from SRC tumors revealed the expression of a subset of c-fos interacting proteins, namely c-jun and v-maf (Figure 7B). C-jun and v-maf proteins can form heterodimers with c-fos to form an AP-1 transcription factor complex. In our study, c-fos was overexpressed, but not other components of the AP-1 transcription factor complex. It is possible that no increase in tumor progression was observed in SRC cells because there was not a concomitant increase in the expression of other proteins that bind to c-fos to make the active AP-1 transcription factor complex. Overexpression of c-fos may lead to the formation of inactive c-fos homodimers that do not possess the transcriptional ability required to promote tumor progression. Inactive c-fos homodimers may interrupt the normal state of AP-1 transcription in the SRC tumors, and this may explain how tumor growth was inhibited in SRC tumors that overexpressed c-fos. In osteosarcoma, co-overexpression of c-fos and c-jun resulted in an increase in tumor formation compared to cells that were overexpressing either c-fos or c-jun (Wang et al. 1995). This osteosarcoma study indicates that the tumorigenic potential of c-fos is dependent upon

the proteins that interact with c-fos to produce active heterodimeric AP-1 transcription factor complexes.

Although c-fos overexpression did not promote an increase in tumor growth, c-fos and AP-1 signaling have been associated with chondrosarcoma development (Papachristou et al. 2005). Another possibility is that c-fos overexpression may promote other aspects of tumor progression. For example, c-fos signaling may influence the invasiveness of human chondrosarcoma cells through the activation of matrix metalloproteases (Hou et al. 2009; Tan et al. 2009). C-fos/AP-1 activity may result from signaling interactions between the SRC tumor cells and the local microenvironment. The signaling mediators and effectors of c-fos/AP-1 interactions may vary depending on the microenvironment of the transplantation site, but they may be the result of signaling from growth factors, cytokines, or other signaling molecules.

Changes in growth factor expression were also detected in the SRC tumors (Figure 7C), and the expression of these growth factors may influence gene expression in the tumors. VEGF, TGFB2, and CTGF are expressed in human chondrosarcoma, and the potential function of these growth factors range from cell motility, to cell growth, to angiogenesis (Furumatsu et al. 2002; Masi et al. 2002; Yosimichi et al. 2001). In our study, incubation with CTGF led to a decrease in the invasiveness of the SRC cells (Figure 12). Although this result may appear counterintuitive to a role for CTGF in tumor progression, CTGF has recently been shown to enhance cell adhesion of a human chondrosarcoma cell line through interaction with fibronectin (also expressed in the SRC cells; Figure 6A) (Hoshijima et al. 2006). CTGF is expressed in normal lung cells (Rishikof et al. 2002; Wu et al. 2009), and an intriguing hypothesis is that CTGF may play a role in the adhesion of tumor cells in the lung. In addition to a role in cellular adhesion, CTGF has previously been shown to influence cell proliferation and angiogenesis (Brigstock 2002; Shimo et al. 1999), but additional experiments are needed to determine if CTGF affects these pathways in the SRC.

The mode of growth factor induction in the SRC tumors is not known, but growth factor induction could be mediated through AP-1 signaling. Binding sites for AP-1 have been identified in the promoter region of CTGF (Xia et al. 2007) and TGF $\beta$ -2 (Noma et al. 1991). AP-1 is capable of activating the IGF-2 promoter (Caricasole and Ward 1993), and the expression of VEGF has previously been shown to be mediated through AP-1 (Cho et al. 2006). The induction of growth factors in the SRC may, in part, be regulated by AP-1. Alternatively, changes in AP-1 expression may also be influenced by growth factor expression (Karin et al. 1997; Lo and Cruz 1995; Piechaczyk and Blanchard 1994).

Taken together, these experiments highlight the importance of the tumor microenvironment in SRC tumorigenesis. Transplantation of a SRC tumor into different microenvironments in the rat resulted in phenotypic changes in the tumor. The changes in the phenotype were accompanied by epigenetic changes as well as gene expression changes. The epigenetic analysis demonstrated that methylation patterns were altered following tumor transplantation, indicating that the transplantation site can affect the DNA methylation of the SRC tumors. The gene expression analysis revealed that the SRC tumors exhibit unique gene expression profiles that are related to their transplantation site. Subsequent functional analysis provided insight into the mechanisms of SRC tumorigenesis, and suggests that thymosin- $\beta$ 4 may play a role in influencing the malignancy of the SRC tumors.

Further research is needed to examine the function of thymosin- $\beta$ 4 in chondrosarcoma, and more research is needed to identify factors that influence thymosin- $\beta$ 4 expression. For example, the promoter region of the human thymosin- $\beta$ 4 gene contains a CpG Island (Yang et al. 2005), which indicates that DNA methylation could play a role in the regulation of thymosin- $\beta$ 4. Additionally, experiments are needed to determine how biologic signaling at the transplantation site affects DNA methylation, and to determine if these changes in DNA methylation have an effect on SRC tumorigenesis.

Table 1. Effect of transplantation site on tumor weight.

Tumor Transplantation site	Average tumor weight	Standard Deviation
Subcutaneous SRC tumor	35.05g	+/- 5.66g
Tibia SRC tumor	75.22mg	+/- 24.83mg
Lung SRC tumor	13.52mg	+/- 5.81mg

Note: The average tumor weight and standard deviation are shown. For the subcutaneous SRC tumor, the weight was calculated from 6 animals. For the tibia SRC tumor, the weight was calculated based on tibia tumors isolated from 14 separate animals. For the lung tumor, the weight represents the average weight of individual metastasis collected from 7 animals. The lung tumors were isolated from animals that had SRC tumor transplanted into the tibia (7 of 14 animals had lung tumors).

Table 2. Summary of SAGE tags generated from each normal cartilage and the SRC tumors.

SAGE Library Summary				
	Femoral Head Cartilage (5 week old rats)	Rat Chondrosarcoma Subcutaneous Tumor	Rat Chondrosarcoma Tibia Tumor	Rat Chondrosarcoma Lung Tumor
Tag Count	120,220	89,798	101,859	108,781
Unique Tags	22,323	20,354	23,577	24,648

Note: The total number of SAGE tags and the number of unique tags are listed for each SAGE library. For data presentation, all SAGE libraries were normalized to 100,000 tags. Full SAGE data is presented in Appendix A.

Table 3. Pathway analysis of differentially expressed genes between RNC and SRC tumors.

Rank	Category	P-value
1	Skeletal and Muscular System Development and Function	5.07E-12
2	Cellular Growth and Proliferation	4.21E-07
3	Cellular Assembly and Organization	1.74E-06
4	Cellular Function and Maintenance	1.74E-06
5	Connective Tissue Development and Function	5.06E-05

Note: The list of genes differentially expressed between RNC and all SRC tumors analyzed with the pathway-mapping program Ingenuity. The top five functional pathways and their corresponding p-values are displayed in table.

Table 4. Summary of subcutaneous tumor weight following transplantation of SRC cells that overexpress thymosin- $\beta$ 4 or c-fos.

Summary of subcutaneous SRC tumor weight					
Control tumors		Thymosin- $\beta$ 4 tumors		c-fos tumors	
Animal Number	Final Tumor Weight (g)	Animal Number	Final Tumor Weight (g)	Animal Number	Final Tumor Weight (g)
1	0.705	1	1.078	1	0.272
2	0.653	2	0.6	2	0.303
3	1	3	0.795	3	0.513
4	0.803	4	1.323	4	0.201
5	1.02	5	1.836	5	0.4
6	0.658	6	0.65	6	0.191
7	1	7	0.454	7	0.441
8	1.112	8	0.759	8	0.442
9	0.359	9	1.015	9	0.363
10	1.074	10	0.04 <sup>1</sup>	10	0.281

Note: Tumors were harvested 33 day following subcutaneous tumor transplantation.

<sup>1</sup>: This animal died 2 weeks into the experiment. Histologic analysis of this animal revealed multiple chondrosarcoma lung metastases. Lung metastases were not found in any tumors from control or c-fos expressing cells.

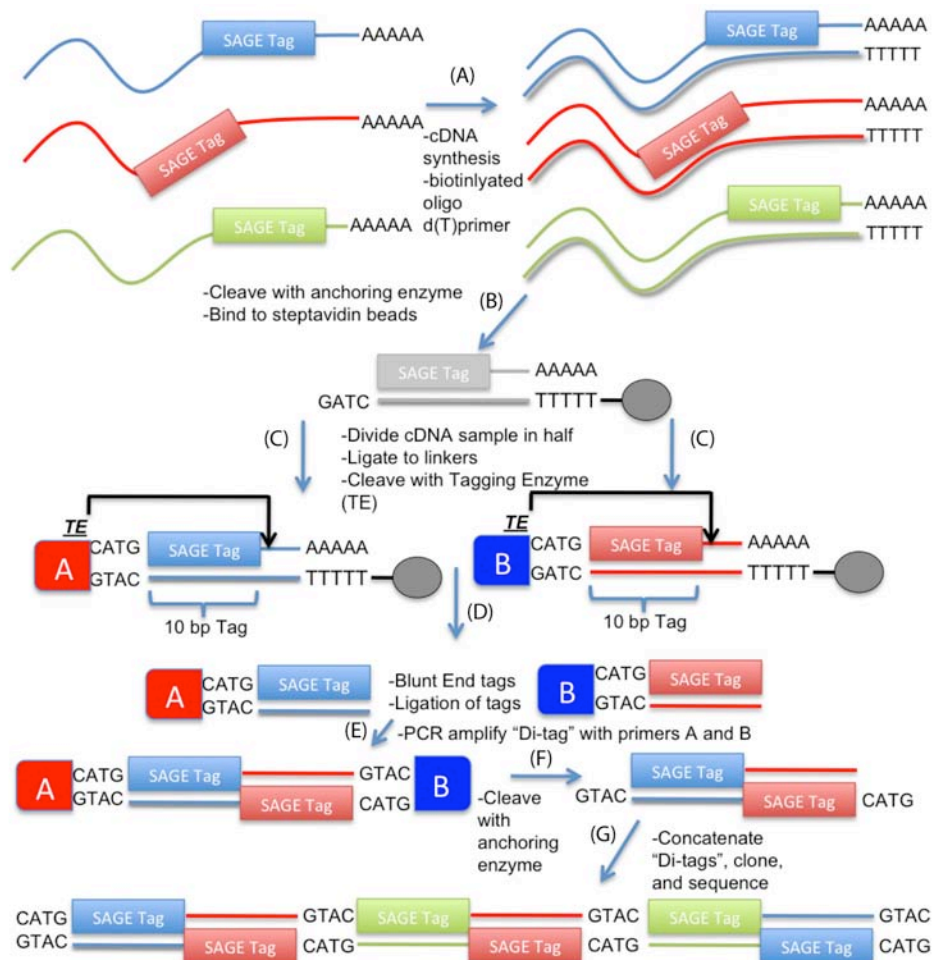


Figure 1. Schematic diagram of a SAGE experiment. SAGE (Serial Analysis of Gene expression) generates an expression profile that is based on the quantification of "tags", which are a short nucleotide sequence that correspond to a mRNA transcript. (A) Polyadenylated RNA is used to construct a biotin-oligo d(T)-primed cDNA library. (B) The cDNA is cleaved with an anchoring enzyme, and the resulting 3' end of the cDNA is isolated with streptavidin beads. (C) The cDNA is then split in half; one half is ligated to linker "A" and the other half is ligated to linker "B". The linkers contain a tagging enzyme (TE) recognition site. Digestion with TE thus releases the "linker-SAGE tag" cDNA fragments of ~20bp (D) The two pools of tags are blunt ended, and then the pools are ligated to each other to form "Di-tags". (E) The ligated "Di-Tags" are then PCR amplified with primer specific to linkers "A" and "B". (F) The PCR amplified "Di-tags" are digested with the anchoring enzyme to remove the linker sequence (freeing the "Di-tag"). (G) Lastly the "Di-tags" are ligated and sequenced. The sequence is then computationally analyzed and the tags are quantified. Figure modified from (Velculescu *et al.*, 1995).

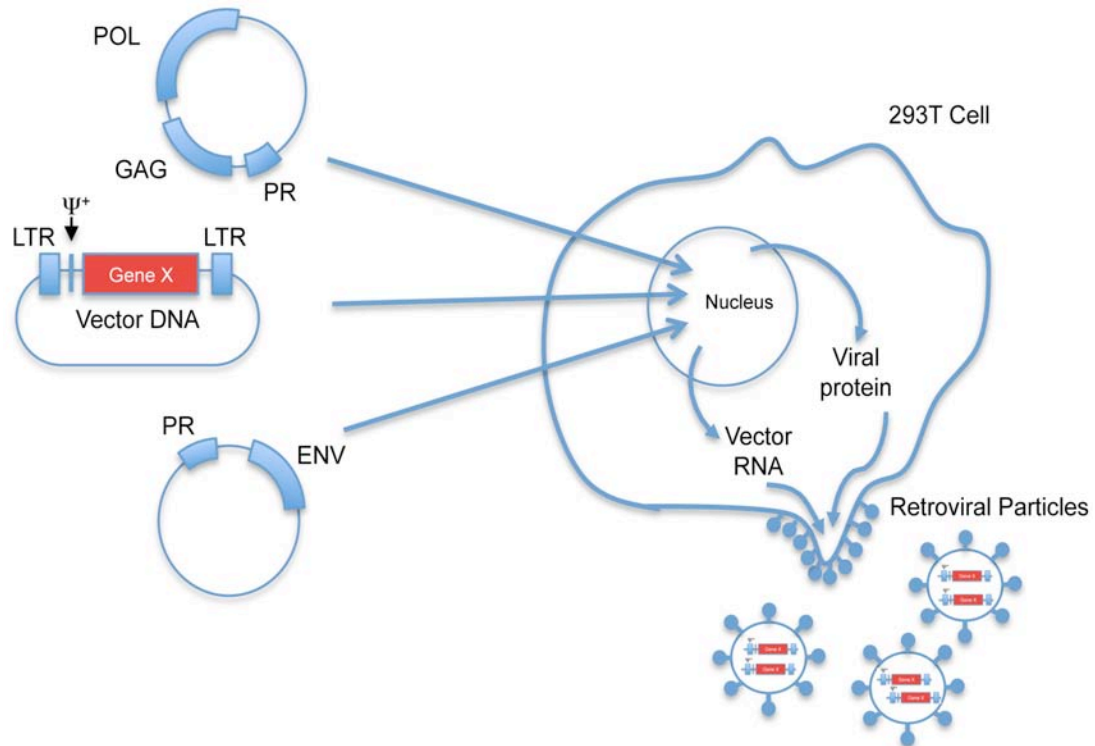


Figure 2. Transient transfection of 293T cells to produce viral particles. The viral vector has been modified so that it cannot, by itself, make proteins required for additional rounds of replication. The viral proteins that are needed for the initial infection can be provided in *trans*. 5' and 3' LTRs contain transcription factor recognition sites. The GAG sequence encodes for proteins that form the shell of the complete retroviral particle. The POL sequence encodes for reverse transcriptase, integrase and ribonuclease H (important for viral integration into host DNA). The ENV sequence encodes for an envelope glycoprotein that extends from the membrane of the viral particle (the ENV protein is the ligand for the receptor on the host cell). The "PR" sequence in the vector DNA contains the promoter sequence that drives the expression of the GAG-POL and ENV. "Ψ<sup>+</sup>" denotes the packaging signal (note that the packaging sequence is only present in the vector containing the gene of interest). The complete description of the viral vectors is located in the Materials and methods.

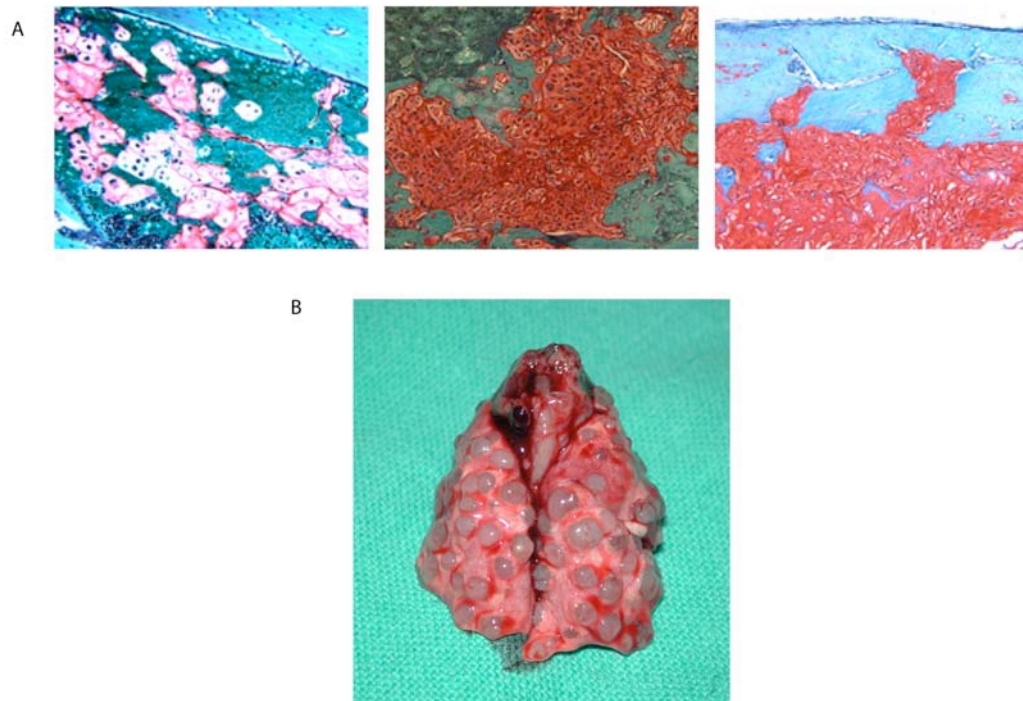


Figure 3. Phenotype of the Swarm Rat chondrosarcoma varies based on tumor transplantation site. (A) Transplantation of the SRC tumor into the tibia of Sprague-Dawley rats. Histologic micrographs at day 0, day 7, and day 34. Successive histologic micrographs revealed increased tumor volume and invasion of the tumor into the bony cortex. Cells stained with safranin O and fast green. (B) SRC tumor detected in the lung of a rat that had the SRC tumor transplanted into the tibia. Note the presence of multiple SRC tumors. Lung tumors were detected in 50% of the animals that had the SRC tumor transplanted into the tibia. The number of metastases in a single animal numbered from 1 to 54 (average=10). The average size of the tumors was 2mm. No lung tumors were detected in the animals with subcutaneous tumor transplants.

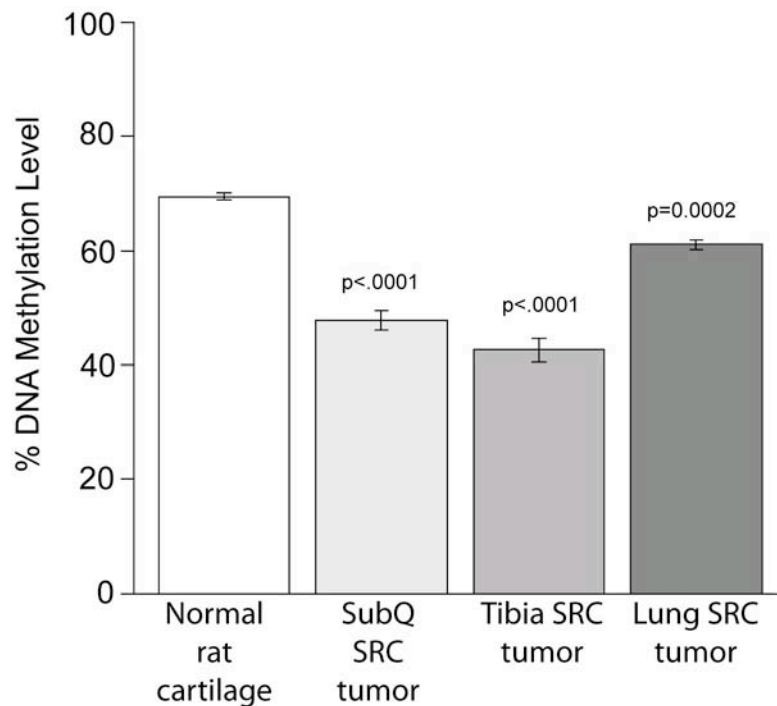


Figure 4. Transplantation microenvironment influences DNA methylation in SRC tumors. Pyrosequencing revealed that Satellite 1 DNA was hypomethylated compared to DNA from rat normal cartilage (control tissue). The satellite 1 DNA in the subcutaneous SRC tumor and the tibia SRC tumor was hypomethylated compared to the DNA in the lung SRC tumor. The graph illustrates the average DNA methylation that was calculated from a pool of tissues from each transplantation site. For each transplantation site, tissue was pooled from at least 10 separate animals. The error bars represent technical replicates of the pooled tissue samples. The p-values represent the significance of the comparison of a specific sample with normal rat cartilage (p-value<0.05 represents a statistically significant difference).

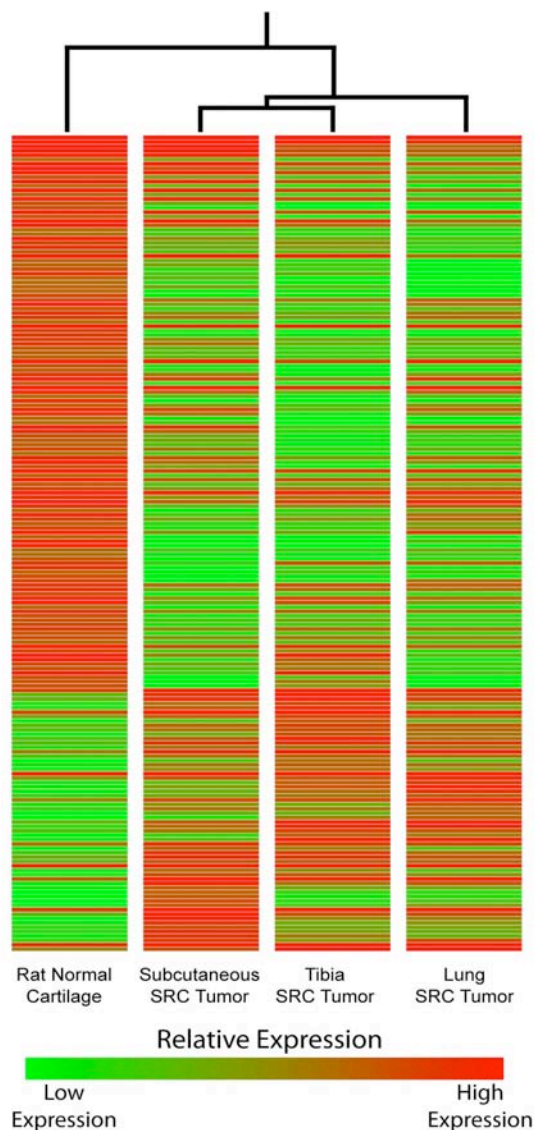


Figure 5. Heat map displaying the differentially expressed genes between RNC and SRC tumor tissues. Rat normal (articular) cartilage has a unique expression profile when compared to the expression profiles of the SRC tumors. The changes in gene expression may represent critical differences between normal cartilage cells and chondrosarcoma, and they may also represent changes important for the development and progression of chondrosarcoma. Heat map displays the differentially expressed genes that were expressed at a level of at least 25 tags in one library. Color bar illustrates relative gene expression levels. Columns represent SAGE libraries and rows represent the expression of individual SAGE tags. For complete gene list and annotation see Appendix B.

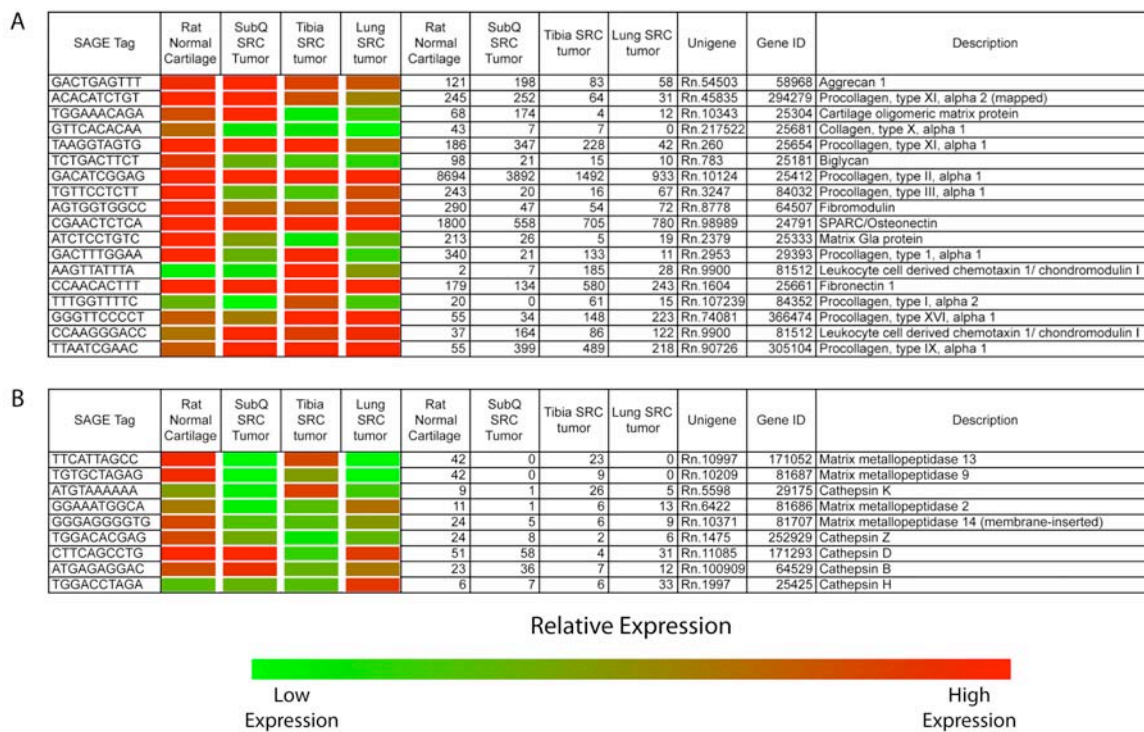


Figure 6. SAGE reveals gene expression differences between the SRC tumors and normal cartilage as well as gene expression differences between SRC tumors. (A) Expression of extracellular matrix genes. (B) Expression of extracellular matrix modifying proteases. Heat map displays relative expression values. Actual expression values are listed to the right of the heat map.

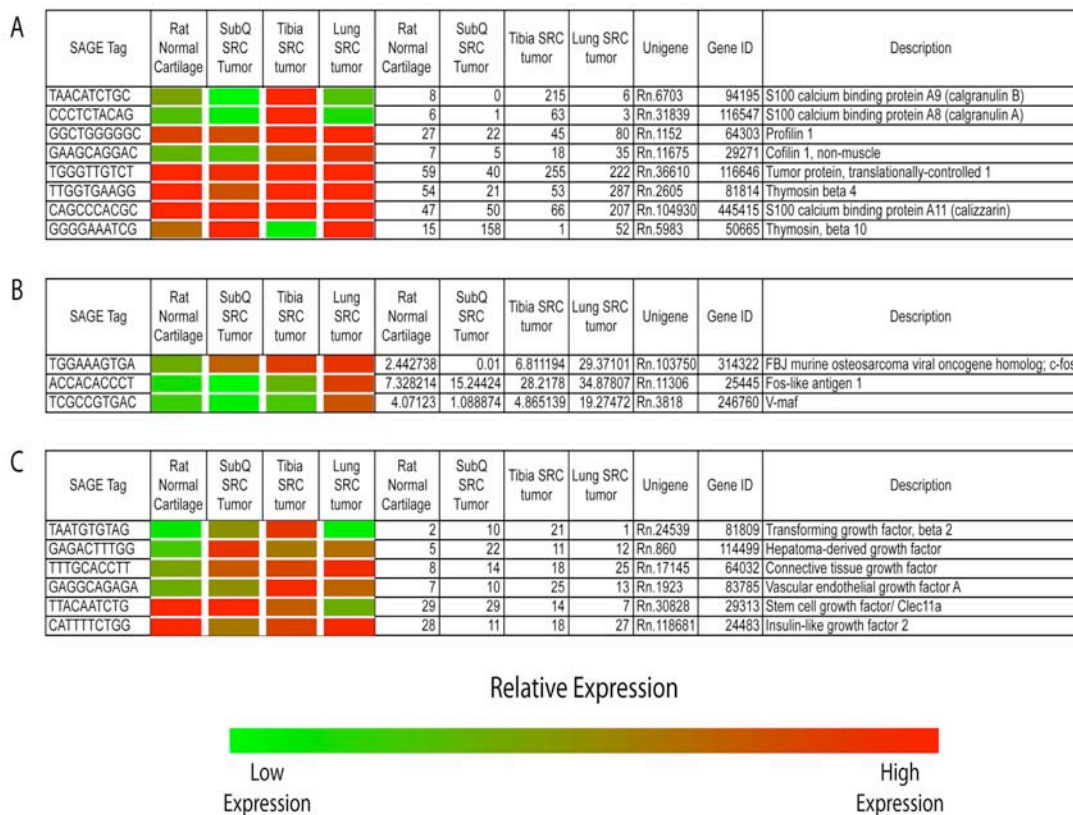


Figure 7. SAGE reveals gene expression differences between the SRC tumors and normal cartilage as well as gene expression differences between SRC tumors. (A) Expression of genes related to cell motility. (B) Expression of components of the AP-1 transcription factor complex. (C) Expression of growth factors. Heat map displays relative expression values. Actual expression values are listed to the right of the heat map.

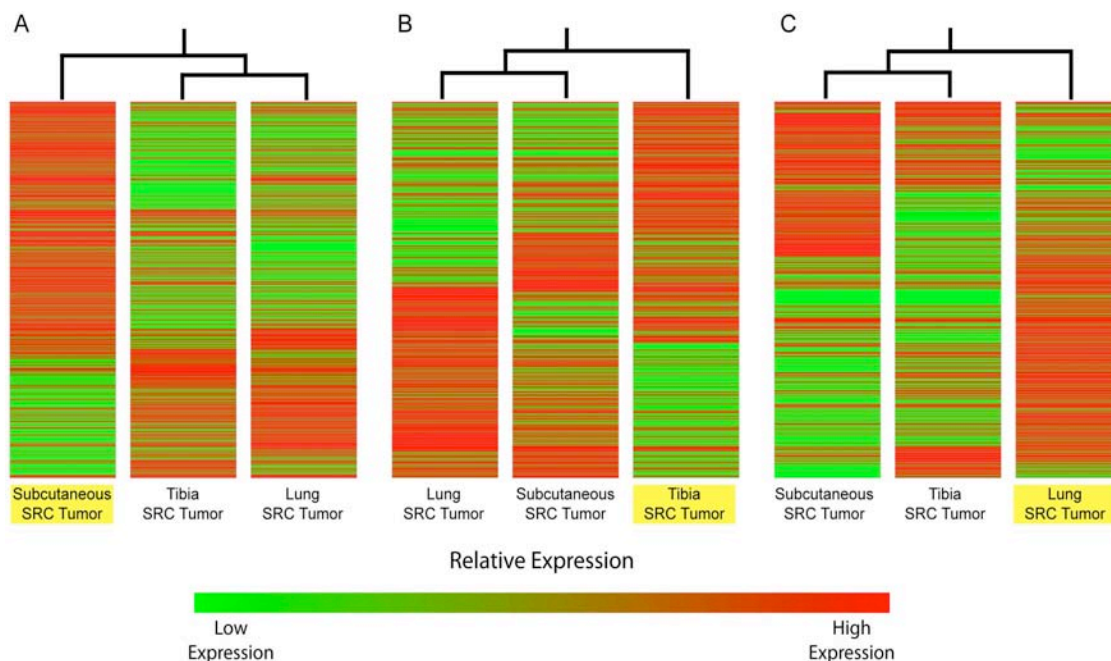


Figure 8. Tumor transplantation site significantly alters the gene expression profiles of the SRC tumors. Since the SRC tumors at different transplant sites originated from the same source tumor, the unique SRC gene expression profiles at each transplant site are likely a result of interactions in the microenvironment between tumor cells and host cells. (A) Differential gene expression between the Subcutaneous SRC tumor (highlighted in yellow) and SRC tumors at the other transplantation sites (200 genes upregulated and 107 genes downregulated in the Subcutaneous SRC tumor). (B) Differential gene expression between the Tibia SRC tumor (highlighted in yellow) and the SRC tumors at the other transplantation sites (106 genes upregulated and 108 genes downregulated in the tibia SRC tumor). (C) Differential gene expression between the Lung SRC tumor (highlighted in yellow) and the SRC tumors at the other transplantation sites (157 genes upregulated and 73 genes downregulated in the lung SRC tumor). Only genes with significantly different gene expression were included in each analysis ( $z > 1.96$ ; see Materials and methods). SAGE tags also needed to have an expression level of at least 25 in one tissue to be included in the analysis. Condition trees illustrate the relationship between the SAGE libraries with respect to the set of differentially expressed genes. Color bar illustrates relative gene expression levels. See Appendix C for complete data set and annotation of the genes presenting within this figure.

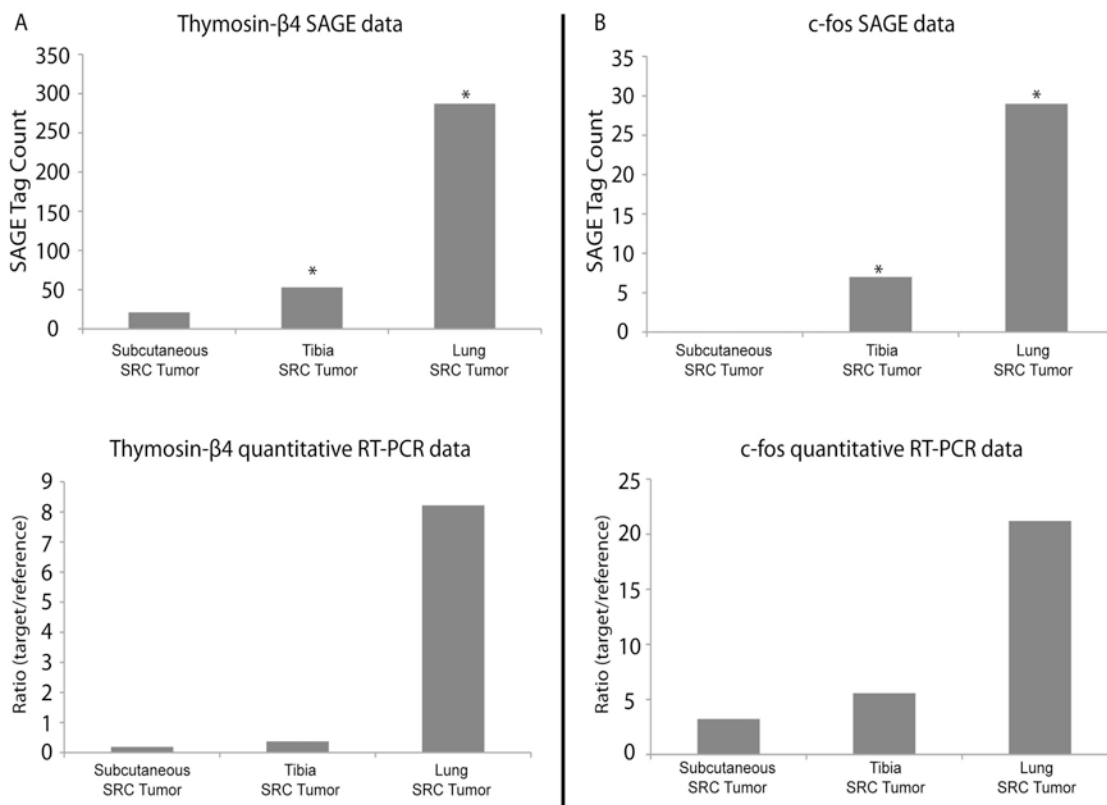
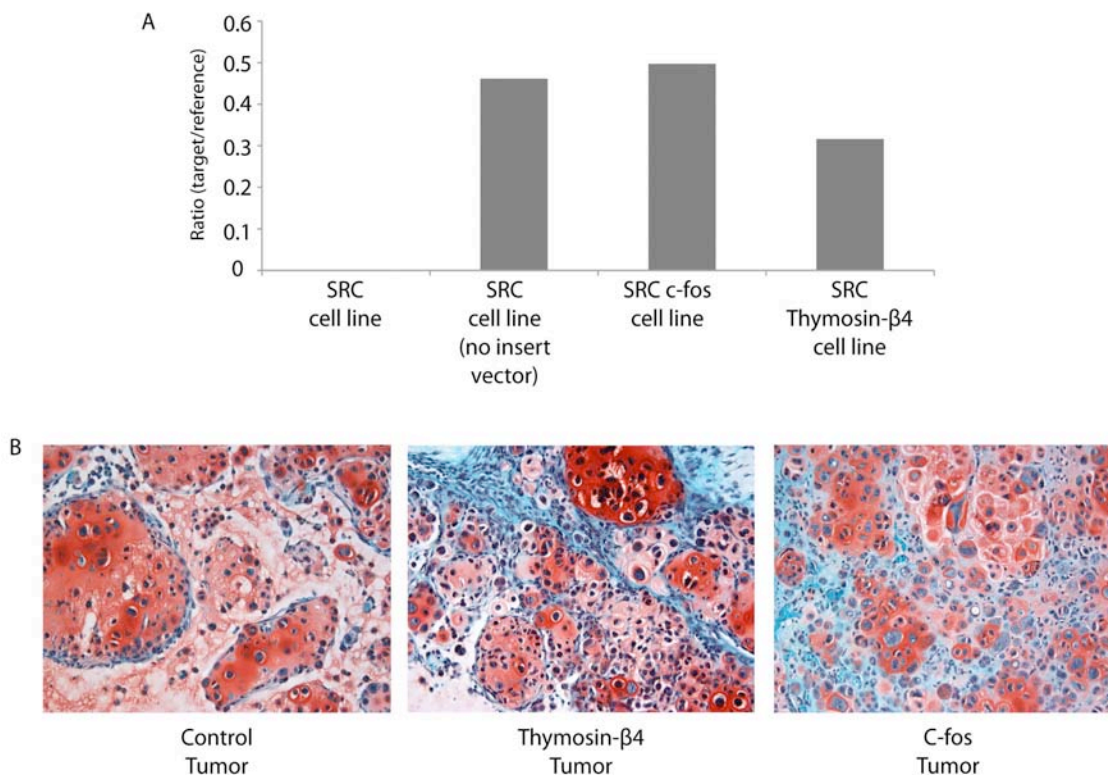


Figure 9. SAGE and quantitative RT-PCR confirm the expression of thymosin-β4 and c-fos in the SRC tumors. (A) Thymosin-β4 expression in the SRC tumors (SAGE analysis top panel; quantitative RT-PCR bottom panel). (B) C-fos expression in the SRC tumors (SAGE analysis top panel; quantitative RT-PCR bottom panel). Similar expression patterns were observed in both the SAGE and RT-PCR analysis. Note the increased expression of thymosin-β4 and c-fos in the tibia and lung SRC tumors. The bars in the RT-PCR graph represent the average expression ratio calculated on RNA that was collected from pooled tumor tissue. For RT-PCR at each transplantation site, tissue was pooled from at least 10 separate tumors. SAGE data was normalized to 100,000 tags/library for analysis. For the SAGE data, “\*” indicates expression levels that are significantly different than the “Subcutaneous SRC tumor” sample ( $z > 1.96$ ).



**Figure 10.** Thymosin-β4 and c-fos overexpression in the SRC cells and histology following subcutaneous transplantation. (A) Confirmation of Thymosin-β4 and c-fos overexpression in the SRC cell line using real time quantitative-PCR. Expression of the transgene construct was detected in all cell lines that were transduced with the viral vector (SRC cell line-no insert vector, SRC c-fos cell line, and SRC Thymosin-β4 cell line). No expression of the transgene construct was detected in the un-transduced SRC cell line (SRC cell line). The expression of the exogenous genes were detected with PCR primers specific for a sequence that is present in all of the expression constructs (see Material and methods). (B) Photomicroscopy of histological sections obtained from SRC tumors (20x magnification). Tumors induced from control cells (SRC cells expressing the empty viral vector), and from SRC cells overexpressing either Thymosin-β4 (Thymosin-β4 tumor) or c-fos (C-fos tumor). Approximately 30 days following tumor induction animals were sacrificed and tumors were removed for histology. Sections representative of each tumor are shown. All tumors were classified as histologic grade II chondrosarcomas. The SRC cells are stained with Safranin O (red).

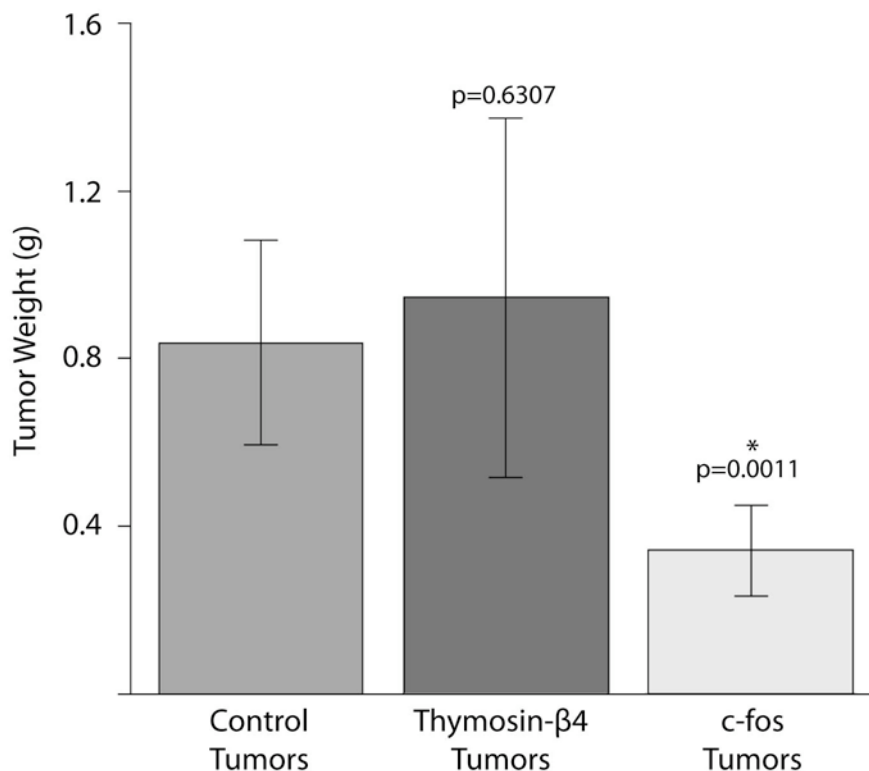


Figure 11. Tumor weight following induction of subcutaneous tumors with SRC cells overexpressing either thymosin-β4 or c-fos. Control tumors were initiated with SRC cells that express the MSCV viral vector with no insert (pMSCV-I-Hyrgo vector). C-fos tumors were initiated with SRC cells that overexpress c-fos (MSCV-cfos-I-Puro). Thymosin-β4 tumors were initiated with SRC cells that overexpress thymosin-β4 (MSCV-Thyβ4-I-Puro). Overexpression of c-fos resulted in the formation of tumors that were significantly smaller than control tumors. The bar represents the average invasion indices of biologic replicates, and the error bars represent the standard deviation of the biologic replicates. n=10 for control tumors and c-fos tumors. n=9 for thymosin-β4 tumors (one animal died prematurely and was found to have multiple chondrosarcoma lung metastases). See Table 4 for individual tumor weights. ‘\*’ Indicates that the tumor weight is significantly different than the tumor weight of the control tumors (p-value <0.05 considered significant).

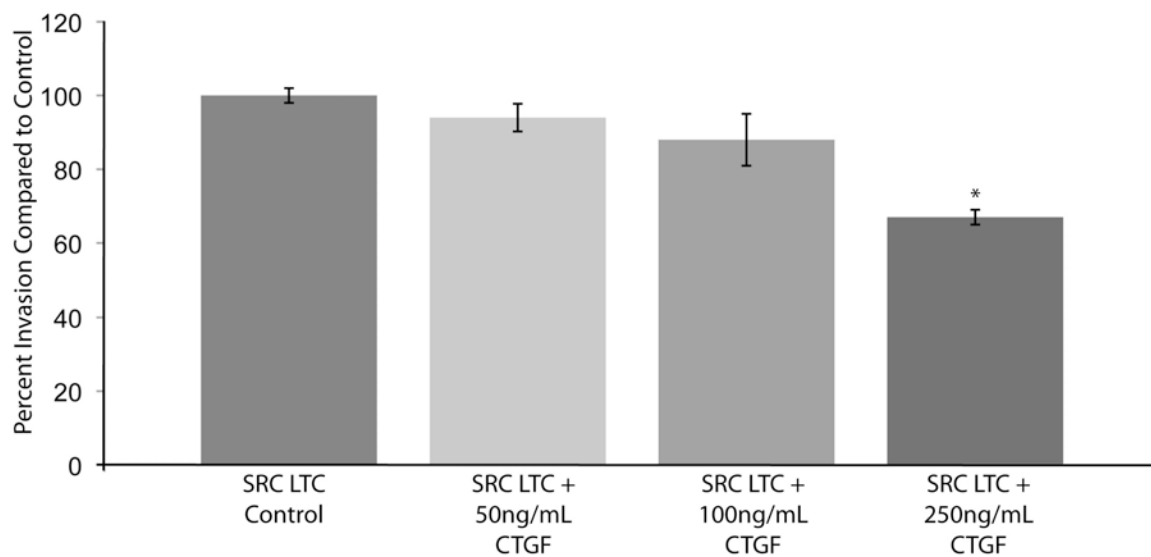


Figure 12. CTGF treatment decreases the invasiveness of SRC cells. Invasiveness was measured in control SRC cells (SRC Control) and in SRC cells treated with CTGF (50, 100, and 250ng/mL) at the start of the invasion assay. Twenty-four hours later, the invasiveness was calculated for all samples and the results are displayed as experimental sample compared to the untreated control SRC cells (100% invasion). The bar represents the average invasion indices of biologic replicates, and the error bars represent the standard deviation of 3 biologic replicates. ‘\*’ Indicates values that are significantly different than the “SRC Control” sample ( $p < .05$ ).

CHAPTER III  
GLOBAL DEMETHYLATION OF RAT  
CHONDROSARCOMA CELLS AFTER TREATMENT  
WITH 5-AZA-2'-DEOXYCYTIDINE RESULTS IN  
INCREASED TUMORIGENICITY

Introduction

Aberrant DNA methylation is thought to play an integral role in the complex process of tumorigenesis (Brena and Costello 2007). Abnormal hypermethylation may result in the silencing of genes that are members of pathways ranging from cell division to tumor suppression. Reintroducing the expression of abnormally silenced genes may restore control of these various signaling and regulatory pathways.

5-Aza-2-deoxycytidine

Current epigenetic therapies are aimed at bringing on hypomethylation with the goal of reverting hypermethylation-induced gene silencing (Mund et al. 2006). One such therapeutic agent is 5-Aza-2-deoxycytidine, which is a deoxycytidine analog that becomes incorporated into DNA and inhibits the activity of DNA methyltransferases (Chen et al. 1991; Santi et al. 1984). The incorporation of 5-Aza-2-deoxycytidine and subsequent inhibition of DNA methyltransferases results in reduced levels of DNA methylation (Mund et al. 2005; Yang et al. 2006). 5-Aza-2-deoxycytidine has been shown to have clinical benefits in the treatment of myelodysplastic syndrome and it has also been shown to be effective in the treatment of other myeloid malignancies (Issa et al. 2004).

Despite the potential benefits of 5-aza-2-deoxycytidine, the complete ramifications of treating tumor cells with a global DNA hypomethylating agent are unknown. The phenomenon of global DNA hypomethylation has been observed in several types of cancer (Hoffmann and Schulz 2005), and DNA hypomethylation has also been associated with tumor aggressiveness (Fraga et al. 2004). Evidence also

suggests that DNA hypomethylation may play a causal role in tumorigenesis (Eden et al. 2003; Gaudet et al. 2003).

#### Induction of DNA hypomethylation in a rat model for human chondrosarcoma

To study the impact of global DNA hypomethylation on the behavior of tumor cells we treated swarm rat chondrosarcoma (SRC) cells with 5-aza-2-deoxycytidine and monitored its effect both *in vitro* and *in vivo*. We selected the SRC tumor model based on its extensive characterization and the ability of the SRC cells to be grown and studied both *in vitro* and *in vivo* (Choi et al. 1971; King and Kimura 2003; Maibenco et al. 1967; Morcuende et al. 2002; Stevens et al. 2005).

#### 5-Aza-2-deoxycytidine treatment of SRC cells

SRC cells were treated *in vitro* with a low dose of 5-Aza-2-deoxycytidine for 30 days to induce genome-wide hypomethylation and their level of methylation was assessed using rat specific pyrosequencing assays. Treatment with 5-Aza-2-deoxycytidine led to demethylation of both LINE and microsatellite regions throughout the genome. The effects of long-term exposure to epigenetic agents are not completely known, and a potential concern is that such treatment may lead to the expression of genes that are normally epigenetically silenced. In addition, it may cause illegitimate transcription events (Costa et al. 2006; Stresemann and Lyko 2008). Indeed, invasion assays performed with treated and untreated SRC cells indicated that loss of methylation is accompanied by an increase in invasiveness. Furthermore, microarray analysis revealed that 5-Aza-2-deoxycytidine treatment leads to alterations in expression of several developmentally regulated genes.

#### Midkine and sox-2

Based on their differential expression in the microarray analyses, two of these genes, midkine and sox-2, were selected for additional expression and epigenetic

analyses. Midkine, a growth factor (Kadomatsu and Muramatsu 2004), and sox-2, a pluripotent transcription factor (Niwa 2007), are expressed at higher levels following 5-Aza-2-deoxycytidine treatment. Treatment with 5-Aza-2-deoxycytidine leads to loss of methylation in the promoter regions of both midkine and sox-2 genes, thus suggesting that methylation may play a role in the transcriptional regulation of these genes.

#### Effect of DNA hypomethylation in tumorigenesis

Since 5-Aza-2-deoxycytidine-induced hypomethylation resulted in several phenotypic changes in the SRC cells *in vitro*, we wanted to determine if the treatment would affect cell growth *in vivo*. Following subcutaneous transplantation, the 5-Aza-2-deoxycytidine treated SRC cells formed larger tumors than the corresponding untreated SRC cells. Methylation and expression analyses of the *in vivo* SRC cells revealed that the effect of 5-Aza-2-deoxycytidine could be observed for at least 60 days following treatment discontinuation.

Altogether the *in vivo* and *in vitro* results suggest that induction of genome-wide hypomethylation by 5-Aza-2-deoxycytidine results in an increase in the tumorigenicity of the SRC cells. The SRC experiments also highlight the importance that epigenetic modifications may have in cancer and suggest that DNA hypomethylation may have a functional role in tumor progression.

#### Materials and methods

##### Establishment of a bioluminescent rat chondrosarcoma cell line

A Murine Stem Cell Virus-Luciferase-Internal ribosomal entry site-Hygromycin (MSCV-Luc-I-Hygro) retroviral vector was prepared by transfecting 293T cells with three plasmids; pMSCV-Luc-I-Hygro (which encodes the Luciferase and hygromycin phosphotransferase), pEQ-Pam3(-E) (which encodes retroviral gag and pol) and pSR $\alpha$ -G (which encodes glycoprotein G from Vesicular Stomatitis Virus) (Rose and Gallione

1981). Forty-eight hours post-transfection media containing retroviral vector was collected, aliquoted, frozen, and stored at  $-80^{\circ}\text{C}$ . This vector was then used to transduce the Swarm rat chondrosarcoma cell line (SRC-LTC (Long Term Culture) (King and Kimura 2003), [obtained from Jeff W. Stevens, University of Iowa]), in the presence of  $5\mu\text{g/ml}$  polybrene on three successive days allowing the cells to recover in the media generally used overnight (Figure 13). Transduced cells were selected by incubation with hygromycin B (Sigma-Aldrich, St. Louis, MO) at a concentration of  $500\mu\text{g/ml}$  for 14 days. Once the hygromycin resistant population was established, the cells were maintained in media containing  $500\mu\text{g/ml}$  of hygromycin B. The newly established rat chondrosarcoma cell line was named SRC-MSCV3-LTC.

#### Cell culture conditions and 5-Aza-2-deoxycytidine treatment

SRC-MSCV3-LTC cells were cultured in DMEM high glucose ( $4.5\text{g glucose/ml}$ ) supplemented with 10% FBS and Penicillin/Streptomycin. Cells were plated at  $2.5 \times 10^4$  cells with  $6\text{ml}$  of media in a  $25\text{ cm}^2$  T flask. Cells were grown until they became 80-90% confluent (6 days), and at this time the cells were trypsinized/split and plated as described. For the 5-Aza-2-deoxycytidine treatment, the media was supplemented with  $0.1\mu\text{M}$  5-Aza-2-deoxycytidine on the day that the cells were passaged. Cell viability was assessed 72 hours following (0, 0.1, and  $1.0\mu\text{M}$ ) 5-Aza-2-deoxycytidine treatment (Figure 14). Viability was determined using the Guava EasyCyte Mini Flow Cytometry System, and the Guava ViaCount Reagent (Millipore; cat no. 4000-0040).

The Swarm rat chondrosarcoma line SRC-MSCV3-LTC, was treated with  $0.1\mu\text{M}$  5-Aza-2-deoxycytidine for 5 passages (30 days). Control cells were grown for 5 passages without 5-Aza-2-deoxycytidine. After 5 passages, cells were either frozen for subsequent DNA and RNA analysis, or they were passaged for five additional passages (30 days) without any drug treatment after which they were frozen for future analysis.

For *in vivo* experiments, cells were grown *in vitro* for 5 passages with or without 5-Aza-2-deoxycytidine. For the treated cells, the 5-Aza-2-deoxycytidine treatment was removed on the day of the injection and the cells did not receive further 5-Aza-2-deoxycytidine treatment.

#### Tumor inductions

Following growth for 5 passages, cells were injected subcutaneously into the lower lumbar region of 4 week old nude mice (Males; Charles River, Strain code: 088). The SRC cells were grown until they were 80% confluent, the cells were then washed with PBS, and then cells were removed from the plate using TrypLE Express (GIBCO cat#: 12605-010) according to manufactures instructions. Following removal of SRC cells from plates, the cells were washed with PBS, centrifuged, and resuspended in PBS. Either  $1 \times 10^6$ ,  $5 \times 10^6$ , or  $10 \times 10^6$  cells were injected subcutaneously. For each experiment one animal was injected with untreated control SRC cells, and one animal was injected with 5-Aza-2-deoxycytidine treated cells. The animals did not receive any dose of 5-Aza-2-deoxycytidine.

Following the injection, the animals were monitored twice weekly for 60 days. After 60 days the animals were euthanized by CO<sub>2</sub> gas inhalation followed by cervical dislocation. Immediately following euthanization, tumors and other tissues were frozen in liquid nitrogen or placed in paraformaldehyde for histology.

#### *In vivo* imaging

All *in vivo* imaging was performed with the Xenogen IVIS 200 imaging system. Ten minutes prior to imaging, D-luciferin (150mg/kg of body weight) was injected into the intraperitoneal cavity of the mice. During the image acquisition animals were anesthetized with isoflurane inhalation at 1 to 2%.

### Primer design and pyrosequencing

Rat genome sequence (rn4/ version 3.4, Nov. 2004) and the annotation for repetitive elements were obtained from the UCSC Genome Database. Based on genomic co-ordinates of LINE elements provided by the UCSC database, 899,092 LINE sequences were extracted and subjected to *in silico* bisulfite treatment. 8,460 L1 elements with length over 6000bp were identified and used for alignment to generate LINE nucleotide base matrix. A region within L1 elements with dense CpG dinucleotides was selected for PCR primer design. An electronic PCR was performed with the novel primers designed for rat LINEs. 827 LINE elements in the rat genome would be targeted in PCR reactions with the primer set designed. With two sequencing primers, a total number of 7 CpG dinucleotides were sequenced for each LINE element targeted. The global methylation data generated was derived from a minimum number of 5,700 CpG dinucleotides in LINE elements. A similar approach was taken to design novel primers for rat satellite repeats. Primers targeting a minimum number of 137 distinct Satellite I elements and five distinct Satellite II elements were designed. For each Satellite element targeted, the methylation profiles were determined for three CpG dinucleotides. Primer sequence and reaction conditions are available in Table 5.

The pyrosequencing analysis for midkine promoter was carried out using the following primers: MDK-2-c-F1: biotin/GTTAAGGTTTTTTTTGTTTTTAGAAT; MDK-2-c-F1: TAAATAACACAAACACAAAAATCC; (Sequencing primer) MDK-2-c-S1: ACAAACACAAAAATCCC. The pyrosequencing analysis for sox-2 promoter was carried out using the following primers: Sox\_2\_CpG47-3-F1: ttgtgtaattagtaggggtaatg; Sox\_2\_CpG47-3-R1: biotin/CAACTTCCTAACATCCCA; (Sequencing primer) Sox\_2\_CpG47-3-S1: TGTGTTAATTAGTAGGGGTA. Five CpG sites were examined with the midkine promoter primers. Eight CpG sites were examined with the sox-2 promoter primers.

## Microarray

Microarray analysis was used to examine the gene expression profiles of the SRC cells (+) or (-)5-Aza-2-deoxycytidine treatment. Microarray was carried out using the NimbleGen microarray service. The *Rattus norvegicus* 1-plex array (14 probes/target; 26739 genes; cat#: A6184-00-01) was used for each hybridization. Two hybridizations were performed on 5-Aza-2-deoxycytidine treated SRC cells and three hybridizations were performed on untreated control SRC cells. Data were processed and displayed using Genespring software (Agilent Technologies). Genespring was used to identify differentially expressed genes that had a 5-fold difference between the 5-Aza-2-deoxycytidine treated samples and the untreated control samples. Additionally, Genespring was used to create a gene tree (Pearson coefficient) to graphically represent the data.

The list of differentially expressed genes was analyzed using a pathway-mapping program (Ingenuity Pathway Analysis version 7.0). Ingenuity was used to sort the list of differentially expressed genes (977genes) based on their role in cellular function and disease. Ingenuity identified 135 cancer related genes. For the heat map, the cancer gene list was further filtered by requiring a minimum expression level of at least 1,000 relative fluorescence units in at least 2 different hybridizations.

Genespring was used for hierarchical clustering, to create a gene tree (Pearson coefficient; centroid linkage clustering), and to generate the heat map used to graphically represent the data.

The list of genes with a 5-fold difference (977genes) was also analyzed using GeneGo to identify pathways that were altered following 5-Aza-2-deoxycytidine treatment.

All presented microarray data is MIAME compliant. The raw microarray data has been deposited in a MIAME compliant database. The microarray data has been deposited at GEO (GEO accession number: GSE17598).

### Real-Time quantitative PCR

Total RNA was isolated using Trizol; RNA was treated with TURBO DNA-free (Ambion Cat# AM1907). Total RNA (1 $\mu$ g) was used to make cDNA with the iScript cDNA Synthesis kit (BioRad). Rat Midkine real time PCR was performed with the iQ SYBR Green Supermix (BioRad), and midkine rat specific primers (Forward: CCCAAGATGTAACCCACCAG; Reverse: GCTCACTTCCCAGAATCCC). For SYBR green PCR's, 18S-RNA was used as a reference gene (Zhu and Altmann 2005) (Forward: GGGAGGTAGTGACGAAAATAACAAT; Reverse: TTGCCCTCCAATGGATCCT).

Rat sox-2 real time PCR was performed with iQ Supermix (Biorad) using Roche universal probe #119 (cat. no. 04693531001) and rat specific primers (forward: ATTACCCGCAGCAAATGAC and Reverse: TTTTTCGTTAATTTGGATGG). For PCR's with the Roche probes 18S-RNA was used as a reference gene (Probe #22 (cat. no. 04686969001 with primers: Forward: GGTGCATGGCCGTTCTTA; Reverse: TCGTTCGTTATCGGAATTAACC).

The Pfaffl method was used to calculate the normalized gene expression (Pfaffl 2001). For each real time PCR analysis the individual sample being examined was used as the test sample in the Pfaffl method. The calibrator sample, for the Pfaffl method, was an equal mixture of cDNA from SRC control cells and 5-Aza-2-deoxycytidine SRC cells. All real time qPCR results are displayed as a ratio of the target gene relative to the reference gene, in a specific test sample, compared to the expression of the target gene relative to the reference gene in the calibrator sample.

### CpG island identification

CpG islands were located by searching the midkine and sox-2 genes in BLAT (Kent et al. 2002). Each CpG island was more closely examined using "CpG Island Searcher" (Takai and Jones 2003) and each island was classified as either a high-CpG

promoter, an intermediate CpG promoter, or as a low-CpG promoter as previously described (Weber et al. 2007).

#### Analysis of DNA methylation by sequencing of sodium bisulfite-treated DNA

Genomic DNA was obtained by digestion with proteinase K (Quiagen) followed by phenol/chloroform extraction, and was subjected to sodium bisulfite treatment to modify unmethylated cytosine to uracil using the ‘CpGenome<sup>TM</sup> DNA Modification Kit’ (Chemicon International, CA). Bisulfite-treated DNA was amplified by a nested-PCR protocol using the primers described in Table 6. PCR was performed in a volume of 25  $\mu$ l containing PCR Buffer (Quiagen); 1.5mM of MgCl<sub>2</sub> (Quiagen); 200  $\mu$ M of dNTPs (Invitrogen); 0.32  $\mu$ M of each primer and 1U of Hot Start Taq Plus DNA Polymerase (Quiagen). The PCR conditions were: 94°C for 10 min, 94°C for 3 min, 48°C for 3 min, 72°C for 2 min, one cycle; 94°C for 3 min, 50°C for 3 min, 72°C for 2 min, five cycles; and 94°C for 1 min, 52°C for 1 min, 72°C for 1 min, 35 cycles for the first reaction and the same annealing temperatures (48°, 50° and 52°C) for the nested reaction. Amplified products were purified using the Gel Purification Kit (Quiagen) and were ligated to a vector using the TOPO TA Cloning Kit (Invitrogen). Twenty-four positive clones were sequenced for each sample using the vector’s forward and reverse primers. DNA sequencing reactions were performed using the ‘DNA dRhodamine Terminator Cycle Sequencing Ready reaction’ kit (Applied Biosystems) and an ABI3730xl sequencer (Applied Biosystems) according to the manufacturer’s instructions.

#### Invasion assay

A Membrane Invasion Culture System (MICS) was used to measure the *in vitro* invasiveness of all SRC cell lines as previously described (Hendrix et al. 1987). Briefly, a polycarbonate membrane with 10- $\mu$ m pores was uniformly coated with a defined matrix. Both upper and lower wells of the chamber were filled with RPMI. SRC cells

were seeded into upper wells at a concentration of  $5 \times 10^5$  cells per well. After a 24-hour incubation in a humidified incubator at  $37^\circ\text{C}$  with 5%  $\text{CO}_2$ , cells that had invaded through the basement membrane were collected, stained, and counted by light microscopy (Sood et al. 2004).

#### Statistical analysis

Analysis of Variance (ANOVA) or two-sample t-test was used to analyze changes of DNA methylation level among different treatment conditions for Line1-S1, Line1-S2, Satellites 1 and 2, respectively. Tukey's method or Dunnett method was used to adjust p-values due to multiple comparisons in ANOVA analysis.

A linear regression method was applied to analyze tumor weight between two tumor groups (SRC Control and SRC 5AZA) after adjusting for the number of cells injected. Tumor weight and number of cells were transformed using the logarithm so that data distribution was appropriate for the analysis methods used.

We used 0.05 as the significance level for comparisons. SAS 9.1 and R software was used for data analysis and graphing.

#### Ethics statement

All animals were handled in strict accordance with good animal practice as defined by the relevant national and/or local animal welfare bodies, and all animal work was approved by the Institutional Animal Care and Use Committee (Children's Memorial Research Center; protocol IACUC #2006-30).

### Results

#### 5-Aza-2-deoxycytidine induces hypomethylation of LINE1 and Satellites 1 and 2

Methylation levels of cytosines in CpG dinucleotides of repetitive elements has been used as a surrogate marker for genome-wide methylation (Yang et al. 2004), in this

study, LINE (Long Interspersed Element) 1 and Satellites 1 and 2 were selected as surrogate methylation markers. Rat specific pyrosequencing assays were designed to examine methylation levels of these repetitive sequences throughout the genome. The pyrosequencing assays were used to determine the methylation levels in untreated cells, in cells treated with a low dose of 5-Aza-2-deoxycytidine, and in cells that were treated with 5-Aza-2-deoxycytidine followed by an additional recovery period without the drug (30 days).

The level of DNA methylation in LINE, Satellite 1 and Satellite 2 regions of SRC cells decreases following 5-Aza-2-deoxycytidine treatment (Figure 15). The SRC cells were grown for 30 additional days after removal of 5-Aza-2-deoxycytidine. Following withdrawal of the drug, methylation was restored to levels that were indistinguishable from those of control cells based on the LINE1 and Satellite 2 assays (Figure 15). Methylation was partially restored for Satellite 1, but it did not completely regain the level that was observed in control cells. This result suggests that the demethylating effects of 5-Aza-2-deoxycytidine treatment may persist after five additional passages (30 days) without the drug.

#### Invasion Assay

The invasiveness of the SRC cells increased 40% following 5-Aza-2-deoxycytidine treatment (Figure 16). Thirty days post-removal of treatment, the invasive activity dropped to a level that was indistinguishable from that of control cells. The invasion assays demonstrated that 5-Aza-2-deoxycytidine-induced DNA hypomethylation leads to an increase in the *in vitro* invasiveness of SRC cells, and that following withdrawal of the drug, the invasive activity of the SRC cells returns to the levels observed for control cells.

### Microarray analysis

Based on the invasion assays it was hypothesized that the 5-Aza-2-deoxycytidine may alter gene expression of the SRC cells. Microarray analysis was carried out to identify changes in gene expression in untreated and in treated cells. The expression level of several genes increased after treatment with 5-Aza-2-deoxycytidine (Figure 17). Data analysis revealed that 977 genes (603 genes upregulated and 374 downregulated) exhibited a 5-fold expression difference in the untreated and treated SRC cells (see Appendix D for gene list). The pathway-mapping program, Ingenuity, was used to analyze the group of genes with a 5-fold difference in expression. Ingenuity revealed that the differentially expressed genes might play a role in several cancer-relevant pathways (Table 7). The top pathway, Cancer (135 genes), was selected for further analysis. A subset of the cancer related genes with a 5-fold difference are shown in a heat map (Figure 17). As illustrated by the heat map, 5-Aza-2-deoxycytidine treatment can lead to the alterations in the expression of genes that may play a role in different aspects of cancer, ranging from cell growth and proliferation, to cell cycle control, and to cell death.

One potential explanation of the microarray results is that 5-Aza-2-deoxycytidine treatment results in the derepression of genes that were epigenetically silenced. As a result, we may observe an increase or a decrease in expression (e.g. derepression of a negative regulator). To examine this possibility, expression and methylation analyses were performed on two of the cancer related genes (midkine: Figure 18 and 19; sox-2: Figure 20 and 21). The genes, midkine and sox-2, were selected on the basis of their differential expression compared to control cells, and because they have CpG islands in their promoter regions (we have previously demonstrated that both sox-2 and midkine are not expressed in the control tissue, normal rat articular cartilage, data not shown; GEO: GSM25926). Midkine and sox-2 were also selected because they are developmentally regulated genes, and studies have indicated that these genes may play functional roles in stem cells (Park et al. 2008; Zou et al. 2006). Therefore, we wanted to determine if 5-

Aza-2-deoxycytidine-induced DNA hypomethylation could lead to the expression of stem cell related genes in the SRC cells.

### Midkine and sox-2

The increase in expression of midkine (Figure 18) and sox-2 (Figure 20), following exposure to 5-Aza-2-deoxycytidine, was confirmed by real-time quantitative RT-PCR. The expression of each midkine and sox-2 decreased to a level that is slightly higher than that of control cells thirty days following discontinuation of 5-Aza-2-deoxycytidine treatment. These data suggest that midkine and sox-2 expression increases as a result of exposure to 5-Aza-2-deoxycytidine, and that 30 days after discontinuation of 5-Aza-2-deoxycytidine *in vitro*, the expression of these genes begins to decrease. Although their expression level decreases, both midkine and sox-2 are expressed at levels that are higher than those observed in untreated control cells (Figures 19 and 20). This suggests that SRC cells may continue to express midkine and sox-2 at high levels for at least 30 days following removal of 5-Aza-2-deoxycytidine.

Both midkine and sox-2 contain CpG islands at their transcription start sites. The CpG islands in the promoters of midkine and sox-2 can be classified as intermediate CpG islands, which is relevant because the activity of promoters containing intermediate CpG islands correlates negatively with their methylation status (Weber et al. 2007). Additionally, intermediate CpG islands may be preferential targets for *de novo* methylation in somatic cells during development (Weber et al. 2007).

The methylation statuses of both midkine and sox-2 CpG islands were examined using bisulfite sequencing (Figures 19 and 21) and pyrosequencing (Figure 22). Two CpG islands were identified in the rat midkine gene. One CpG island encompasses the midkine transcriptional start site and the other is slightly downstream from it (Figure 19). Both midkine CpG islands were heavily methylated in untreated SRC cells, and they became hypomethylated in 5-Aza-2-deoxycytidine treated cells (Figure 19).

Two CpG islands were also examined for *sox-2* (Figure 21). The CpG island encompassing the *sox-2* transcriptional start site (CpG 154) was not methylated in either control or treated cells (Figure 21B). However, a CpG island (CpG 47) located less than 1kb upstream of the *sox-2* transcriptional start site was methylated in untreated SRC cells. Following 5-Aza-2-deoxycytidine, this CpG island became hypomethylated (Figure 21A).

These results suggest that 5-Aza-2-deoxycytidine treatment can lead to the demethylation of CpG islands at or near the transcriptional start site of *midkine* (Figures 19) and *sox-2* genes (Figure 21). The decrease in CpG island methylation was accompanied by an increase in the expression of *sox-2* and *midkine* (Figures 18 and 20), consistent with the hypothesis that methylation may play a role in the regulation of these genes.

#### *In vivo* tumor formation

SRC cells were transplanted into nude mice to test tumorigenicity following 5-Aza-2-deoxycytidine-induced DNA hypomethylation. The SRC cell line used for all aforementioned experiments stably expresses luciferase, which enables tumor growth to be examined *in vivo*. SRC cells treated with 5-Aza-2-deoxycytidine produced larger tumors than those induced with control SRC cells (Figure 23 and 24, and Table 8).

Subcutaneous tumors were induced with  $1 \times 10^6$ ,  $5 \times 10^6$ ,  $7 \times 10^6$ , or  $10 \times 10^6$  cells. In preparation for injections, SRC cells were treated *in vitro* for 30 days with 5-Aza-2-deoxycytidine, after which the treatment was stopped and the cells were transplanted into nude mice. Control tumors were induced with untreated SRC cells. Tumors were resected sixty days after transplantation. As it has been documented with human chondrosarcoma (Soderstrom et al. 2001a; Soderstrom et al. 2001b), the SRC cells produced tumors with varying degrees of heterogeneity (Figure 24A and 24B). Albeit relevant, histological grading is not predictive of outcome (Aigner 2002), and no markers

of prognostic value have been identified to date for human chondrosarcoma (Lee et al. 1999). Hence, we examined another characteristic of the tumor, tumor weight, which demonstrated that 5-Aza-2-deoxycytidine treated cells produced larger tumors than those derived from untreated cells (Figure 24 and Table 8).

Histological analysis detected the presence of SRC cells in the lungs of mice injected with control cells and in the lungs of mice injected with 5-Aza-2-deoxycytidine treated cells (Table 8). However, it should be noted that SRC cells were detected macroscopically in the lungs of mice injected with 5-Aza-2-deoxycytidine-treated cells (3 out of 9 mice; Figure 26). SRC cells could not be detected macroscopically in the lungs of mice injected with untreated control cells. These results indicated that 5-Aza-2-deoxycytidine-treated SRC cells may grow more aggressively than untreated SRC cells in the lung of subcutaneously injected mice.

Taken together, the *in vivo* analyses demonstrated that DNA hypomethylation, induced by 5-Aza-2-deoxycytidine, led to the formation of more aggressive tumors than the tumors formed from untreated control SRC cells both locally, at the site of injection, and distantly, in the lungs.

#### Methylation of SRC cells *in vivo*

The tumors derived from untreated SRC cells were methylated to a greater extent than the tumors derived from 5-Aza-2-deoxycytidine treated cells (Figures 27). *In vivo* the 5-Aza-2-deoxycytidine treated cells were injected and allowed to grow *in vivo* without treatment for 60 days. After 60 days of growth *in vivo*, tumors derived from 5-Aza-2-deoxycytidine-treated SRC cells exhibited a significantly lower level of methylation (Figure 27; LINE-1, LINE1-S2, Satellite 1, and Satellite 2) than that of the tumors derived from untreated control cells. This result is of note since *in vitro* the SRC cells were treated for 30 days and subsequently grown *in vitro* for 30 days without treatment, but these cells did reestablish methylation levels that were similar to control

cells (Figure 15; LINE-1, LINE1-S2, and Satellite2). These results suggest that 5-Aza-2-deoxycytidine treated SRC cells more efficiently reestablish hypermethylation *in vitro* than *in vivo*.

### Discussion

Aberrant DNA hypermethylation has been observed in a variety of cancers including chondrosarcoma (Asp et al. 2001; Asp et al. 2000; Ropke et al. 2003). 5-Aza-2-deoxycytidine treatment is thought to lead to the reactivation of aberrantly hypermethylated genes (Karpf and Jones 2002), and treatment of leukemias with 5-Aza-2-deoxycytidine has been shown to have clinical benefits (Issa et al. 2004). However, genome-wide hypomethylation has also been observed in several types of cancer (Hoffmann and Schulz 2005), and it has been suggested that DNA hypomethylation may play a role in tumorigenesis (Eden et al. 2003; Gaudet et al. 2003). Although 5-Aza-2-deoxycytidine does have clinical benefits, one potential concern with a drug that induces DNA hypomethylation is the possibility that, in addition to reintroducing the expression of abnormally silenced genes, it may also lead to the expression of genes that are normally epigenetically silenced or it may lead to an increase of illegitimate transcription events (Stresemann and Lyko 2008). Genome-wide derepression of transcription of genes that are normally epigenetically silenced is likely to have a dramatic impact in cancer cells that already possess abnormal genetic, epigenetic, or gene expression profiles.

In this study, we examined the effect of 5-Aza-2-deoxycytidine-induced genome-wide hypomethylation on SRC cells *in vitro* and *in vivo*, using pyrosequencing assays. As expected, treatment with 5-Aza-2-deoxycytidine led to a decrease in the global methylation levels of SRC cells. This decrease in methylation was accompanied by an increase in the invasiveness of the SRC cells *in vitro*. Subsequent global gene

expression analysis revealed that 5-Aza-2-deoxycytidine treatment leads to (abnormal) expression of several cancer related genes.

More detailed analysis of two of the cancer related genes, *sox-2* and *midkine*, confirmed that their expression levels increased following 5-Aza-2-deoxycytidine treatment. Methylation analysis of CpG islands at their transcription start site revealed that these genes were methylated in control cells and that they lost methylation after treatment with 5-Aza-2-deoxycytidine. This result suggests that loss of methylation may play a role in the activation of both *sox-2* and *midkine* in 5-Aza-2-deoxycytidine-treated SRC cells.

Analysis of the *sox-2* CpG island revealed that the 5' end of the island is heavily methylated in control and treated SRC cells but the 3' end of the island is unmethylated. This finding is noteworthy because the pattern of DNA methylation changes from 90% methylated to less than 10% DNA methylated in a distance that is shorter than 50 base pairs (Figure 21 A and B). The abrupt change in DNA methylation may be explained by observations made in a homologous region of the *sox-2* promoter in the human gene. The CpG island, examined in Figure 21, shares 90% sequence similarity with the human *sox-2* promoter region. Interestingly the *sox-2* promoter region in humans has been shown by chromatin immunoprecipitation (ChIP) assays to contain a CTCF (CCCTC-binding factor) binding site 500bp upstream from the *sox-2* promoter CpG island (Rosenbloom et al. 2009). CTCF has previously been shown to act as an insulator that is capable of blocking enhancer activity and spread of heterochromatin (Bell et al. 1999; Cho et al. 2005). CTCF may act as an insulator in the *sox-2* promoter whereby it prevents the downstream spread of heterochromatin to the *sox-2* promoter. The methylation pattern that is observed in the *sox-2* promoter in SRC control cells may be indicative of a change in the DNA from a condensed state that is characteristic of heterochromatin to a less-condensed state that is characteristic of euchromatin, and CTCF may act as an insulator between these two epigenetic states.

It is noteworthy that *sox-2* and *midkine* contain “intermediate-type” CpG islands (Weber et al. 2007). Transcriptional activity of genes with such type of CpG islands is known to correlate negatively with their level of methylation (Weber et al. 2007). The expression of these genes may, at least in part, explain the increase in invasiveness following 5-Aza-2-deoxycytidine treatment, as both *sox-2* and *midkine* may play roles in tumor progression (Kato et al. 2000; Sanada et al. 2006; Tanabe et al. 2008).

*Sox-2* and *midkine* may also have a function in stem cells. *Midkine* is involved in the growth of neuronal stem cells (Zou et al. 2006), and the expression of *sox-2* has been shown to be an important factor for restoring somatic cells to a pluripotent state (Park et al. 2008). An intriguing possibility is that 5-Aza-2-deoxycytidine may induce the expression of genes or networks that allow the cells to acquire stem cell-like properties. Pathway analysis of the differentially expressed genes led to the identification of a network of stem cell related genes that became upregulated following 5-Aza-2-deoxycytidine treatment (Figure 27). Based on the network, *sox-2* plays a role in the regulation of *Dppa5* (Tanaka et al. 2002), *Alpha crystallin B* (Ijichi et al. 2004) and *P-cadherin* (Boyer et al. 2005), and this is consistent with the microarray data (see Figure 17 and Appendix E). Although products of these genes may have functions in stem cells, their role in the SRC cells is not known. It is important to note that these genes may have additional cellular functions. For example, besides their putative roles in stem cells, *midkine* and *Alpha crystallin B* may also play a role in drug resistance (Ivanov et al. 2008; Mirkin et al. 2005). These examples demonstrate the complex nature of gene expression changes that occur following 5-Aza-2-deoxycytidine treatment.

A number of genes are also downregulated following 5-Aza-2-deoxycytidine treatment. Among these are genes with diverse cellular functions (see Figure 17 and Appendix E). One potential explanation for this observation is that 5-Aza-2-deoxycytidine treatment may lead to the activation of genes that negatively regulate other genes. These negative regulators may include protein-coding genes, as well as

microRNA genes that could negatively regulate gene expression (Lujambio et al. 2008). Another intriguing possibility is that 5-Aza-2-deoxycytidine treatment might lead to the expression of other noncoding antisense RNAs that could in turn negatively regulate gene expression (Cayre et al. 2003; Costa 2008; Stuart et al. 2000; Tufarelli et al. 2003).

5-Aza-2-deoxycytidine-induced changes in gene expression had a significant impact on the phenotype of the SRC cells as tumors derived from 5-Aza-2-deoxycytidine treated cells produced larger tumors than tumors derived from untreated cells (Figure 23 and 24). Tumors derived from 5-Aza-2-deoxycytidine treated cells had a lower level of methylation (60 days after tumor induction) than those derived from control untreated cells (Figure 27) This is a notable observation because *in vitro*, 30 days following 5-Aza-2-deoxycytidine removal, the SRC cells had reestablished a methylation level that was similar to that of control cells (Figure 15). It is possible that the *in vivo* microenvironment may provide more favorable growth conditions that would allow selection and/or propagation of hypomethylated cells. *In vitro* cells do not encounter the same selective pressure as *in vivo* cells do, and this difference in selective pressure may provide an explanation as to why the tumor cells maintain a lower level of methylation.

While it can be speculated that the microenvironment may exert some selective pressure on the SRC cells *in vivo*, the possibility cannot be ruled out that the *in vitro* cells may have a faster doubling time than that of the cells *in vivo*. The faster doubling time would presumably allow the *in vitro* cells to more quickly regain DNA methylation, whereas the cells *in vivo* may have a slower doubling time and therefore would require more time for the cells to reestablish the same methylation level that was observed *in vitro*.

It is important to note that 5-Aza-2-deoxycytidine is not currently used for the treatment of human chondrosarcoma, and the treatment schedule presented in this paper was designed for the treatment of cells *in vitro* and therefore it does not match a standard clinical treatment regimen. Consequently, the results obtained with 5-Aza-2-

deoxycytidine may be specific for the SRC cell line and the conditions of the experiment. It should be noted that in our studies, the SRC cell line was treated with 5-Aza-2-deoxycytidine *in vitro*. This treatment was removed and the cells were transplanted *in vivo*. *In vivo*, the animals did not receive any 5-Aza-2-deoxycytidine. This is in contrast to other 5-Aza-2-deoxycytidine studies where a tumor xenograft was induced, and then the animal was treated with 5-Aza-2-deoxycytidine (Morita et al. 2006). Treating the animal with 5-Aza-2-deoxycytidine will result in changes in DNA methylation to both the tumor cells and the surrounding host cells in the microenvironment. 5-Aza-2-deoxycytidine-induced changes to host cells may influence the phenotype of the tumor xenograft. Since our studies did not treat the animals, we do not know the impact that 5-Aza-2-deoxycytidine might have on the cells of the host animal and what the subsequent impact will be on the tumor xenografts. Future 5-Aza-2-deoxycytidine studies that involve treatment of the SRC tumor xenografts *in vivo* will be more appropriate to address the impact that 5-Aza-2-deoxycytidine has on the microenvironment of the host cells and what impact this has on tumor progression. It should be emphasized, however, that we chose to pre-treat the cells *in vitro* so that we could work with a single variable and hence be able to associate loss of methylation with changes in behavior.

Despite the nontraditional use of 5-Aza-2-deoxycytidine, our results suggest that genome-wide DNA hypomethylation, induced by 5-Aza-2-deoxycytidine, may actually promote certain aspects of tumorigenesis in SRC cells. This observation may initially seem counterintuitive based on the use of 5-Aza-2-deoxycytidine as a chemotherapeutic agent, but previous studies have demonstrated that 5-Aza-2-deoxycytidine can be mutagenic (Jackson-Grusby et al. 1997), and that DNA hypomethylation can promote the formation of tumors (Eden et al. 2003; Gaudet et al. 2003). Recent studies have also shown that chromatin modifying agents, including 5-Aza-2-deoxycytidine, are capable of inducing pluripotency associated genes (Ruau et al. 2008) and it is possible to speculate that the activation of pluripotency associated genes may have a substantial impact on

tumor cells. However, further studies are needed to attain a greater understanding of the effect that these epigenetic modifying drugs have on tumor cells. Finally, additional studies are needed to investigate the specific mechanisms by which genome-wide loss of methylation may promote tumorigenesis.

Table 5. Pyrosequencing primer design and PCR conditions.

Name	PCR Primer	PCR Primer sequence	Annealing temperature	PCR conditions (template amplification)	Sequencing primer	Sequencing Primer Sequence
rat LINE1	rLINE(F)	ttggtgagttgggat	53.7C	Step-1:95C 5min	rLINE-seq-1	tagaatttttta ggat
	rLINE(R)	biotin- aaatctaaaacaaaaactact ac	-----	Step-2: 94C 15s	rLINE-seq-2	ataggaagttt atatt
				Step-3: __C (annealing temp) 10s		
rat Satellite 1	rSat1(F)	gagagtttggttagta	54.9C	Step-4: go to Step-2 49x	rSat1-seq	gtgggtagtat ttta
	rSat1(R)	biotin- aaaaattaatcttacctataatcc c	-----	step-5: 72C 60s		
				step-6: 4C o/n		
rat Satellite 2	rSat2(F)	gaatttggtgtaatgaagt	54.9C		rSat2-seq	gtgtattgaagt ttt
	rSat2(R)	biotin- caacaacaaaaaacctac	-----			

Table 6. Bisulfite treated DNA primer design.

Region	Primer <sup>1,2</sup>	Primer Sequence
Midkine CpG 1	Midkine CpG 1 (15)-EF	AAGTTTTATTAAAGATATATTTTG
	Midkine CpG 1 (15)-ER	CTACTACCACCAAAAAAAAAATAAAATAA
	Midkine CpG 1 (15)-IF	TTTTTAAATTTTTTTTTTTTAGTTGTAGG
	Midkine CpG 1 (15)-IR	AATAATAACTTCAAATCCTCCC
Midkine CpG 2	Midkine CpG 2 (17)-EF	TTATTTTATTTTTTTTGGTGGTAG
	Midkine CpG 2 (17)-ER	AAAATTTACCAAATTCAATTCTATATAC
	Midkine CpG 2 (17)-IF	TTGGAGGGATAGGGGTTATAG
	Midkine CpG 2 (17)-IR	AACTCTTAAACCTTCCTTATTC
Sox-2 CpG 154.1	Sox-2 CpG 154.1-EF	TAATTTTTGGTTTGTGTTTGTGAG
	Sox-2 CpG 154.1-ER	TAATTAATTTTTAAAAAACTTAAACC
	Sox-2 CpG 154.1-IF	ATAAGGTTGGAAGAGGGGTTG
	Sox-2 CpG 154.1-IR	CTTCTTCTCCCAACCCTAATC
Sox-2 CpG 47	Sox-2 CpG 47-EF	GGTTGATTTGGGGTAGATGAG
	Sox-2 CpG 47-ER	CCAACCTTATTACCAACACCC
	Sox-2 CpG 47-IF	GTTTTAATAAGAGAGTGAAGG
	Sox-2 CpG 47-IR	CAAACAAACCAAAAATTAACCC

<sup>1</sup> EF/R: external forward/reverse primer

<sup>2</sup> IF/R: internal forward/reverse primer

Table 7. Top pathways altered following 5-Aza-2-deoxycytidine treatment.

Rank	Function and Diseases	p-value	#Molecules
1	Cancer	9.84E-06	135
2	Cellular Growth and Proliferation	9.84E-06	68
3	Gastrointestinal Disease	9.84E-06	14
4	Nervous System Development and Function	2.23E-05	28
5	Ophthalmic Disease	1.21E-04	11
6	Cellular Function and Maintenance	3.74E-04	17
7	Reproductive System Development and Function	7.29E-04	11
8	Reproductive System Disease	7.40E-04	55
9	Cell Cycle	9.11E-04	20
10	Cell Death	1.16E-03	34

Note: The list of genes with a 5-fold difference (977 genes) in gene expression between untreated SRC control cells and 5-Aza-2-deoxycytidine treated cells was analyzed using Ingenuity Pathway Analysis software. The top 10 functions and diseases are shown in the table. The function, its associated p-value, and the number of molecules in the specific pathway are shown.

Table 8. In vivo: Subcutaneous transplantation of SRC tumor cells.

Experiment	Cells Injected	Lungs evaluated	SRC Cells detected in Lung	Tumor Weight	Surface Radiance
1a	1x10 <sup>6</sup>	No	-	0.07g	1.70E+09
1b	1x10 <sup>6</sup>	No	-	0.174g	4.19E+09
2a	1x10 <sup>6</sup>	Yes	No	NDT <sup>1</sup>	2.38E+04
2b	1x10 <sup>6</sup>	Yes	No	* <sup>2</sup>	2.12E+06
3a	5x10 <sup>6</sup>	No	-	0.34g	3.76E+09
3b	5x10 <sup>6</sup>	Yes	No	0.86g	1.00E+10
4a	5x10 <sup>6</sup>	No	-	0.07g	4.11E+08
4b	5x10 <sup>6</sup>	Yes	Yes	3.75g	2.14E+10
5a	5x10 <sup>6</sup>	Yes	Yes	0.53g	3.33E+09
5b	5x10 <sup>6</sup>	Yes	Yes	4.27g	9.84E+09
6a	5x10 <sup>6</sup>	Yes	Yes	0.72g	1.23E+09
6b	5x10 <sup>6</sup>	Yes	Yes	3.58g	3.38E+09
7a	7x10 <sup>6</sup>	Yes	No	2g** <sup>3</sup>	9.78E+08
7b	7x10 <sup>6</sup>	Yes	No	10.0g** <sup>3</sup>	1.78E+09
8a	10x10 <sup>6</sup>	Yes	No	0.38g	1.48E+09
8b	10x10 <sup>6</sup>	Yes	Yes	1.71g	4.46E+09
9a	10x10 <sup>6</sup>	Yes	Yes	0.28g	6.95E+09
9b	10x10 <sup>6</sup>	No	-	1.60g	2.39E+10

<sup>1</sup> NDT: No detectible tumor.

<sup>2</sup> Tumor too small to weigh, but was detected with *in vivo* imaging.

<sup>3</sup> Animals were allowed to grow for an additional 60 days post cell injection.

Table 9. Upregulation of *dppa5*, *cryaB*, *cdh3*, and *sox-2* following 5-aza-2-deoxycytidine treatment.

Gene	5AZA p6[1]	5AZA p6[2]	SRC-No- Treat-P6- [1]	SRC-No- Treat-P6- [2]	SRC-No- Treat-P6- [3]	gene ID	Description
<i>Dppa5</i>	594	1057	63	53	64	301101	developmental pluripotency associated 5
<i>CryaB</i>	12897	13078	1465	3596	1378	25420	crystallin, alpha B
<i>Cdh3</i>	1128	1645	163	231	165	116777	cadherin 3, type 1, P-cadherin (placental)
<i>Sox2</i>	7700	7380	1000	630	1001	499593	SRY (sex determining region Y)-box 2

Note: Upregulation of *Dppa5*, *CryaB*, *Cdh3*, and *Sox2* following 5-aza-2-deoxycytidine treatment. Expression values extracted from normalized microarray data.

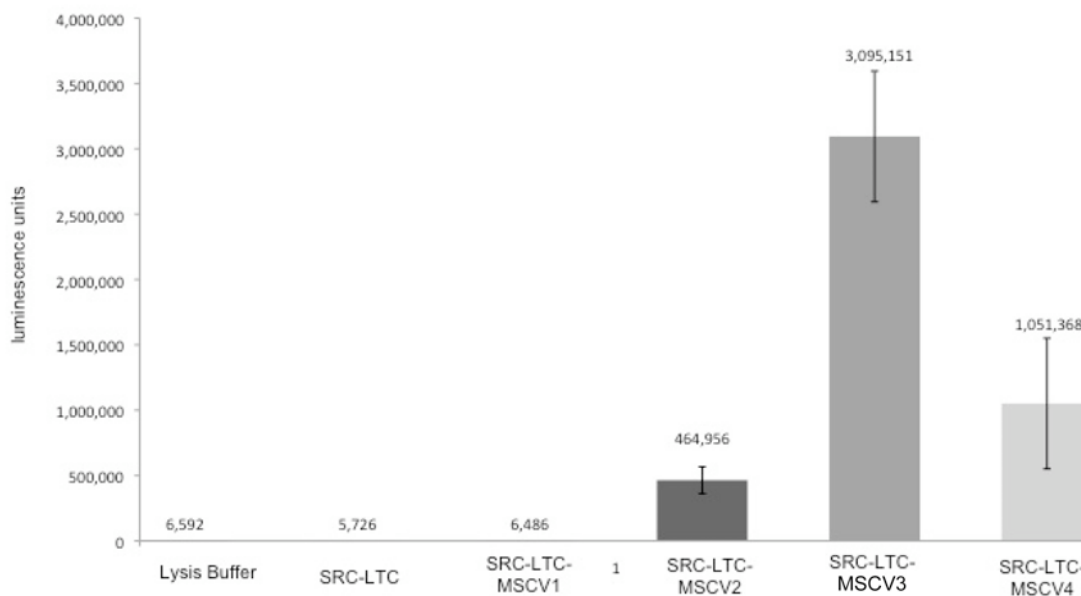


Figure 13. Expression of luciferase in a SRC cell line. SRC cells were transduced with a retrovirus containing the MSCV-Luc-I-Hyrgo plasmid (see Materials and methods). The number of transductions ranged from a single transduction to four transductions. Multiple transductions were done on consecutive days. Following antibiotic selection, the cell lines were tested for luciferase activity. The cell line with the highest luciferase activity was selected for use in subsequent experiments (SRC-LTC-MSCV3). The average luminescence signal is listed above each bar on the graph (the average was calculated from at least 5 biologic replicates).

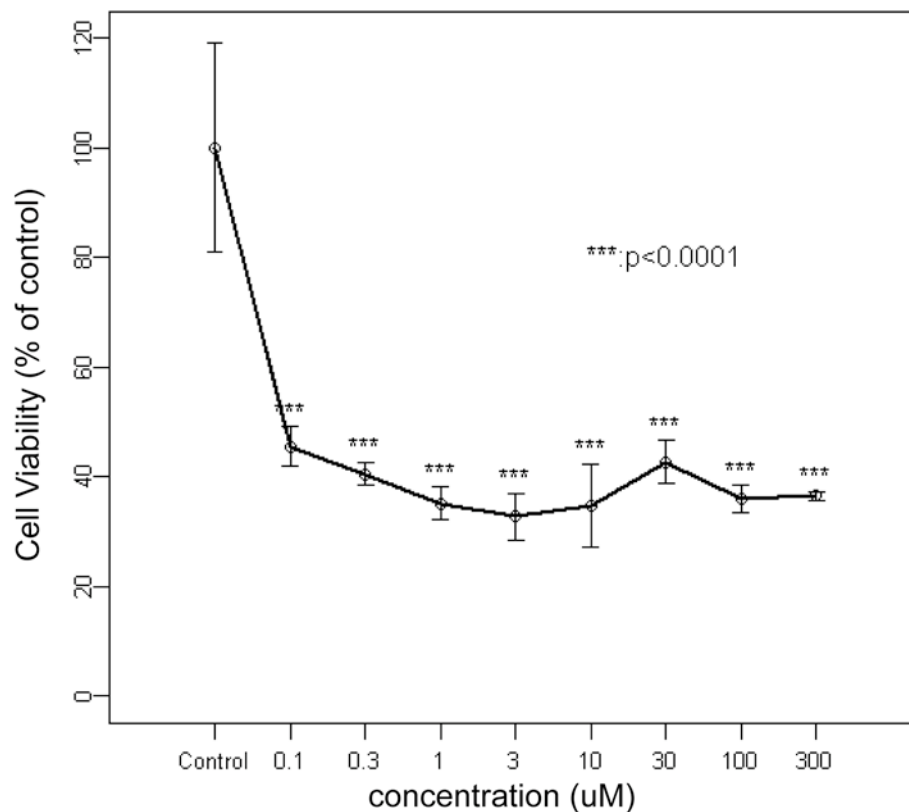


Figure 14. Percent viability of SRC cells following 72-hour incubation with 5-Aza-2-deoxycytidine. Percent viability of SRC cells 72-hours following treatment with 0, 0.1, 0.3, 1.0, 3.0, 10, 30, 100, and 300uM 5-Aza-2-deoxycytidine. Each point on the graph represents the average viability of three biologic replicates, and the error bars represent the standard deviation of the biologic replicates. “\*\*\*” indicates a significant difference between a given sample and the control sample (0.0uM: no treatment).

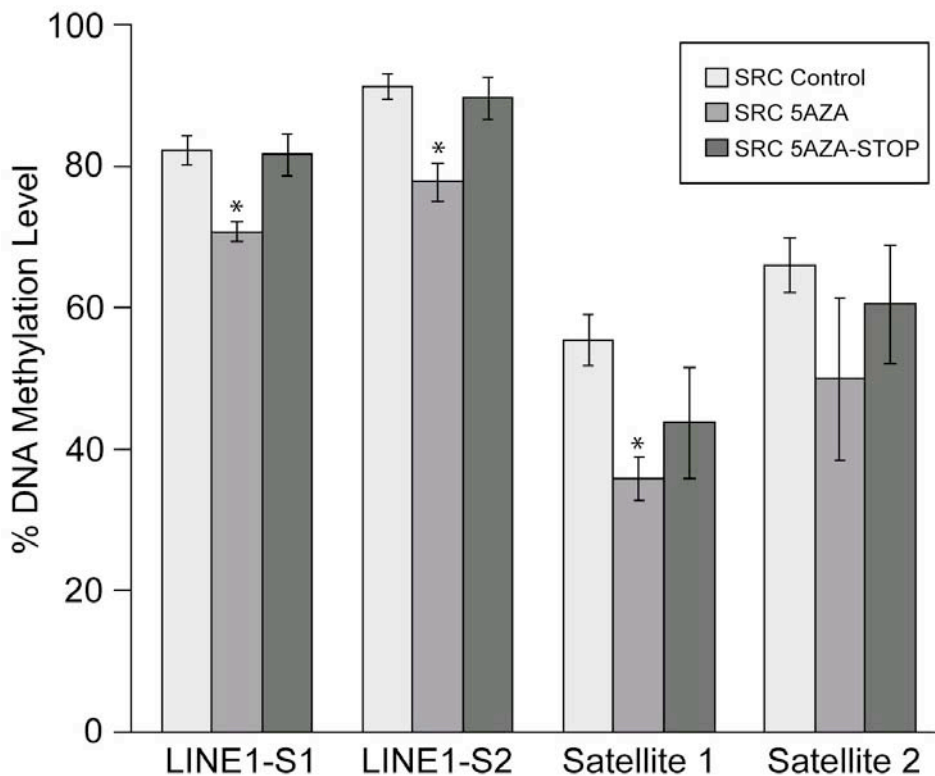


Figure 15. Pyrosequencing of LINE and Satellite 1 and 2 *in vitro*. For each experiment the methylation pattern was analyzed in SRC untreated control cells (SRC-Control), SRC cells treated with 5-Aza-2-deoxycytidine for 5 passages (SRC 5AZA), and in SRC cells that were treated with 5-Aza-2-deoxycytidine for 5 passages and then allowed to grow for 5 additional passages without treatment (SRC 5AZA-STOP). Pyrosequencing assay: LINE1-S1; [2481 CpG's], LINE1-S2; [3308 CpG's]; Satellite I [15CpG's], and Satellite II [411 CpG's]. Treatment of MSCV3-LTC chondrosarcoma cells with 5-Aza-2-deoxycytidine leads to demethylation that can be detected throughout the genome. Altered DNA methylation patterns can be detected several weeks following removal of 5-Aza-2-deoxycytidine treatment. Bars represent the average DNA methylation % of biologic replicates, and error bars represent the standard deviation of these replicates. "\*" Indicates values that are significantly different than the "SRC Control" sample ( $p < .05$ ).

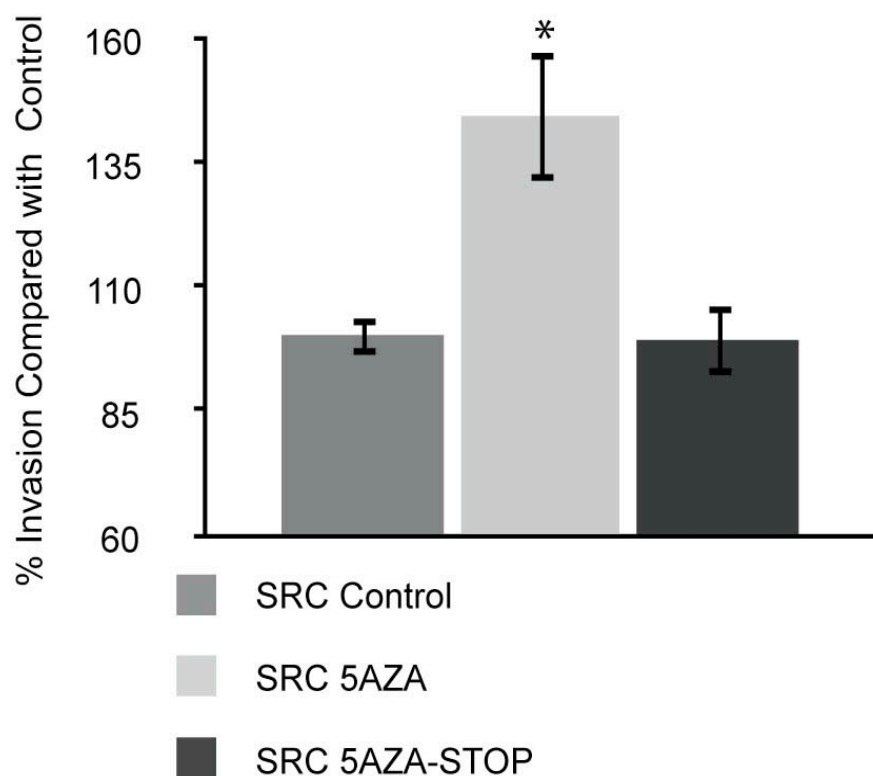


Figure 16. 5-Aza-2-deoxycytidine treatment increases the invasiveness of rat chondrosarcoma cells. Invasiveness was measured in control SRC cells (SRC Control), SRC cells that were treated for 5 passages with 5-Aza-2-deoxycytidine (SRC 5AZA), and SRC cells 5-with 5 passages Aza-2-deoxycytidine and then grown for 5 additional passages without treatment (5AZA-STOP). The invasiveness was calculated for all samples and the results are displayed as experimental sample compared to the untreated control SRC cells (100% invasion). The bar represents the average invasion indices of biologic replicates, and the error bars represent the standard deviation of the biologic replicates. ‘\*’ Indicates values that are significantly different than the “SRC Control” sample ( $p < .05$ ).

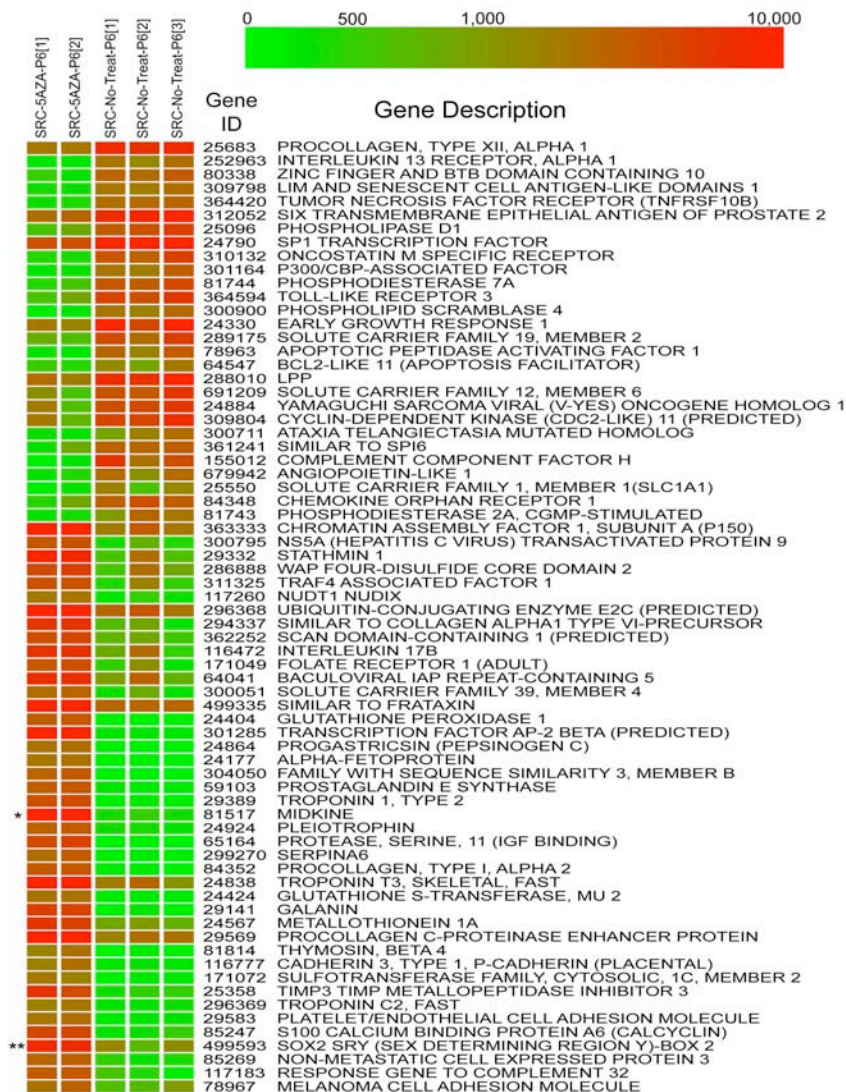


Figure 17. Heat map of differentially expressed genes between SRC cells treated 5-Aza-2-deoxycytidine and untreated control SRC cells. Genes with at least a 5-fold difference were selected for analysis using the pathway program Ingenuity. Ingenuity revealed that, of the 977 differentially expressed genes (603 genes upregulated and 374 downregulated), 135 were identified as cancer related. A subset of these cancer related genes (see Materials and methods; see Appendix E for complete gene list and expression values) was then used for hierarchical clustering, and the results of that clustering are presented in this figure. Each vertical column represents microarray hybridizations from separate individual experiments. Microarray hybridizations were carried out on SRC cells treated with 5-Aza-2-deoxycytidine for 5 passages (SRC-5-AZA-P6 [1] and [2]), and microarray hybridizations were also carried out on SRC cells grown for 5 passages without 5-Aza-2-deoxycytidine treatment (SRC-No-Treat-P6 [1], [2], and [3]). ‘\*’ Indicates midkine and ‘\*\*’ indicates sox-2 in the heat map. The color bar corresponds to the expression level in relative fluorescent units.

### Expression of Midkine in 5-Aza-2-deoxycytidine treated SRC cells

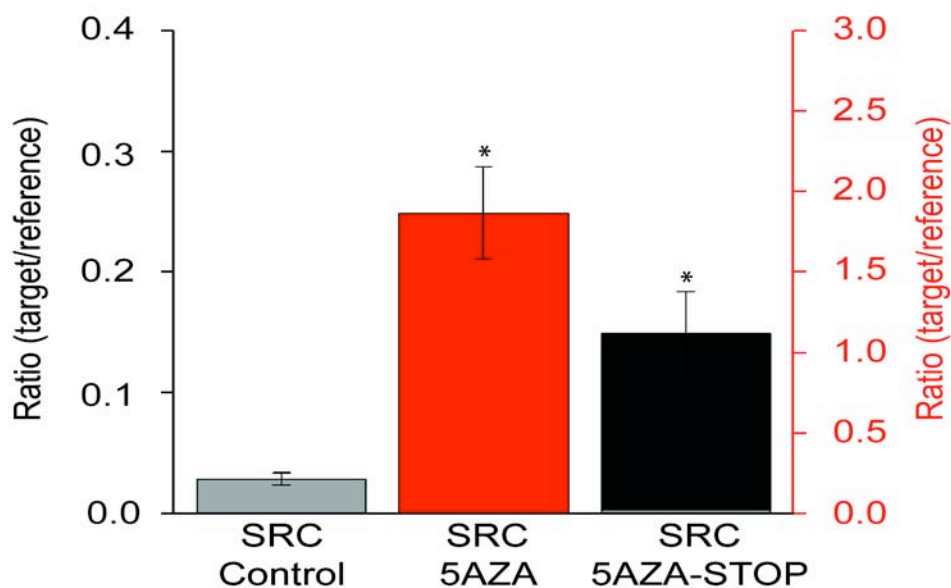


Figure 18. Expression analysis of midkine. Quantitative real time PCR analysis of midkine expression in control SRC cells (SRC Control), SRC cells that were treated for 5 passages with 5-Aza-2-deoxycytidine (SRC 5AZA), and SRC cells 5-with 5 passages Aza-2-deoxycytidine and then grown for 5 additional passages without treatment (5AZA-STOP). Treatment with 5-Aza-2-deoxycytidine induces midkine expression. Five passages following 5-Aza-2-deoxycytidine removal the expression of midkine has dropped but it is greater than that of untreated control cells. Bars represent the average expression of three biologic replicates, and error bars represent the standard deviation of these replicates. ‘\*’ Indicates values that are significantly different than the “SRC Control” sample ( $p < .05$ ). Note that for graphical representation two different vertical scale bars are shown; the vertical scale bar on the left corresponds to the SRC Control and SRC 5AZA-STOP samples, and the vertical Scale bar on the right corresponds with the SRC 5AZA-STOP sample.

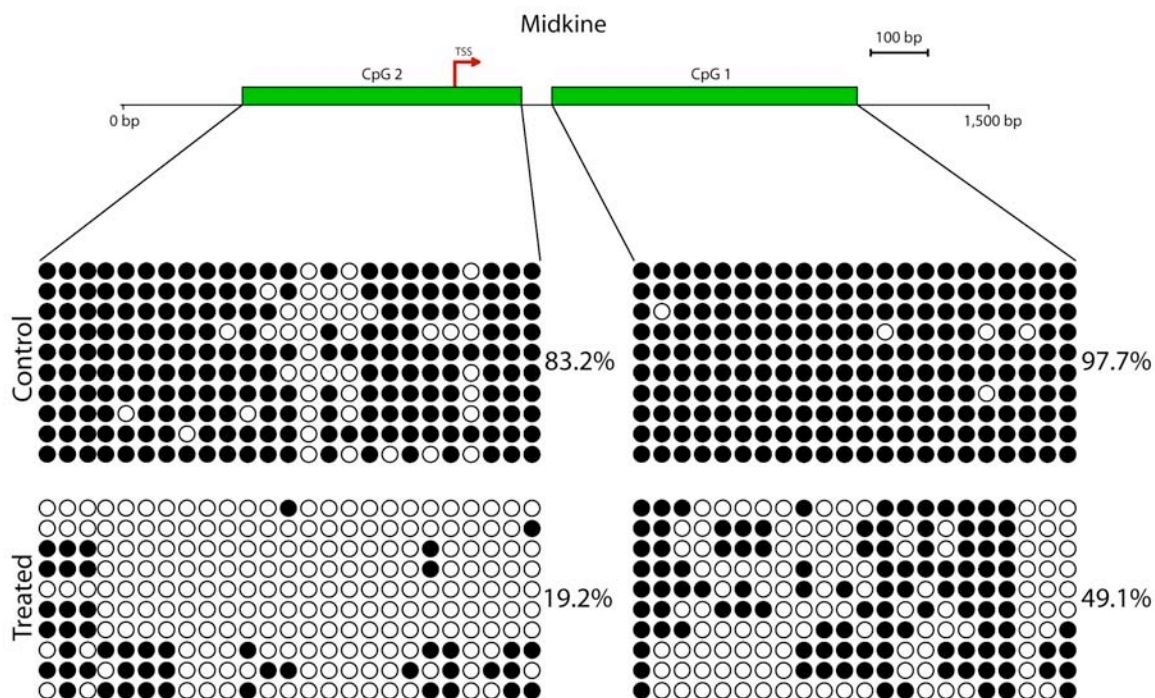


Figure 19. Epigenetic analysis of Midkine methylation in SRC cells. Schematic representation of analyzed CpG islands in relation to the midkine transcriptional start site (TSS). Green bars indicate regions that were targeted for bisulfite sequencing. Bisulfite sequencing of midkine CpG Island 1 and CpG Island 2. Each row indicates an individual cloned sequence. Circles represent CpG sites. Black circles indicate a methylated CpG site and white circles indicate an unmethylated CpG site. These results demonstrate that 5-Aza-2-deoxycytidine treatment leads to the hypomethylation of CpG islands that span regions of the rat midkine gene.

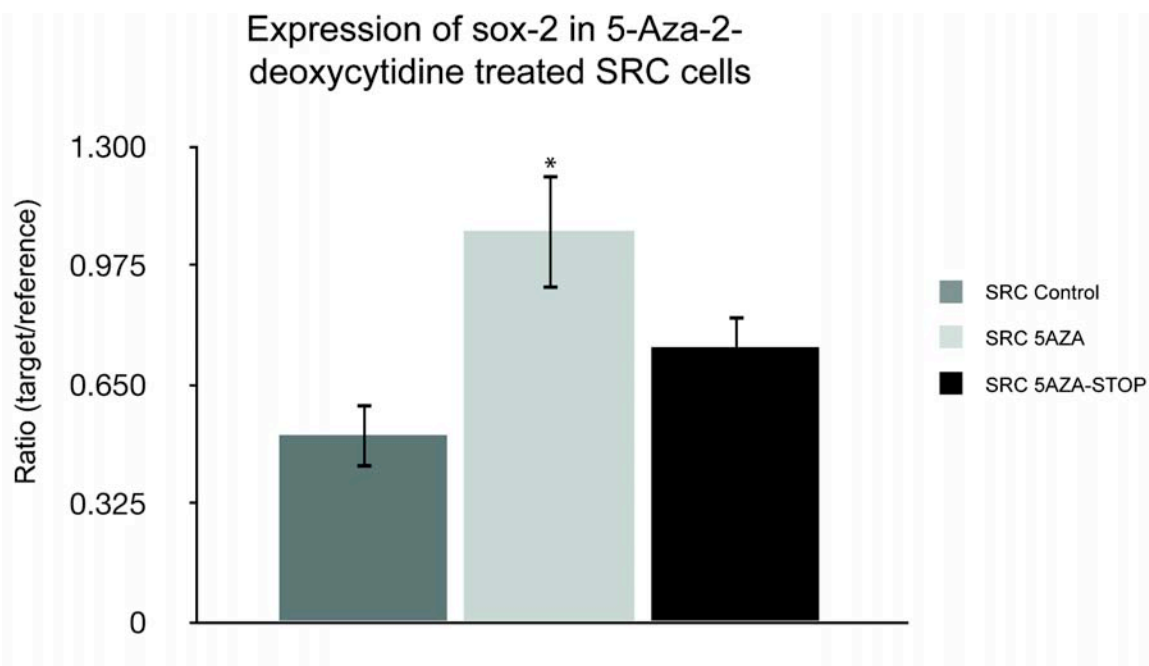


Figure 20. Expression analysis of sox-2 in SRC cells. Quantitative real time PCR analysis of sox-2 expression in control SRC cells (SRC Control), SRC cells that were treated for 5 passages with 5-Aza-2-deoxycytidine (SRC 5AZA), and SRC cells 5-with 5 passages Aza-2-deoxycytidine and then grown for 5 additional passages without treatment (5AZA-STOP). Treatment with 5-Aza-2-deoxycytidine induces sox-2 expression. Five passages following 5-Aza-2-deoxycytidine removal the expression of sox-2 has dropped. Bars represent the average expression of three biologic replicates, and error bars represent the standard deviation of these replicates. ‘\*’ Indicates values that are significantly different than the “SRC Control” sample ( $p < .05$ ).

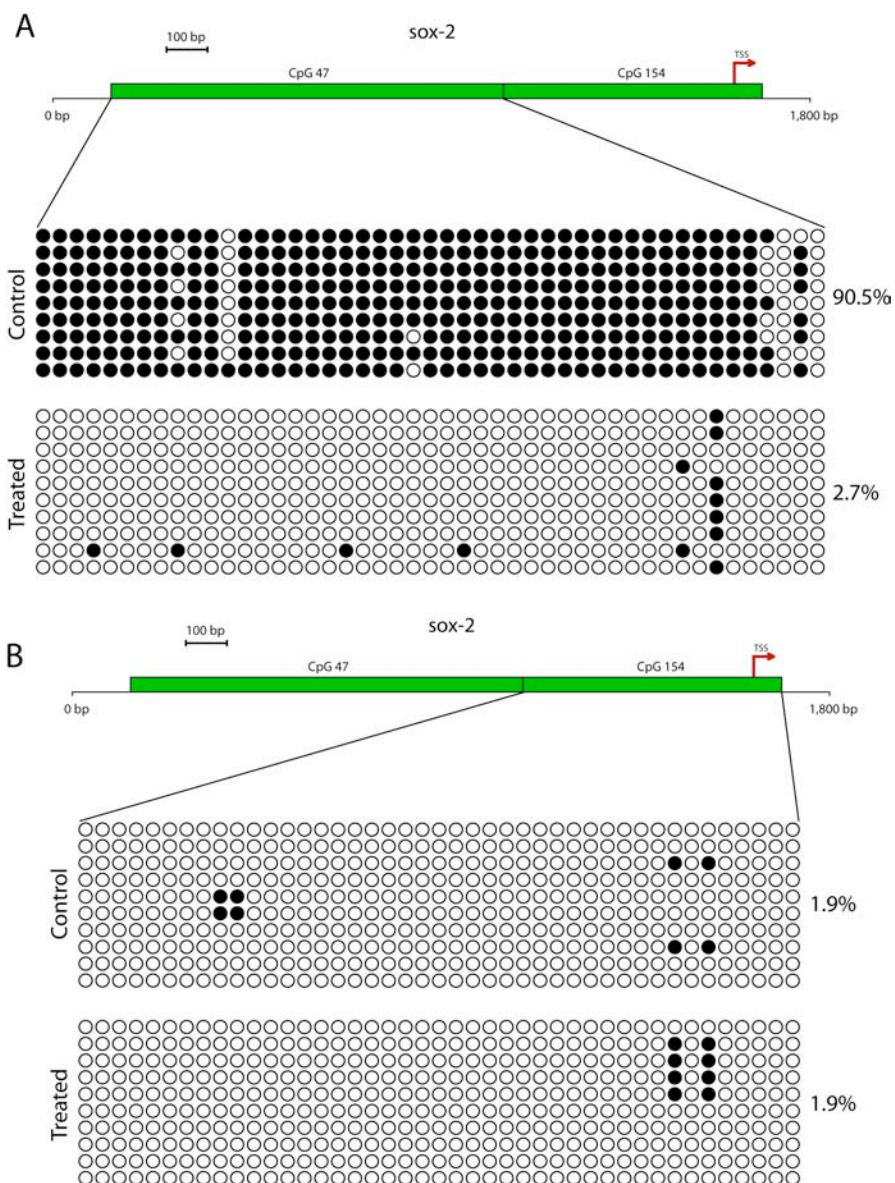


Figure 21. Epigenetic analysis of *sox-2*. Schematic representation of analyzed CpG islands in relation to the *sox-2* transcriptional start site (TSS). Green bars indicate regions that were targeted for bisulfite sequencing. Bisulfite sequencing of *sox-2* CpG Island 47 and CpG Island 154. Each row indicates an individual cloned sequence. Circles represent CpG sites. Black circles indicate a methylated CpG site and white circles indicate an unmethylated CpG site. (A) CpG 47 Island was methylated in untreated SRC cells but following 5-Aza-2-deoxycytidine treatment it became hypomethylated. (B) CpG Island 154 was not methylated in either control or treated cells.

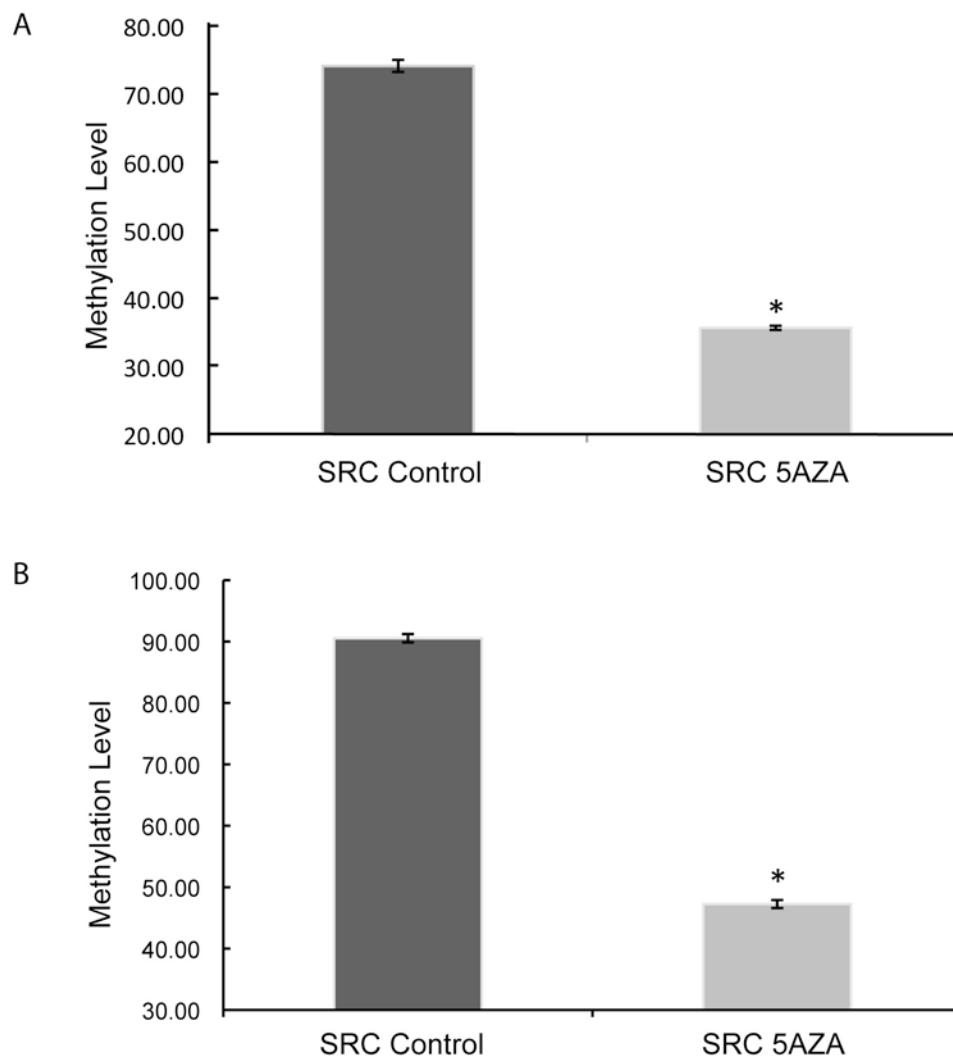


Figure 22. Pyrosequencing of the midkine and sox-2 promoter. CpG sites in the midkine (A) and sox-2 (B) promoter sequence are methylated in untreated SRC cells but following 5-Aza-2-deoxycytidine treatment they become hypomethylated. The promoter regions of midkine and sox-2 were analyzed for DNA methylation status. Pyrosequencing was used to analyze bisulfite treated DNA with primers specific for midkine or sox-2. The bar represents the average DNA methylation of technical replicates, and the error bars represent the standard deviation of the technical replicates. '\*' Indicates that the values are significantly different than the "SRC Control" sample ( $p < .05$ ). Five CpG sites were examined with the midkine promoter analysis. Eight CpG sites were examined in the sox-2 analysis.

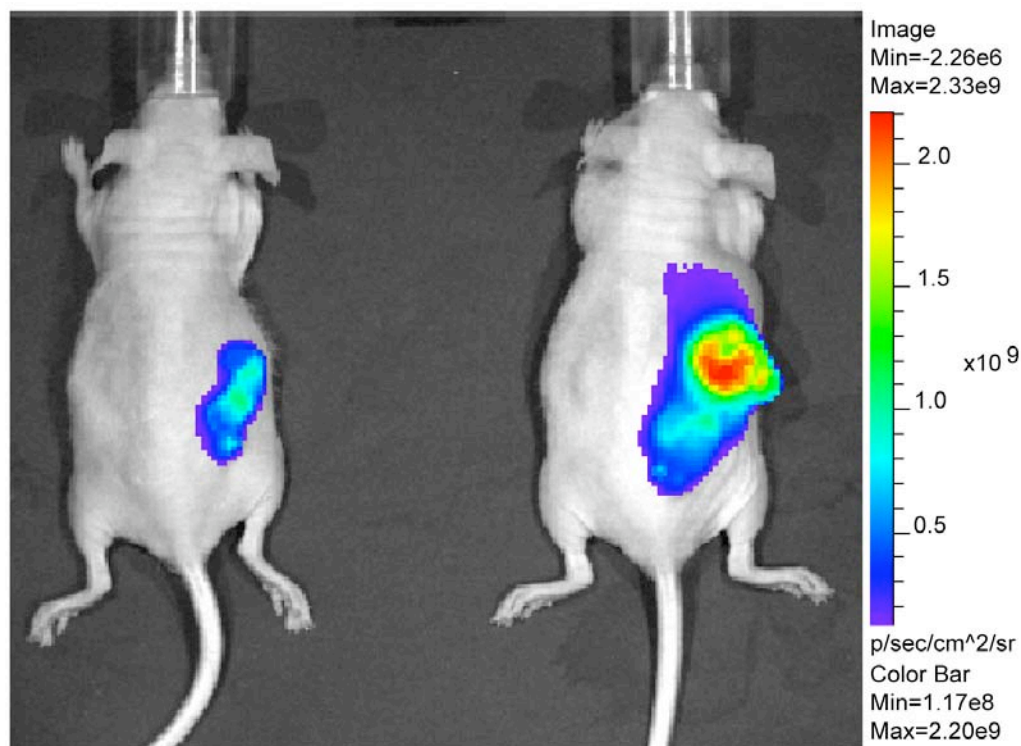


Figure 23. 5-Aza-2-deoxycytidine treated SRC cells produced larger tumors than untreated SRC cells. (A) *In vivo* bioluminescent imaging of SRC cells in nude mice.  $5 \times 10^6$  Control cells [animal a; left] and  $5 \times 10^6$  5-Aza-2-deoxycytidine treated cells [animal B; right] were injected subcutaneously. This image was collected 6 weeks after tumor induction. This Image corresponds to animal 3a and 3b in Table 8.

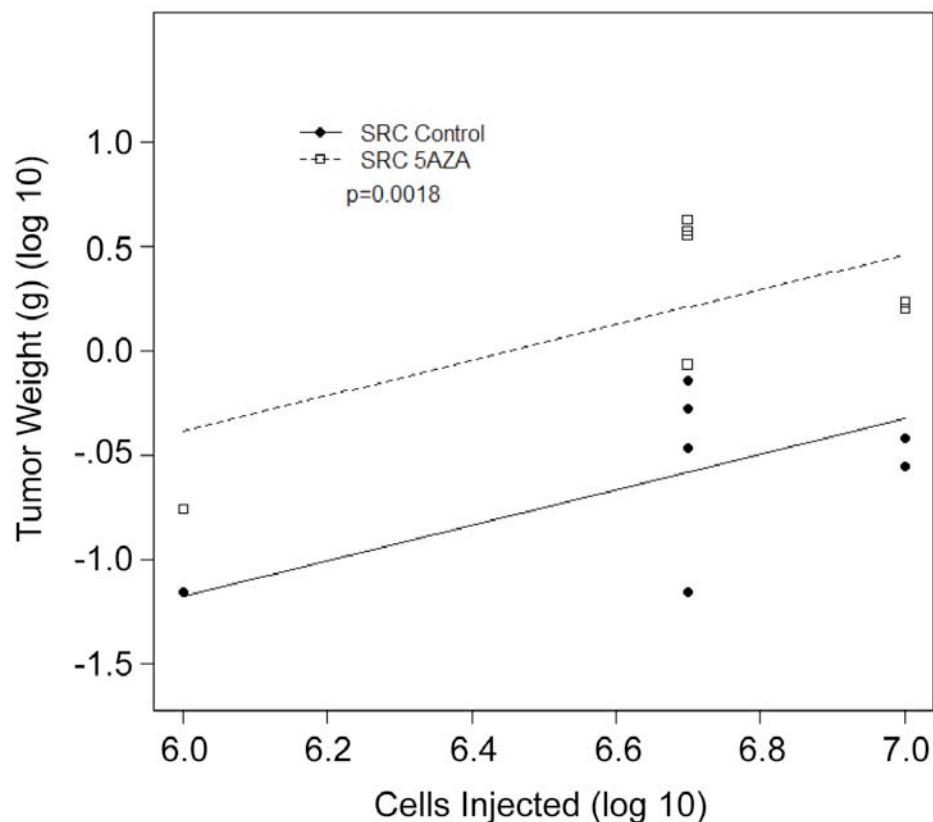


Figure 24. Summary of *in vivo* SRC injections. Tumors induced with 5-Aza-2-deoxycytidine-treated SRC cells produced larger tumors than the tumors induced with SRC control cells. A linear regression method was applied to analyze tumor weight between two tumor groups (SRC Control and SRC 5AZA) after adjusting for the number of cells injected. For graphical representation the tumor weights and the number of cells injected was log transformed. p-value is for comparison of the two tumor groups (SRC Control and SRC 5AZA), and indicates that there is a significant difference in tumor weight between the two groups. Results are shown for 7 animals with tumors induced from untreated cells (SRC control) and for 7 animals with tumors induced from 5-Aza-2-deoxycytidine-treated cells (SRC 5AZA). Detailed *in vivo* tumor summary is presented in Table 8.

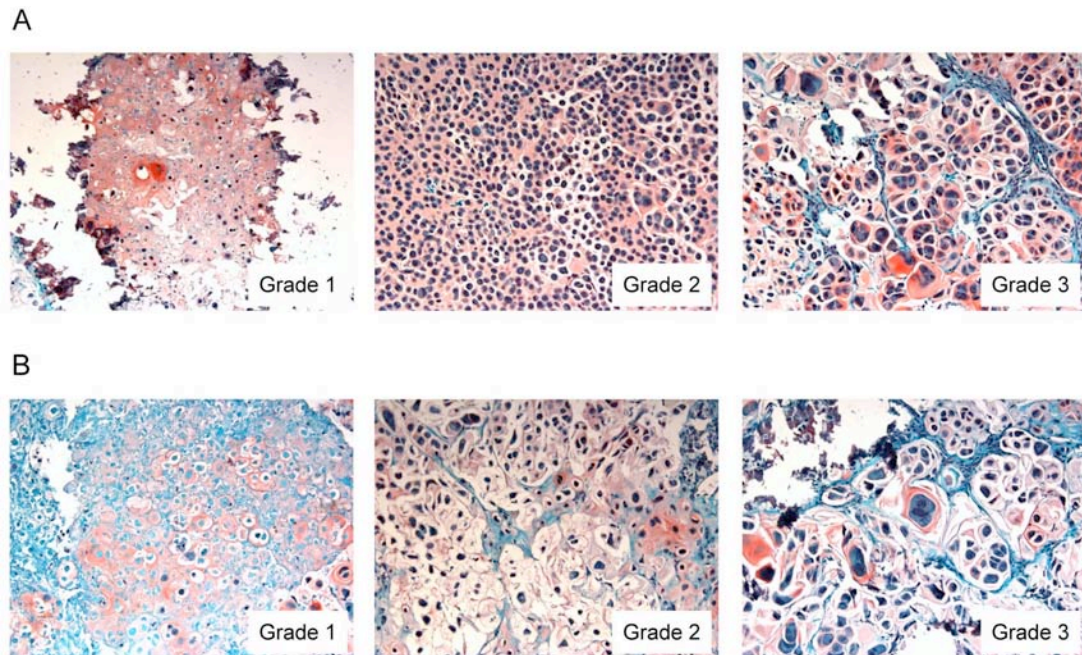


Figure 25. Photomicroscopy of histological sections obtained from SRC tumors (20x magnification). (A) Subcutaneous tumor induced from untreated SRC control cells. (B) Subcutaneous tumor induced from 5-Aza-2-deoxycytidine SRC cells. Approximately 60 days following tumor induction animals were sacrificed and tumors were removed for histology. Tumors from the SRC control cells and the 5-Aza-2-deoxycytidine cells showed considerable heterogeneity. There was no clear histological difference between tumors initiated from control cells or treated cells. Low grade (Grade 1) – Small nuclei with low variation in size and abundant cartilage matrix. Intermediate grade (Grade 2) – Higher cellularity, larger nuclei with increased atypia and hyperchromasia. High grade (Grade 3) – Pleomorphic cells with greater degree atypia and nuclear size. The SRC cells are stained with Safranin O (red).



Figure 26. Macrometastasis detected in the lungs of mice injected with 5-Aza-2-deoxycytidine treated SRC cells. Macrometastases were detected in 3 of 9 animals injected with 5-Aza-2-deoxycytidine treated cells, but no macrometastases were detected in the lungs of mice injected with untreated cells. Metastases of varying size were detected in the in the lungs of the same animal. The SRC tumor cells form nodules of different sizes and resemble hyaline cartilage. Lungs from 3 separate mice are displayed in the figure.

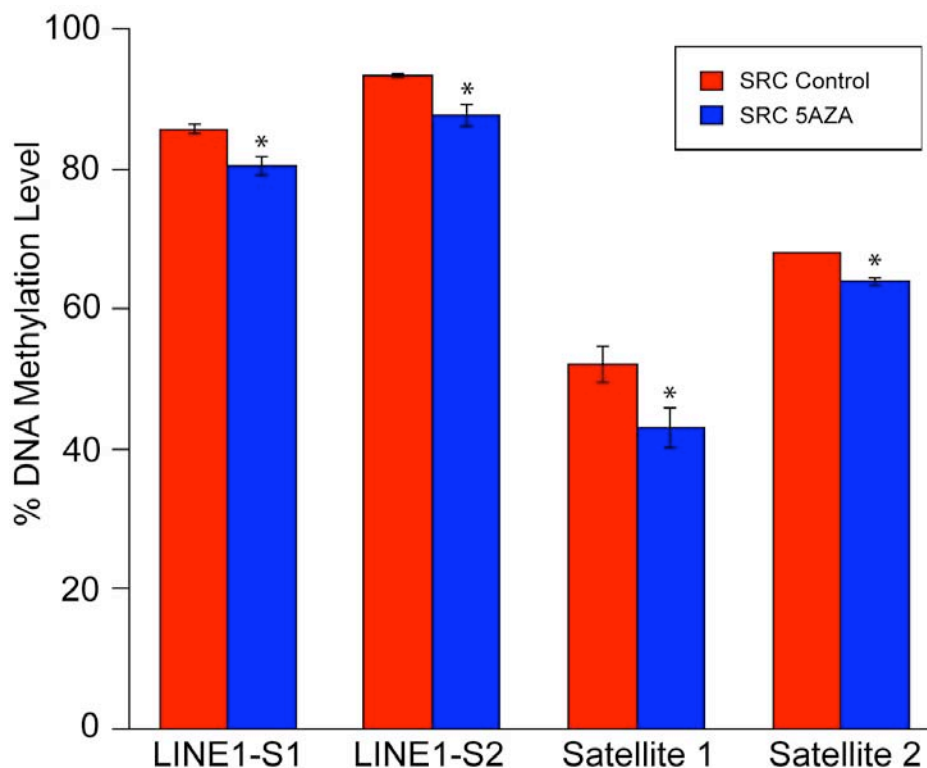


Figure 27. Pyrosequencing of LINE and Satellite 1 and 2 *in vivo*. Pyrosequencing results are also displayed from tumor samples: tumors initiated from untreated SRC cells (SRC Control) and tumors initiated from SRC cells that were treated for 5 passages with 5-Aza-2-deoxycytidine (SRC 5AZA). Results are shown for 3 SRC Control tumors and 3 SRC 5AZA tumors. Pyrosequencing assay: LINE1-S1; [2481 CpG's], LINE1-S2; [3308 CpG's], Satellite I [15CpG's], Satellite II [411 CpG's]. In all regions examined by pyrosequencing the SRC 5AZA tumors have a significantly lower level of methylation than the SRC Control tumors. Bars represent the average DNA methylation % of biologic replicates, and error bars represent the standard deviation of these replicates. "\*" Indicates values that are significantly different than the "SRC Control" sample ( $p < .05$ ).

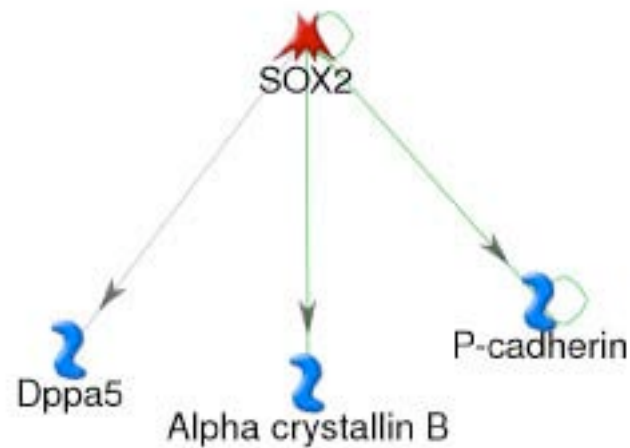


Figure 28. Identification of Sox-2 regulated genes. Genes with a 5-fold difference between control and 5-Aza-2-deoxycytidine treated cells were imported into the pathway program GeneGO. GenGO identified a network whereby sox-2 putatively activates the expression of Dppa5, Alpha crystallin B, and P-cadherin. Microarray data demonstrates that Dppa5, CryaB, Cdh3, and Sox2 are upregulated following 5-aza-2-deoxycytidine treatment (Table 9). The relative expression ratios of Dppa5, Alpha crystallin B, and P-cadherin are similar to that of sox-2, suggesting that sox-2 may play a role in the regulation of these genes.

## CHAPTER IV

### CONCLUSION

Over 1.4 million new cases of cancer are diagnosed each year in the United States, and it is estimated that more than half a million people die each year to this disease (Jemal et al. 2008). Research is needed to uncover the molecular mechanisms underlying tumorigenesis and metastasis so that non-invasive, sensitive methods can be developed for improved detection, diagnosis, prognosis, and ultimately for safer and more effective treatment of cancer.

In this thesis we characterize a rat model (SRC: Swarm rat chondrosarcoma) of human cancer chondrosarcoma, with the goal of attaining a greater understanding of the molecular basis for its development and progression. Specifically, we examined the impact of genome-wide hypomethylation and the contribution of the tumor microenvironment in the SRC model. The microenvironment has a direct impact on tumor cells and epigenetic alterations constitute a hallmark of cancer (Hanahan and Weinberg 2000). Albeit regarded as a common epigenomic alteration in cancer (Pogribny and Beland 2009), the genome-wide pattern of DNA hypomethylation and its consequence to tumorigenesis are still poorly understood.

Previous studies indicated that the SRC tumor microenvironment can influence SRC malignancy (Kenan and Steiner 1991). However, no studies had previously examined its biologic basis. To address this issue we carried out epigenetic and gene expression studies on the SRC tumors that were initiated at different transplantation sites. Global methylation analysis revealed that the DNA of the SRC tumor was hypomethylated compared to that of normal tissue, and it also revealed that the tumor transplantation site influenced the extent of DNA hypomethylation.

To complement the epigenetic analysis, SAGE (Velculescu et al. 1995) was used to derive gene expression profiles from the SRC tumors. This study revealed that the

gene expression profiles of the SRC tumors were unique to each transplantation site. We identified several site-specific alterations in gene expression that may contribute to the increase in malignancy that is observed in SRC tumors grown in the tibia. For example, the expression of mRNAs coding for structural extracellular matrix proteins decreased, and that of proteases increased in SRC tumors. Changes to the extracellular matrix are necessary for tissue invasion and metastasis (Hanahan and Weinberg 2000), and these gene expression alterations may contribute to the invasive phenotype of the tibia SRC tumors (Kenan and Steiner 1991). Such alterations in gene expression of extracellular matrix proteins have also been observed in human chondrosarcoma (Aigner et al. 2002), which provides further evidence for the similarity between the SRC rat model and human chondrosarcoma.

Additional analysis revealed changes in the expression of genes regulating skeletal development, cell proliferation and cell motility. Expression of two of these genes, c-fos and thymosin- $\beta$ 4, has been documented in human chondrosarcoma (Papachristou et al. 2005). These genes have been implicated in several aspects of tumorigenesis (Cha et al. 2003; Kobayashi et al. 2002; Tuckermann et al. 2001). To investigate the role of these genes, we independently overexpressed c-fos and thymosin- $\beta$ 4 in a SRC cell line. Overexpression of neither c-fos nor thymosin- $\beta$ 4 affected tumorigenesis based on average tumor weights. It is noteworthy, however, that multiple lung metastases were detected in one animal with a thymosin- $\beta$ 4-overexpressing tumor. More studies are needed to determine the significance of this finding but, the detection of SRC lung metastases is in agreement with previous studies that indicated that thymosin- $\beta$ 4 can regulate tumor cell motility and metastasis (Kobayashi et al. 2002).

Taken together these studies indicate that the microenvironment can induce significant alterations in the epigenetic and gene expression profiles of SRC tumors, which in turn affect tumorigenesis.

In the third chapter of this thesis we examined the influence of DNA hypomethylation on SRC tumorigenesis. The occurrence of DNA hypomethylation in tumors is well documented (Jones and Baylin 2002). DNA hypomethylation can lead to genomic instability (Howard et al. 2008), and it may also result in the expression of genes that should otherwise be silenced (Pogribny and Beland 2009). Evidence suggests that hypomethylation promotes tumor formation, but the role of DNA hypomethylation in chondrosarcoma is unclear. In the second chapter we examined the methylation profiles of the SRC tumors. Interestingly, we found that the tumor most aggressive tumor, that which was grown in the tibia, was also the most hypomethylated.

To further investigate the role of DNA hypomethylation in tumorigenesis we induced DNA hypomethylation with 5-Aza-2'-deoxycytidine. 5-Aza-2'-deoxycytidine inhibits DNA methyltransferases (Chen et al. 1991) thus leading to reduced levels of DNA methylation (Mund et al. 2005).

5-Aza-2'-deoxycytidine was used to induce DNA hypomethylation in the SRC cells. The resulting decrease in methylation was accompanied by an increase in the invasiveness of the SRC cells. *In vitro*, methylation was reestablished following removal of 5-Aza-2'-deoxycytidine. Once reestablished, the invasiveness of the cell line returned to a level similar to that observed in control cells. *In vivo*, DNA hypomethylation led to the formation of tumors that were more aggressive than those derived from control cells.

Microarray analysis revealed that DNA hypomethylation induced several gene expression alterations in the SRC cells. Two of these genes, midkine and sox-2, were selected for further analysis based on their differential expression and putative role in tumorigenesis (Kato et al. 2000; Sanada et al. 2006; Tanabe et al. 2008). Analysis of the promoter regions of these genes revealed the presence of CpG dinucleotides that were methylated prior to but not post treatment with 5-Aza-2'-deoxycytidine. This result suggests that both midkine and sox-2 genes may be epigenetically regulated and that their

expression may contribute to the increased tumorigenicity that is observed following treatment with 5-Aza-2'-deoxycytidine.

Although 5-Aza-2-deoxycytidine has previously been shown to have clinical benefits in the treatment of specific forms of leukemia (Plimack et al. 2007), our results suggest that 5-Aza-2-deoxycytidine treatment may promote certain aspects of tumorigenesis in SRC cells. The clinical benefits of 5-Aza-2-deoxycytidine are thought to be mediated by the drug's ability to induce DNA hypomethylation. However, it has been shown that chromosomal instability and tumor formation are also promoted by genome-wide loss in DNA methylation (Eden et al. 2003). Additionally, 5-Aza-2-deoxycytidine has been shown to induce DNA damage (Juttermann et al. 1994; Palii et al. 2008). Our studies in SRC cells demonstrate that 5-Aza-2-deoxycytidine treatment can lead to the induction of genes that can regulate pluripotency in stem cells (Figure 28). The expression of pluripotency related genes may lead to the activation of transcriptional programs that could confer stem cell-like properties to the tumor cells (Schoenhals et al. 2009), and this would ultimately promote further tumor progression. Taken together, our results highlight the potential negative impact that epigenetic drugs may have on tumor outcome. Experimental treatment of other tumor types with 5-Aza-2-deoxycytidine should therefore be done with great caution.

Overall this thesis demonstrates that the tumor microenvironment can induce epigenetic alterations and changes in gene expression in the SRC cells. Subsequent functional analysis of differentially expressed genes provided insight into the role that two genes, *c-fos* and *thymosin- $\beta$ 4*, may play in chondrosarcoma tumorigenesis. This thesis also demonstrates that DNA hypomethylation can promote aspects of chondrosarcoma tumorigenesis. These changes in tumorigenesis may be mediated by the expression of genes that are epigenetically silenced in normal cells. Interestingly, *thymosin- $\beta$ 4* was found to be upregulated in both the SAGE data derived from SRC tumors, and the microarray data obtained from hypomethylated SRC cells. Examination

of the thymosin- $\beta$ 4 promoter revealed that both human and rat thymosin- $\beta$ 4 genes have CpG islands in their promoter regions (Figure 29), thus suggesting that thymosin- $\beta$ 4 expression in chondrosarcoma cells may be epigenetically regulated by DNA methylation.

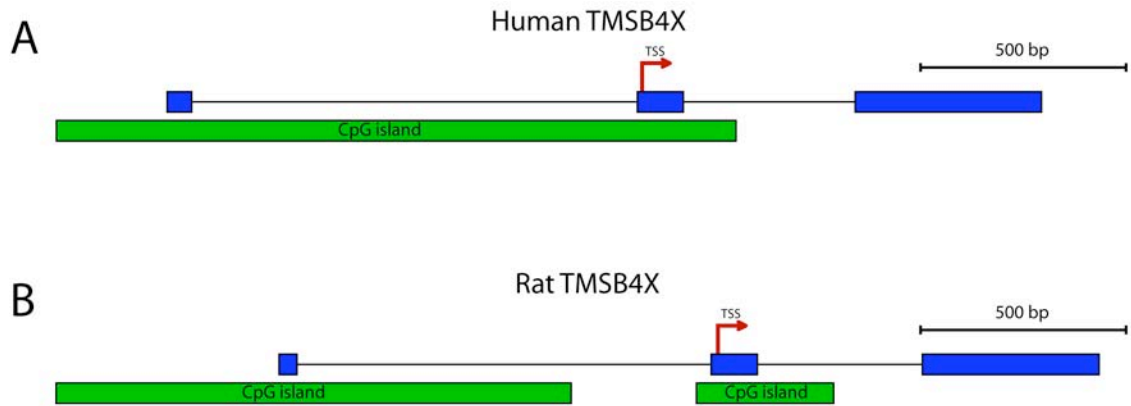


Figure 29. Schematic representation of the thymosin- $\beta$ 4 promoter. The thymosin- $\beta$ 4 promoter sequence in human (A) and rat (B) was examined for CpG islands. CpG islands were found to cover the first two exons of the thymosin- $\beta$ 4 gene in both species. Diagram is drawn to scale. Blue boxes represent exons. The green boxes represent the location of the CpG islands.

## APPENDIX A COMPLETE SAGE DATA

The gene expression data generated with the SAGE experiments are provided in Appendix A. The data is presented as a table. The first row of the table describes each column of the table. Each subsequent row corresponds to a single SAGE tag. Each tag is identified by its 10 base-pair nucleic acid sequence. The adjacent columns provide the expression value for each tag in a given SAGE library. The raw expression data and the normalized expression values are given for each SAGE library (for the normalized data the tags were normalized to 100,000 tags/library). For each SAGE tag, the Unigene number and gene name description are given if known.

This SAGE data file is documented as a file named Appendix\_A with Microsoft Excel, and stored in the attached DVD.

## APPENDIX B DIFFERENTIALLY EXPRESSED SAGE TAGS

The complete list of differentially expressed genes obtained from the comparison of “Rat Normal Cartilage” vs. all 3 SRC SAGE libraries (“Subcutaneous SRC tumor”, “Tibia SRC tumor”, and “Lung SRC tumor”) is provided in Appendix B. The criteria for selection was as follows:  $z\text{-value} > 1.96$  (for differential gene expression) and expression of at least 25 tags in one SAGE library. The data is presented as a table. The first row of the table describes each column of the table. Each subsequent row corresponds to a single SAGE tag. Each tag is identified by its 10 base-pair nucleic acid sequence. The adjacent columns provide the expression value for each tag in a given SAGE library. For each SAGE tag, the Unigene number and gene name description are given if known.

This SAGE data file is documented as a file named Appendix\_B with Microsoft Excel, and stored in the attached DVD.

## APPENDIX C GENE LIST OF UNIQUE SAGE PROFILES

The complete list of differentially expressed genes for the following comparisons are presented in Appendix C: “Subcutaneous SRC tumor” vs. “Tibia SRC tumor” and “Lung SRC tumor”, “Tibia SRC tumor” vs. “Subcutaneous SRC tumor” and “Lung SRC tumor”, and “Lung SRC tumor “ vs. “Subcutaneous SRC tumor” and “Tibia SRC tumor”. The criteria for selection was as follows:  $z\text{-value} > 1.96$  (for differential gene expression) and expression of at least 25 tags in one SAGE library. The first row of the table describes each column of the table. Each subsequent row corresponds to a single SAGE tag. Each tag is identified by its 10 base-pair nucleic acid sequence. The adjacent columns provide the expression value for each tag in a given SAGE library. For each SAGE tag, the Unigene number and gene name description are given if known.

This SAGE data file is documented as a file named Appendix\_C with Microsoft Excel, and stored in attached DVD. Each tab of the spreadsheet corresponds to an as specific comparison of expression data as follows: Tab 1=“Subcutaneous SRC tumor” vs. “Tibia SRC tumor” and “Lung SRC tumor, Tab 2= “Tibia SRC tumor” vs. “Subcutaneous SRC tumor” and “Lung SRC tumor”, and Tab 3= “Lung SRC tumor “ vs. “Subcutaneous SRC tumor and “Tibia SRC tumor”.

## APPENDIX D COMPLETE MICROARRAY DATA

The complete microarray data for the gene expression experiment (Chapter III) is provided in Appendix D. The data for 5 microarray hybridizations is presented in a table. The five hybridizations: SRC-5AZA-1(treated sample), SRC-5AZA-2(treated sample), SRC-No-Treat-1(control sample), SRC-No-Treat-2(control sample), and SCR-No-Treat-3(control sample). The first row of the table describes the annotation for of each column of the table. The unique identifier for each set of probes on the microarray is listed under the column “SEQ\_IDs”. The annotation for each of the “SEQ\_IDs” is presented in the second tab of the excel workbook. For the expression analysis, a “SEQ\_ID” occupies the first column in a row, and the adjacent columns contain the expression values( Tab 1: Normalized data). The microarray was carried out using the NimbleGen microarray service. The *Rattus norvegicus* 1-plex array (14 probes/target; 26739 genes; cat#: A6184-00-01) was used for each hybridization.

All presented microarray data is MIAME compliant. The raw microarray data has been deposited in a MIAME compliant database. The microarray data has been deposited at the Gene Expression Omnibus database (GEO accession number: GSE17598).

This microarray data file is documented as a file named Appendix\_D with Microsoft Excel, and stored in the attached DVD.

APPENDIX E  
DIFFERENTIALLY EXPRESSED GENES IDENTIFIED  
BY MICROARRAY ANALYSES

The complete list of differentially expressed genes for the comparison of 5-AZA-2-deoxycytidine treated SRC-LTC cells (SRC-5AZA) vs. untreated SRC-LTC cells (SRC-No-Treat) are presented in Appendix E. For inclusion in this analysis the genes had to have a 5-fold difference between control and 5-Aza-2-deoxycytidine treated cells.

The data is presented as a table. The first row of the table describes each column of the table. Each subsequent row corresponds to a gene/set of probes on the microarray data. The first column lists the GenBank number. The adjacent columns provide the expression value for each tag in a given hybridization.

This microarray data file is documented as a file named Appendix\_E with Microsoft Excel, and stored in the attached DVD.

## REFERENCES

- Adams MD, Soares MB, Kerlavage AR, Fields C, Venter JC (1993) Rapid cDNA sequencing (expressed sequence tags) from a directionally cloned human infant brain cDNA library. *Nat Genet* 4: 373-80
- Adler CP, Herget GW, Neuburger M (1995) Cartilaginous tumors: prognostic applications of cytophotometric DNA analysis. *Cancer* 76: 1176-80
- Aigner T (2002) Towards a new understanding and classification of chondrogenic neoplasias of the skeleton--biochemistry and cell biology of chondrosarcoma and its variants. *Virchows Arch* 441: 219-30
- Aigner T, Muller S, Neureiter D, Illstrup DM, Kirchner T, Bjornsson J (2002) Prognostic relevance of cell biologic and biochemical features in conventional chondrosarcomas. *Cancer* 94: 2273-81
- Albini A, Sporn MB (2007) The tumour microenvironment as a target for chemoprevention. *Nat Rev Cancer* 7: 139-47
- Allfrey VG, Faulkner R, Mirsky AE (1964) Acetylation and Methylation of Histones and Their Possible Role in the Regulation of Rna Synthesis. *Proc Natl Acad Sci U S A* 51: 786-94
- Anisimov SV (2005) A large-scale screening of the normalized mammalian mitochondrial gene expression profiles. *Genet Res* 86: 127-38
- Argani P, Rosty C, Reiter RE, Wilentz RE, Murugesan SR, Leach SD, Ryu B, Skinner HG, Goggins M, Jaffee EM, Yeo CJ, Cameron JL, Kern SE, Hruban RH (2001) Discovery of new markers of cancer through serial analysis of gene expression: prostate stem cell antigen is overexpressed in pancreatic adenocarcinoma. *Cancer Res* 61: 4320-4
- Asp J, Inerot S, Block JA, Lindahl A (2001) Alterations in the regulatory pathway involving p16, pRb and cdk4 in human chondrosarcoma. *J Orthop Res* 19: 149-54
- Asp J, Sangiorgi L, Inerot SE, Lindahl A, Molendini L, Benassi MS, Picci P (2000) Changes of the p16 gene but not the p53 gene in human chondrosarcoma tissues. *Int J Cancer* 85: 782-6
- Balkwill F, Mantovani A (2001) Inflammation and cancer: back to Virchow? *Lancet* 357: 539-45
- Bando H, Toi M, Kitada K, Koike M (2003) Genes commonly upregulated by hypoxia in human breast cancer cells MCF-7 and MDA-MB-231. *Biomed Pharmacother* 57: 333-40
- Barrios C, Castresana JS, Kreicbergs A (1994) Clinicopathologic correlations and short-term prognosis in musculoskeletal sarcoma with c-myc oncogene amplification. *Am J Clin Oncol* 17: 273-6
- Bell AC, West AG, Felsenfeld G (1999) The protein CTCF is required for the enhancer blocking activity of vertebrate insulators. *Cell* 98: 387-96

- Bhowmick NA, Neilson EG, Moses HL (2004) Stromal fibroblasts in cancer initiation and progression. *Nature* 432: 332-7
- Blain EJ, Mason DJ, Duance VC (2002) The effect of thymosin beta4 on articular cartilage chondrocyte matrix metalloproteinase expression. *Biochem Soc Trans* 30: 879-82
- Boyer LA, Lee TI, Cole MF, Johnstone SE, Levine SS, Zucker JP, Guenther MG, Kumar RM, Murray HL, Jenner RG, Gifford DK, Melton DA, Jaenisch R, Young RA (2005) Core transcriptional regulatory circuitry in human embryonic stem cells. *Cell* 122: 947-56
- Breitkreutz D, Diaz de Leon L, Paglia L, Gay S, Swarm RL, Stern R (1979) Histological and biochemical studies of a transplantable rat chondrosarcoma. *Cancer Res* 39: 5093-100
- Brena RM, Costello JF (2007) Genome-epigenome interactions in cancer. *Hum Mol Genet* 16 Spec No 1: R96-105
- Brigstock DR (2002) Regulation of angiogenesis and endothelial cell function by connective tissue growth factor (CTGF) and cysteine-rich 61 (CYR61). *Angiogenesis* 5: 153-65
- Bromme D, Okamoto K, Wang BB, Biroc S (1996) Human cathepsin O2, a matrix protein-degrading cysteine protease expressed in osteoclasts. Functional expression of human cathepsin O2 in *Spodoptera frugiperda* and characterization of the enzyme. *J Biol Chem* 271: 2126-32
- Bui C, Ouzzine M, Talhaoui I, Sharp S, Prydz K, Coughtrie MW, Fournel-Gigleux S (2009) Epigenetics: methylation-associated repression of heparan sulfate 3-O-sulfotransferase gene expression contributes to the invasive phenotype of H-EMC-SS chondrosarcoma cells. *FASEB J*
- Caricasole A, Ward A (1993) Transactivation of mouse insulin-like growth factor II (IGF-II) gene promoters by the AP-1 complex. *Nucleic Acids Res* 21: 1873-9
- Cayre A, Rossignol F, Clottes E, Penault-Llorca F (2003) aHIF but not HIF-1alpha transcript is a poor prognostic marker in human breast cancer. *Breast Cancer Res* 5: R223-30
- Cha HJ, Jeong MJ, Kleinman HK (2003) Role of thymosin beta4 in tumor metastasis and angiogenesis. *J Natl Cancer Inst* 95: 1674-80
- Chang CC, Shih JY, Jeng YM, Su JL, Lin BZ, Chen ST, Chau YP, Yang PC, Kuo ML (2004) Connective tissue growth factor and its role in lung adenocarcinoma invasion and metastasis. *J Natl Cancer Inst* 96: 364-75
- Chen L, MacMillan AM, Chang W, Ezaz-Nikpay K, Lane WS, Verdine GL (1991) Direct identification of the active-site nucleophile in a DNA (cytosine-5)-methyltransferase. *Biochemistry* 30: 11018-25
- Chiang PK, Gordon RK, Tal J, Zeng GC, Doctor BP, Pardhasaradhi K, McCann PP (1996) S-Adenosylmethionine and methylation. *FASEB J* 10: 471-80

- Cho DH, Thienes CP, Mahoney SE, Analau E, Filippova GN, Tapscott SJ (2005) Antisense transcription and heterochromatin at the DM1 CTG repeats are constrained by CTCF. *Mol Cell* 20: 483-9
- Cho ML, Jung YO, Moon YM, Min SY, Yoon CH, Lee SH, Park SH, Cho CS, Jue DM, Kim HY (2006) Interleukin-18 induces the production of vascular endothelial growth factor (VEGF) in rheumatoid arthritis synovial fibroblasts via AP-1-dependent pathways. *Immunol Lett* 103: 159-66
- Choi HU, Meyer K, Swarm R (1971) Mucopolysaccharide and protein-polysaccharide of a transplantable rat chondrosarcoma. *Proc Natl Acad Sci U S A* 68: 877-9
- Comb M, Goodman HM (1990) CpG methylation inhibits proenkephalin gene expression and binding of the transcription factor AP-2. *Nucleic Acids Res* 18: 3975-82
- Costa FF (2008) Non-coding RNAs, epigenetics and complexity. *Gene* 410: 9-17
- Costa FF, Paixao VA, Cavalher FP, Ribeiro KB, Cunha IW, Rinck JA, Jr., O'Hare M, Mackay A, Soares FA, Brentani RR, Camargo AA (2006) SATR-1 hypomethylation is a common and early event in breast cancer. *Cancer Genet Cytogenet* 165: 135-43
- Dahlin DC, Henderson ED (1956) Chondrosarcoma, a surgical and pathological problem; review of 212 cases. *J Bone Joint Surg Am* 38-A: 1025-38; passim
- Di Cesare PE, Carlson CS, Attur M, Kale AA, Abramson SB, Della Valle C, Steiner G, Amin AR (1998) Up-regulation of inducible nitric oxide synthase and production of nitric oxide by the Swarm rat and human chondrosarcoma. *J Orthop Res* 16: 667-74
- Dorfman HD, Czerniak B (1995) Bone cancers. *Cancer* 75: 203-10
- Dunn BK (2003) Hypomethylation: one side of a larger picture. *Ann N Y Acad Sci* 983: 28-42
- Eden A, Gaudet F, Waghmare A, Jaenisch R (2003) Chromosomal instability and tumors promoted by DNA hypomethylation. *Science* 300: 455
- Eefting D, Schrage YM, Geirnaerd MJ, Le Cessie S, Taminiau AH, Bovee JV, Hogendoorn PC (2009) Assessment of interobserver variability and histologic parameters to improve reliability in classification and grading of central cartilaginous tumors. *Am J Surg Pathol* 33: 50-7
- Eferl R, Wagner EF (2003) AP-1: a double-edged sword in tumorigenesis. *Nat Rev Cancer* 3: 859-68
- Esteller M, Corn PG, Baylin SB, Herman JG (2001) A gene hypermethylation profile of human cancer. *Cancer Res* 61: 3225-9
- Evans HL, Ayala AG, Romsdahl MM (1977) Prognostic factors in chondrosarcoma of bone: a clinicopathologic analysis with emphasis on histologic grading. *Cancer* 40: 818-31
- Fan M, Yan PS, Hartman-Frey C, Chen L, Paik H, Oyer SL, Salisbury JD, Cheng AS, Li L, Abbosh PH, Huang TH, Nephew KP (2006) Diverse gene expression and DNA

methylation profiles correlate with differential adaptation of breast cancer cells to the antiestrogens tamoxifen and fulvestrant. *Cancer Res* 66: 11954-66

Fang J, Shing Y, Wiederschain D, Yan L, Butterfield C, Jackson G, Harper J, Tamvakopoulos G, Moses MA (2000) Matrix metalloproteinase-2 is required for the switch to the angiogenic phenotype in a tumor model. *Proc Natl Acad Sci U S A* 97: 3884-9

Fang J, Yan L, Shing Y, Moses MA (2001) HIF-1 $\alpha$ -mediated up-regulation of vascular endothelial growth factor, independent of basic fibroblast growth factor, is important in the switch to the angiogenic phenotype during early tumorigenesis. *Cancer Res* 61: 5731-5

Feinberg AP (2008) Epigenetics at the epicenter of modern medicine. *JAMA* 299: 1345-50

Feinberg AP, Tycko B (2004) The history of cancer epigenetics. *Nat Rev Cancer* 4: 143-53

Feinberg AP, Vogelstein B (1983) Hypomethylation distinguishes genes of some human cancers from their normal counterparts. *Nature* 301: 89-92

Fraga MF, Herranz M, Espada J, Ballestar E, Paz MF, Ropero S, Erkek E, Bozdogan O, Peinado H, Niveleau A, Mao JH, Balmain A, Cano A, Esteller M (2004) A mouse skin multistage carcinogenesis model reflects the aberrant DNA methylation patterns of human tumors. *Cancer Res* 64: 5527-34

Fromigue O, Louis K, Dayem M, Milanini J, Pages G, Tartare-Deckert S, Ponzio G, Hofman P, Barbry P, Auberger P, Mari B (2003) Gene expression profiling of normal human pulmonary fibroblasts following coculture with non-small-cell lung cancer cells reveals alterations related to matrix degradation, angiogenesis, cell growth and survival. *Oncogene* 22: 8487-97

Furumatsu T, Nishida K, Kawai A, Namba M, Inoue H, Ninomiya Y (2002) Human chondrosarcoma secretes vascular endothelial growth factor to induce tumor angiogenesis and stores basic fibroblast growth factor for regulation of its own growth. *Int J Cancer* 97: 313-22

Gaudet F, Hodgson JG, Eden A, Jackson-Grusby L, Dausman J, Gray JW, Leonhardt H, Jaenisch R (2003) Induction of tumors in mice by genomic hypomethylation. *Science* 300: 489-92

Gitelis S, Bertoni F, Picci P, Campanacci M (1981) Chondrosarcoma of bone. The experience at the Istituto Ortopedico Rizzoli. *J Bone Joint Surg Am* 63: 1248-57

Gold M, Hurwitz J, Anders M (1963) The Enzymatic Methylation of Rna and DNA, Ii. On the Species Specificity of the Methylation Enzymes. *Proc Natl Acad Sci U S A* 50: 164-9

Grimaud E, Damiens C, Rousselle AV, Passuti N, Heymann D, Gouin F (2002) Bone remodelling and tumour grade modifications induced by interactions between bone and swam rat chondrosarcoma. *Histol Histopathol* 17: 1103-11

Hallor KH, Staaf J, Bovee JV, Hogendoorn PC, Cleton-Jansen AM, Knuutila S, Savola S, Niini T, Brosjo O, Bauer HC, Vult von Steyern F, Jonsson K, Skorpil M, Mandahl N, Mertens F (2009) Genomic profiling of chondrosarcoma: chromosomal patterns in central and peripheral tumors. *Clin Cancer Res* 15: 2685-94

Hanahan D, Weinberg RA (2000) The hallmarks of cancer. *Cell* 100: 57-70

Hart IR, Fidler IJ (1980) Role of organ selectivity in the determination of metastatic patterns of B16 melanoma. *Cancer Res* 40: 2281-7

Hendrix MJ, Seftor EA, Seftor RE, Fidler IJ (1987) A simple quantitative assay for studying the invasive potential of high and low human metastatic variants. *Cancer Lett* 38: 137-47

Hess J, Angel P, Schorpp-Kistner M (2004) AP-1 subunits: quarrel and harmony among siblings. *J Cell Sci* 117: 5965-73

Hoffmann MJ, Schulz WA (2005) Causes and consequences of DNA hypomethylation in human cancer. *Biochem Cell Biol* 83: 296-321

Hoshijima M, Hattori T, Inoue M, Araki D, Hanagata H, Miyauchi A, Takigawa M (2006) CT domain of CCN2/CTGF directly interacts with fibronectin and enhances cell adhesion of chondrocytes through integrin alpha5beta1. *FEBS Lett* 580: 1376-82

Hou CH, Hsiao YC, Fong YC, Tang CH (2009) Bone morphogenetic protein-2 enhances the motility of chondrosarcoma cells via activation of matrix metalloproteinase-13. *Bone* 44: 233-42

Howard G, Eiges R, Gaudet F, Jaenisch R, Eden A (2008) Activation and transposition of endogenous retroviral elements in hypomethylation induced tumors in mice. *Oncogene* 27: 404-8

Huang WQ, Wang QR (2001) Bone marrow endothelial cells secrete thymosin beta4 and AcSDKP. *Exp Hematol* 29: 12-8

Iacobuzio-Donahue CA, Argani P, Hempen PM, Jones J, Kern SE (2002) The desmoplastic response to infiltrating breast carcinoma: gene expression at the site of primary invasion and implications for comparisons between tumor types. *Cancer Res* 62: 5351-7

Ijichi N, Tsujimoto N, Iwaki T, Fukumaki Y, Iwaki A (2004) Distal Sox binding elements of the alphaB-crystallin gene show lens enhancer activity in transgenic mouse embryos. *J Biochem* 135: 413-20

Issa JP, Garcia-Manero G, Giles FJ, Mannari R, Thomas D, Faderl S, Bayar E, Lyons J, Rosenfeld CS, Cortes J, Kantarjian HM (2004) Phase 1 study of low-dose prolonged exposure schedules of the hypomethylating agent 5-aza-2'-deoxycytidine (decitabine) in hematopoietic malignancies. *Blood* 103: 1635-40

Ivanov O, Chen F, Wiley EL, Keswani A, Diaz LK, Memmel HC, Rademaker A, Gradishar WJ, Morrow M, Khan SA, Cryns VL (2008) alphaB-crystallin is a novel predictor of resistance to neoadjuvant chemotherapy in breast cancer. *Breast Cancer Res Treat* 111: 411-7

Jackson-Grusby L, Laird PW, Magge SN, Moeller BJ, Jaenisch R (1997) Mutagenicity of 5-aza-2'-deoxycytidine is mediated by the mammalian DNA methyltransferase. *Proc Natl Acad Sci U S A* 94: 4681-5

Jemal A, Siegel R, Ward E, Hao Y, Xu J, Murray T, Thun MJ (2008) Cancer statistics, 2008. *CA Cancer J Clin* 58: 71-96

Jones PA, Baylin SB (2002) The fundamental role of epigenetic events in cancer. *Nat Rev Genet* 3: 415-28

Juttermann R, Li E, Jaenisch R (1994) Toxicity of 5-aza-2'-deoxycytidine to mammalian cells is mediated primarily by covalent trapping of DNA methyltransferase rather than DNA demethylation. *Proc Natl Acad Sci U S A* 91: 11797-801

Kadomatsu K, Muramatsu T (2004) Midkine and pleiotrophin in neural development and cancer. *Cancer Lett* 204: 127-43

Kalinski T, Ropke A, Sel S, Kouznetsova I, Ropke M, Roessner A (2009) Down-regulation of ephrin-A5, a gene product of normal cartilage, in chondrosarcoma. *Hum Pathol*

Karin M, Liu Z, Zandi E (1997) AP-1 function and regulation. *Curr Opin Cell Biol* 9: 240-6

Karpf AR, Jones DA (2002) Reactivating the expression of methylation silenced genes in human cancer. *Oncogene* 21: 5496-503

Kato M, Maeta H, Kato S, Shinozawa T, Terada T (2000) Immunohistochemical and in situ hybridization analyses of midkine expression in thyroid papillary carcinoma. *Mod Pathol* 13: 1060-5

Kenan S, Steiner GC (1991) Experimental transplantation of the Swarm rat chondrosarcoma into bone: radiological and pathological studies. *J Orthop Res* 9: 445-51

Kent WJ, Sugnet CW, Furey TS, Roskin KM, Pringle TH, Zahler AM, Haussler D (2002) The human genome browser at UCSC. *Genome Res* 12: 996-1006

Kim YI, Giuliano A, Hatch KD, Schneider A, Nour MA, Dallal GE, Selhub J, Mason JB (1994) Global DNA hypomethylation increases progressively in cervical dysplasia and carcinoma. *Cancer* 74: 893-9

Kimura JH, Hardingham TE, Hascall VC, Solursh M (1979) Biosynthesis of proteoglycans and their assembly into aggregates in cultures of chondrocytes from the Swarm rat chondrosarcoma. *J Biol Chem* 254: 2600-9

King KB, Kimura JH (2003) The establishment and characterization of an immortal cell line with a stable chondrocytic phenotype. *J Cell Biochem* 89: 992-1004

Kobayashi T, Okada F, Fujii N, Tomita N, Ito S, Tazawa H, Aoyama T, Choi SK, Shibata T, Fujita H, Hosokawa M (2002) Thymosin-beta4 regulates motility and metastasis of malignant mouse fibrosarcoma cells. *Am J Pathol* 160: 869-82

Kondo S, Kubota S, Mukudai Y, Moritani N, Nishida T, Matsushita H, Matsumoto S, Sugahara T, Takigawa M (2006) Hypoxic regulation of stability of connective tissue

- growth factor/CCN2 mRNA by 3'-untranslated region interacting with a cellular protein in human chondrosarcoma cells. *Oncogene* 25: 1099-110
- Lee FY, Mankin HJ, Fondren G, Gebhardt MC, Springfield DS, Rosenberg AE, Jennings LC (1999) Chondrosarcoma of bone: an assessment of outcome. *J Bone Joint Surg Am* 81: 326-38
- Lee JY, Eom EM, Kim DS, Ha-Lee YM, Lee DH (2003) Analysis of gene expression profiles of gastric normal and cancer tissues by SAGE. *Genomics* 82: 78-85
- Lewis JS, Landers RJ, Underwood JC, Harris AL, Lewis CE (2000) Expression of vascular endothelial growth factor by macrophages is up-regulated in poorly vascularized areas of breast carcinomas. *J Pathol* 192: 150-8
- Lo YY, Cruz TF (1995) Involvement of reactive oxygen species in cytokine and growth factor induction of c-fos expression in chondrocytes. *J Biol Chem* 270: 11727-30
- Lujambio A, Calin GA, Villanueva A, Ropero S, Sanchez-Cespedes M, Blanco D, Montuenga LM, Rossi S, Nicoloso MS, Faller WJ, Gallagher WM, Eccles SA, Croce CM, Esteller M (2008) A microRNA DNA methylation signature for human cancer metastasis. *Proc Natl Acad Sci U S A* 105: 13556-61
- Magee PN (1971) The possible role of nucleic acid methylases in the induction of cancer. *Cancer Res* 31: 599-604
- Maibenco HC, Krehbiel RH, Nelson D (1967) Transplantable osteogenic tumor in the rat. *Cancer Res* 27: 362-6
- Mandahl N, Gustafson P, Mertens F, Akerman M, Baldetorp B, Gisselsson D, Knuutila S, Bauer HC, Larsson O (2002) Cytogenetic aberrations and their prognostic impact in chondrosarcoma. *Genes Chromosomes Cancer* 33: 188-200
- Mankin HJ, Fondren G, Hornicek FJ, Gebhardt MC, Rosenberg AE (2002) The use of flow cytometry in assessing malignancy in bone and soft tissue tumors. *Clin Orthop Relat Res*: 95-105
- Masciocchi C, Sparvoli L, Barile A (1998) Diagnostic imaging of malignant cartilage tumors. *Eur J Radiol* 27 Suppl 1: S86-90
- Masi L, Malentacchi C, Campanacci D, Franchi A (2002) Transforming growth factor-beta isoform and receptor expression in chondrosarcoma of bone. *Virchows Arch* 440: 491-7
- Mason RM, Crossman MV, Sweeney C (1989) Hyaluronan and hyaluronan-binding proteins in cartilaginous tissues. *Ciba Found Symp* 143: 107-16; discussion 117-20, 281-5
- McGough RL, Lin C, Meitner P, Aswad BI, Terek RM (2002) Angiogenic cytokines in cartilage tumors. *Clin Orthop Relat Res*: 62-9
- Mignatti P, Rifkin DB (1993) Biology and biochemistry of proteinases in tumor invasion. *Physiol Rev* 73: 161-95

- Mirkin BL, Clark S, Zheng X, Chu F, White BD, Greene M, Rebbaa A (2005) Identification of midkine as a mediator for intercellular transfer of drug resistance. *Oncogene* 24: 4965-74
- Mitchell AD, Ayoub K, Mangham DC, Grimer RJ, Carter SR, Tillman RM (2000) Experience in the treatment of dedifferentiated chondrosarcoma. *J Bone Joint Surg Br* 82: 55-61
- Morcuende JA, Huang XD, Stevens J, Kucaba TA, Brown B, Abdulkawy H, Scheetz TE, Malchenko S, Bonaldo F, Casavant TL, Soares B (2002) Identification and initial characterization of 6,000 expressed sequenced tags (ESTs) from rat normal-growing cartilage and swarm rat chondrosarcoma cDNA libraries. *Iowa Orthop J* 22: 28-34
- Morita S, Iida S, Kato K, Takagi Y, Uetake H, Sugihara K (2006) The synergistic effect of 5-aza-2'-deoxycytidine and 5-fluorouracil on drug-resistant tumors. *Oncology* 71: 437-45
- Moulder JE, Rockwell S (1987) Tumor hypoxia: its impact on cancer therapy. *Cancer Metastasis Rev* 5: 313-41
- Mund C, Brueckner B, Lyko F (2006) Reactivation of epigenetically silenced genes by DNA methyltransferase inhibitors: basic concepts and clinical applications. *Epigenetics* 1: 7-13
- Mund C, Hackanson B, Stresemann C, Lubbert M, Lyko F (2005) Characterization of DNA demethylation effects induced by 5-Aza-2'-deoxycytidine in patients with myelodysplastic syndrome. *Cancer Res* 65: 7086-90
- Naka T, Iwamoto Y, Shinohara N, Ushijima M, Chuman H, Tsuneyoshi M (1997) Expression of c-met proto-oncogene product (c-MET) in benign and malignant bone tumors. *Mod Pathol* 10: 832-8
- Niwa H (2007) How is pluripotency determined and maintained? *Development* 134: 635-46
- Noel A, Jost M, Maquoi E (2008) Matrix metalloproteinases at cancer tumor-host interface. *Semin Cell Dev Biol* 19: 52-60
- Noma T, Glick AB, Geiser AG, O'Reilly MA, Miller J, Roberts AB, Sporn MB (1991) Molecular cloning and structure of the human transforming growth factor-beta 2 gene promoter. *Growth Factors* 4: 247-55
- Ohtani-Fujita N, Fujita T, Aoike A, Osifchin NE, Robbins PD, Sakai T (1993) CpG methylation inactivates the promoter activity of the human retinoblastoma tumor-suppressor gene. *Oncogene* 8: 1063-7
- Ozaki T, Lindner N, Hillmann A, Rodl R, Blasius S, Winkelmann W (1996) Influence of intralesional surgery on treatment outcome of chondrosarcoma. *Cancer* 77: 1292-7
- Paget S (1989) The distribution of secondary growths in cancer of the breast. 1889. *Cancer Metastasis Rev* 8: 98-101
- Palii SS, Van Emburgh BO, Sankpal UT, Brown KD, Robertson KD (2008) DNA methylation inhibitor 5-Aza-2'-deoxycytidine induces reversible genome-wide DNA

damage that is distinctly influenced by DNA methyltransferases 1 and 3B. *Mol Cell Biol* 28: 752-71

Pan LH, Beppu T, Kurose A, Yamauchi K, Sugawara A, Suzuki M, Ogawa A, Sawai T (2002) Neoplastic cells and proliferating endothelial cells express connective tissue growth factor (CTGF) in glioblastoma. *Neurol Res* 24: 677-83

Pant R, Yasko AW, Lewis VO, Raymond K, Lin PP (2005) Chondrosarcoma of the scapula: long-term oncologic outcome. *Cancer* 104: 149-58

Papachristou DJ, Papachristou GI, Papaefthimiou OA, Agnantis NJ, Basdra EK, Papavassiliou AG (2005) The MAPK-AP-1/-Runx2 signalling axes are implicated in chondrosarcoma pathobiology either independently or via up-regulation of VEGF. *Histopathology* 47: 565-74

Park IH, Zhao R, West JA, Yabuuchi A, Huo H, Ince TA, Lerou PH, Lensch MW, Daley GQ (2008) Reprogramming of human somatic cells to pluripotency with defined factors. *Nature* 451: 141-6

Pfaffl MW (2001) A new mathematical model for relative quantification in real-time RT-PCR. *Nucleic Acids Res* 29: e45

Piechaczyk M, Blanchard JM (1994) c-fos proto-oncogene regulation and function. *Crit Rev Oncol Hematol* 17: 93-131

Plimack ER, Kantarjian HM, Issa JP (2007) Decitabine and its role in the treatment of hematopoietic malignancies. *Leuk Lymphoma* 48: 1472-81

Pogribny IP, Beland FA (2009) DNA hypomethylation in the origin and pathogenesis of human diseases. *Cell Mol Life Sci* 66: 2249-61

Porter D, Lahti-Domenici J, Keshaviah A, Bae YK, Argani P, Marks J, Richardson A, Cooper A, Strausberg R, Riggins GJ, Schnitt S, Gabrielson E, Gelman R, Polyak K (2003) Molecular markers in ductal carcinoma in situ of the breast. *Mol Cancer Res* 1: 362-75

Rehman J, Li J, Orschell CM, March KL (2003) Peripheral blood "endothelial progenitor cells" are derived from monocyte/macrophages and secrete angiogenic growth factors. *Circulation* 107: 1164-9

Reynolds TY, Rockwell S, Glazer PM (1996) Genetic instability induced by the tumor microenvironment. *Cancer Res* 56: 5754-7

Ridley A (2000) Molecular switches in metastasis. *Nature* 406: 466-7

Riedel RF, Larrier N, Dodd L, Kirsch D, Martinez S, Brigman BE (2009) The clinical management of chondrosarcoma. *Curr Treat Options Oncol* 10: 94-106

Rishikof DC, Ricupero DA, Kuang PP, Liu H, Goldstein RH (2002) Interleukin-4 regulates connective tissue growth factor expression in human lung fibroblasts. *J Cell Biochem* 85: 496-504

Rong S, Jeffers M, Resau JH, Tsarfaty I, Oskarsson M, Vande Woude GF (1993) Met expression and sarcoma tumorigenicity. *Cancer Res* 53: 5355-60

- Ropke M, Boltze C, Neumann HW, Roessner A, Schneider-Stock R (2003) Genetic and epigenetic alterations in tumor progression in a dedifferentiated chondrosarcoma. *Pathol Res Pract* 199: 437-44
- Rose JK, Gallione CJ (1981) Nucleotide sequences of the mRNA's encoding the vesicular stomatitis virus G and M proteins determined from cDNA clones containing the complete coding regions. *J Virol* 39: 519-28
- Rosenbloom KR, Dreszer TR, Pheasant M, Barber GP, Meyer LR, Pohl A, Raney BJ, Wang T, Hinrichs AS, Zweig AS, Fujita PA, Learned K, Rhead B, Smith KE, Kuhn RM, Karolchik D, Haussler D, Kent WJ (2009) ENCODE whole-genome data in the UCSC Genome Browser. *Nucleic Acids Res*
- Ruau D, Ensenat-Waser R, Dinger TC, Vallabhapurapu DS, Rolletschek A, Hacker C, Hieronymus T, Wobus AM, Muller AM, Zenke M (2008) Pluripotency associated genes are reactivated by chromatin-modifying agents in neurosphere cells. *Stem Cells* 26: 920-6
- Ruijter JM, Van Kampen AH, Baas F (2002) Statistical evaluation of SAGE libraries: consequences for experimental design. *Physiol Genomics* 11: 37-44
- Sakamoto A, Oda Y, Adachi T, Oshiro Y, Tamiya S, Tanaka K, Matsuda S, Iwamoto Y, Tsuneyoshi M (2001) H-ras oncogene mutation in dedifferentiated chondrosarcoma: polymerase chain reaction-restriction fragment length polymorphism analysis. *Mod Pathol* 14: 343-9
- Sanada Y, Yoshida K, Konishi K, Oeda M, Ohara M, Tsutani Y (2006) Expression of gastric mucin MUC5AC and gastric transcription factor SOX2 in ampulla of Vater adenocarcinoma: comparison between expression patterns and histologic subtypes. *Oncol Rep* 15: 1157-61
- Sandberg AA, Bridge JA (2003) Updates on the cytogenetics and molecular genetics of bone and soft tissue tumors: osteosarcoma and related tumors. *Cancer Genet Cytogenet* 145: 1-30
- Sanerkin NG (1980) The diagnosis and grading of chondrosarcoma of bone: a combined cytologic and histologic approach. *Cancer* 45: 582-94
- Santi DV, Norment A, Garrett CE (1984) Covalent bond formation between a DNA-cytosine methyltransferase and DNA containing 5-azacytosine. *Proc Natl Acad Sci U S A* 81: 6993-7
- Scapini P, Morini M, Tecchio C, Minghelli S, Di Carlo E, Tanghetti E, Albin A, Lowell C, Berton G, Noonan DM, Cassatella MA (2004) CXCL1/macrophage inflammatory protein-2-induced angiogenesis in vivo is mediated by neutrophil-derived vascular endothelial growth factor-A. *J Immunol* 172: 5034-40
- Schmid M, Haaf T, Grunert D (1984) 5-Azacytidine-induced undercondensations in human chromosomes. *Hum Genet* 67: 257-63
- Schoenhals M, Kassambara A, De Vos J, Hose D, Moreaux J, Klein B (2009) Embryonic stem cell markers expression in cancers. *Biochem Biophys Res Commun* 383: 157-62
- Shahrzad S, Bertrand K, Minhas K, Coomber BL (2007) Induction of DNA hypomethylation by tumor hypoxia. *Epigenetics* 2: 119-25

- Shakunaga T, Ozaki T, Ohara N, Asaumi K, Doi T, Nishida K, Kawai A, Nakanishi T, Takigawa M, Inoue H (2000) Expression of connective tissue growth factor in cartilaginous tumors. *Cancer* 89: 1466-73
- Shimo T, Nakanishi T, Nishida T, Asano M, Kanyama M, Kuboki T, Tamatani T, Tezuka K, Takemura M, Matsumura T, Takigawa M (1999) Connective tissue growth factor induces the proliferation, migration, and tube formation of vascular endothelial cells in vitro, and angiogenesis in vivo. *J Biochem* 126: 137-45
- Singer-Sam J, Riggs AD (1993) X chromosome inactivation and DNA methylation. *EXS* 64: 358-84
- Soderstrom M, Aro HT, Ahonen M, Johansson N, Aho A, Ekfors T, Bohling T, Kahari VM, Vuorio E (2001a) Expression of matrix metalloproteinases and tissue inhibitors of metalloproteinases in human chondrosarcomas. *Apmis* 109: 305-15
- Soderstrom M, Bohling T, Ekfors T, Nelimarkka L, Aro HT, Vuorio E (2002) Molecular profiling of human chondrosarcomas for matrix production and cancer markers. *Int J Cancer* 100: 144-51
- Soderstrom M, Ekfors T, Bohling T, Aho A, Aro HT, Vuorio E (2001b) Cysteine proteinases in chondrosarcomas. *Matrix Biol* 19: 717-25
- Sood AK, Coffin JE, Schneider GB, Fletcher MS, DeYoung BR, Gruman LM, Gershenson DM, Schaller MD, Hendrix MJ (2004) Biological significance of focal adhesion kinase in ovarian cancer: role in migration and invasion. *Am J Pathol* 165: 1087-95
- Stackpole CW, Alterman AL, Angadi CV, Kim YS, Fornabaio DM (1990) Differences in organization of metastatic and nonmetastatic tumors initiated by the same B16 melanoma clone in mature and young mice. *Clin Exp Metastasis* 8: 255-66
- Stevens JW, Patil SR, Jordan DK, Kimura JH, Morcuende JA (2005) Cytogenetics of swarm rat chondrosarcoma. *Iowa Orthop J* 25: 135-40
- Stevens RL, Hascall VC (1981) Characterization of proteoglycans synthesized by rat chondrosarcoma chondrocytes treated with multiplication-stimulating activity and insulin. *J Biol Chem* 256: 2053-8
- Stresemann C, Lyko F (2008) Modes of action of the DNA methyltransferase inhibitors azacytidine and decitabine. *Int J Cancer* 123: 8-13
- Stuart JJ, Egry LA, Wong GH, Kaspar RL (2000) The 3' UTR of human MnSOD mRNA hybridizes to a small cytoplasmic RNA and inhibits gene expression. *Biochem Biophys Res Commun* 274: 641-8
- Szyf M (2009) The early life environment and the epigenome. *Biochim Biophys Acta* 1790: 878-85
- Takai D, Jones PA (2003) The CpG island searcher: a new WWW resource. *In Silico Biol* 3: 235-40
- Tallini G, Dorfman H, Brys P, Dal Cin P, De Wever I, Fletcher CD, Jonson K, Mandahl N, Mertens F, Mitelman F, Rosai J, Rydholm A, Samson I, Sciort R, Van den Berghe H,

- Vanni R, Willen H (2002) Correlation between clinicopathological features and karyotype in 100 cartilaginous and chordoid tumours. A report from the Chromosomes and Morphology (CHAMP) Collaborative Study Group. *J Pathol* 196: 194-203
- Tan TW, Yang WH, Lin YT, Hsu SF, Li TM, Kao ST, Chen WC, Fong YC, Tang CH (2009) Cyr61 increases migration and MMP-13 expression via  $\alpha$ 5 $\beta$ 3 integrin, FAK, ERK and AP-1-dependent pathway in human chondrosarcoma cells. *Carcinogenesis* 30: 258-68
- Tanabe K, Matsumoto M, Ikematsu S, Nagase S, Hatakeyama A, Takano T, Niikura H, Ito K, Kadomatsu K, Hayashi S, Yaegashi N (2008) Midkine and its clinical significance in endometrial carcinoma. *Cancer Sci* 99: 1125-30
- Tanaka TS, Kunath T, Kimber WL, Jaradat SA, Stagg CA, Usuda M, Yokota T, Niwa H, Rossant J, Ko MS (2002) Gene expression profiling of embryo-derived stem cells reveals candidate genes associated with pluripotency and lineage specificity. *Genome Res* 12: 1921-8
- Terek RM, Healey JH, Garin-Chesa P, Mak S, Huvos A, Albino AP (1998) p53 mutations in chondrosarcoma. *Diagn Mol Pathol* 7: 51-6
- Tsuchiya T, Osanai T, Ogoe A, Tamura G, Chano T, Kaneko Y, Ishikawa A, Orui H, Wada T, Ikeda T, Namba M, Takigawa M, Kawashima H, Hotta T, Tsuchiya A, Ogino T, Motoyama T (2005) Methylation status of EXT1 and EXT2 promoters and two mutations of EXT2 in chondrosarcoma. *Cancer Genet Cytogenet* 158: 148-55
- Tuckermann JP, Vallon R, Gack S, Grigoriadis AE, Porte D, Lutz A, Wagner EF, Schmidt J, Angel P (2001) Expression of collagenase-3 (MMP-13) in c-fos-induced osteosarcomas and chondrosarcomas is restricted to a subset of cells of the osteo-/chondrogenic lineage. *Differentiation* 69: 49-57
- Tufarelli C, Stanley JA, Garrick D, Sharpe JA, Ayyub H, Wood WG, Higgs DR (2003) Transcription of antisense RNA leading to gene silencing and methylation as a novel cause of human genetic disease. *Nat Genet* 34: 157-65
- Unni K (1996) Dahlins' bone tumors: general aspects and data on 11,087 cases, 5th edn. Lippincott Williams & Wilkins, Philadelphia
- Unni KK (2001) Cartilaginous lesions of bone. *J Orthop Sci* 6: 457-72
- van Beerendonk HM, Rozeman LB, Taminiau AH, Sciort R, Bovee JV, Cleton-Jansen AM, Hogendoorn PC (2004) Molecular analysis of the INK4A/INK4A-ARF gene locus in conventional (central) chondrosarcomas and enchondromas: indication of an important gene for tumour progression. *J Pathol* 202: 359-66
- Vaupel P, Kallinowski F, Okunieff P (1989) Blood flow, oxygen and nutrient supply, and metabolic microenvironment of human tumors: a review. *Cancer Res* 49: 6449-65
- Velculescu VE, Zhang L, Vogelstein B, Kinzler KW (1995) Serial analysis of gene expression. *Science* 270: 484-7
- Walter-Yohrling J, Cao X, Callahan M, Weber W, Morgenbesser S, Madden SL, Wang C, Teicher BA (2003) Identification of genes expressed in malignant cells that promote invasion. *Cancer Res* 63: 8939-47

- Wang ZQ, Grigoriadis AE, Mohle-Steinlein U, Wagner EF (1991) A novel target cell for c-fos-induced oncogenesis: development of chondrogenic tumours in embryonic stem cell chimeras. *EMBO J* 10: 2437-50
- Wang ZQ, Liang J, Schellander K, Wagner EF, Grigoriadis AE (1995) c-fos-induced osteosarcoma formation in transgenic mice: cooperativity with c-jun and the role of endogenous c-fos. *Cancer Res* 55: 6244-51
- Watts GS, Futscher BW, Holtan N, Degeest K, Domann FE, Rose SL (2008) DNA methylation changes in ovarian cancer are cumulative with disease progression and identify tumor stage. *BMC Med Genomics* 1: 47
- Weber M, Hellmann I, Stadler MB, Ramos L, Paabo S, Rebhan M, Schubeler D (2007) Distribution, silencing potential and evolutionary impact of promoter DNA methylation in the human genome. *Nat Genet* 39: 457-66
- Weisstein JS, Majeska RJ, Klein MJ, Einhorn TA (2001) Detection of c-fos expression in benign and malignant musculoskeletal lesions. *J Orthop Res* 19: 339-45
- Welkerling H, Kratz S, Ewerbeck V, Delling G (2003) A reproducible and simple grading system for classical chondrosarcomas. Analysis of 35 chondrosarcomas and 16 enchondromas with emphasis on recurrence rate and radiological and clinical data. *Virchows Arch* 443: 725-33
- Wike-Hooley JL, Haveman J, Reinhold HS (1984) The relevance of tumour pH to the treatment of malignant disease. *Radiother Oncol* 2: 343-66
- Wu S, Platteau A, Chen S, McNamara G, Whitsett J, Bancalari E (2009) Conditional Over-expression of Connective Tissue Growth Factor Disrupts Postnatal Lung Development. *Am J Respir Cell Mol Biol*
- Xia W, Kong W, Wang Z, Phan TT, Lim IJ, Longaker MT, Yang GP (2007) Increased CCN2 transcription in keloid fibroblasts requires cooperativity between AP-1 and SMAD binding sites. *Ann Surg* 246: 886-95
- Yang AS, Doshi KD, Choi SW, Mason JB, Mannari RK, Gharybian V, Luna R, Rashid A, Shen L, Estecio MR, Kantarjian HM, Garcia-Manero G, Issa JP (2006) DNA methylation changes after 5-aza-2'-deoxycytidine therapy in patients with leukemia. *Cancer Res* 66: 5495-503
- Yang AS, Estecio MR, Doshi K, Kondo Y, Tajara EH, Issa JP (2004) A simple method for estimating global DNA methylation using bisulfite PCR of repetitive DNA elements. *Nucleic Acids Res* 32: e38
- Yang SP, Lee HJ, Su Y (2005) Molecular cloning and structural characterization of the functional human thymosin beta4 gene. *Mol Cell Biochem* 272: 97-105
- Yoder JA, Walsh CP, Bestor TH (1997) Cytosine methylation and the ecology of intragenomic parasites. *Trends Genet* 13: 335-40
- Yosimichi G, Nakanishi T, Nishida T, Hattori T, Takano-Yamamoto T, Takigawa M (2001) CTGF/Hcs24 induces chondrocyte differentiation through a p38 mitogen-activated protein kinase (p38MAPK), and proliferation through a p44/42 MAPK/extracellular-signal regulated kinase (ERK). *Eur J Biochem* 268: 6058-65

Young SD, Hill RP (1998) Influence of tumor microenvironment on the malignant potential of murine tumor cells. *Clinical and Experimental Metastasis* 6: 66-67

Zhang L, Zhou W, Velculescu VE, Kern SE, Hruban RH, Hamilton SR, Vogelstein B, Kinzler KW (1997) Gene expression profiles in normal and cancer cells. *Science* 276: 1268-72

Zhu LJ, Altmann SW (2005) mRNA and 18S-RNA coapplication-reverse transcription for quantitative gene expression analysis. *Anal Biochem* 345: 102-9

Zou P, Muramatsu H, Miyata T, Muramatsu T (2006) Midkine, a heparin-binding growth factor, is expressed in neural precursor cells and promotes their growth. *J Neurochem* 99: 1470-9